Towards malaria combination therapy:

Characterization of hybrid molecules for HIV/malaria combination therapy and of thiostrepton as a proteasome-targeting antibiotic with a dual mode of action

Die Entwicklung von Malaria-Kombinationstherapien:

Die Charakterisierung von Hybridmolekülen für eine HIV/Malaria-Kombinationstherapie und von Thiostrepton als ein gegen das Proteasom-gerichtetes Antibiotikum mit dualem Wirkmodus

Doctoral thesis for a doctoral degree at the Graduate School of Life Sciences,
Julius-Maximilians-Universität Würzburg,

Immunity and Infection

Submitted by

Makoah Nigel Aminake

From

Yaounde, Cameroon

Würzburg, 2012

Members of the dissertation committee:

Chairperson: Prof. Dr. Thomas Hünig

Supervisors:

1. PD. Dr. Gabriele Pradel
2. Prof. Dr. Axel Rethwilm
3. Prof. Dr. Kelly Chibale

Affidavit

I hereby confirm that my thesis entitled Towards malaria combination therapy: Characterization of hybrid molecules for HIV/malaria combination therapy and of thiostrepton as a proteasome-targeting antibiotic with a dual mode of action is the result of my own work. I did not receive any help or support from commercial consultants. All sources and / or materials applied are listed and specified in the thesis.

Furthermore, I confirm that this thesis has not yet been submitted as part of another examination process neither in identical nor in similar form.

Würzburg, April 4, 2012
Place, Date

Signature

Eidesstattliche Erklärung

Hiermit erkläre ich an Eides statt, die Dissertation Die Entwicklung von Malaria-Kombinationstherapien: Die Charakterisierung von Hybridmolekülen für eine HIV/Malaria-Kombinationstherapie und von Thiostrepton als ein gegen das Proteasom-gerichtetes Antibiotikum mit dualem Wirkmodus eigenständig, d.h. insbesondere selbständig und ohne Hilfe eines kommerziellen Promotionsberaters, angefertigt und keine anderen als die von mir angegebenen Quellen und Hilfsmittel verwendet zu haben.

Ich erkläre außerdem, dass die Dissertation weder in gleicher noch in ähnlicher Form bereits in einem anderen Prüfungsverfahren vorgelegen hat.

Würzburg, 4. April 2012
Ort, Datum

Unterschrift

Acknowledgements

I owe my deepest gratitude to my supervisor, **Dr. Gabriele Pradel**, who gave me the opportunity to join the international research training group (IRTG 1522) and whose encouragement, supervision and support from the preliminary to the concluding level enabled me to develop an understanding of the subject. I would also like to thank her for the advices and guidance towards my future career.

I am grateful to **Prof. Axel Rethwilm**, speaker of our research training group and member of my supervisory committee, for giving me the opportunity to learn beyond my research area, and for his constant support throughout my studies in Wuerzburg.

I am also thankful to **Dr. Marc Kirschner** who introduced me in the field of molecular virology for his constant supervision during the 7 months spent in his laboratory.

I would like to thank **Prof. Kelly Chibale**, who hosted me in his laboratory for 6 months and introduced me to new methods and techniques in the field of pre-clinical pharmacology; I would also like to thank him for his advices and guidance.

I would take this opportunity to extend my thanks to **Prof. P. Smith, Dr. L. Wiesner** and all the member of the big group focused on drug discovery at the University of Cape Town, especially to **D. Taylor, C. de Kock, T. Finch, G. Mugumbate and A. Nchinda** for their substantial contribution to my work.

I would like to thank **Prof. H.-D. Arndt** and **Dr. S. Schoof** for providing thiotrepton and derivatives and for their helpful discussion and suggestions. I would also like to thank **Dr. C. Biot** for providing ciprofloxacin and derivatives and **Dr. S. Tschan** for providing peptidyl sulfonyl fluorides. I am grateful to **Dr. C. Sasse** for providing the GFP positive control for Western blot.

I would like to thank **Prof. G. Krohne** and his team for the assistance with the electron microscopy and **Hilde Merkert** for the assistance with fluorescence microscopy.

I would like to acknowledge the current and former members of the Pradel group for the nice working environment. A special thank goes to **Ludmilla** and **Monika** for their support and contribution to my project and **Dr. M. Scheuermayer** for his advices and for translating my summary into german. I would also like to thank **Nina** and **Shruti** for providing pure ribonucleic acid used to perform RT-PCRs.

Lastly, I would like to thank my family and my friends for their love and constant support.

Table of contents

Summary

Malaria and HIV are among the most important global health problems of our time and together are responsible for approximately 3 million deaths annually. These two diseases overlap in many regions of the world including sub-Saharan Africa, Southeast Asia and South America, leading to a higher risk of co-infection. In this study, we generated and characterized hybrid molecules to target *P. falciparum* and HIV simultaneously for a potential HIV/malaria combination therapy. Hybrid molecules were synthesized by covalent fusion between azidothymidine (AZT) and dihydroartemisinin (DHA), tetraoxane or chloroquine (CQ); and a small library was generated and tested for antiviral and antimalarial activity. Our data suggest that dihyate is the most potent molecule *in vitro*, with antiplasmodial activity comparable to that of DHA (IC_{50} = 26 nM, SI > 3000), a moderate activity against HIV (IC_{50} = 2.9 µM; SI > 35) and safe to HeLa cells at concentrations used in the assay (CC_{50} > 100 µM). Pharmacokinetic studies further revealed that dihyate is metabolically unstable and is cleaved following an O-dealkylation once in contact with cytochrome P450 enzymes. The later further explains the uneffectiveness of dihyate against the CQ-sensitive *P. berghei* N strain in mice when administered by oral route at 20 mg/kg. Here, we report on a first approach to develop antimalarial/anti-HIV hybrid molecules and future optimization efforts will aim at producing second generation hybrid molecules to improve activity against HIV as well as compound bioavailability.

With the emergence of resistant parasites against all the counterpart drugs of artemisinin derivatives used in artemisinin based combination therapies (ACTs), the introduction of antibiotics in the treatment of malaria has renewed interest on the identification of antibiotics with potent antimalarial properties. In this study we also investigated the antiplasmodial potential of thiostrepton and derivatives, synthesized using combinations of tail truncation, oxidation, and addition of lipophilic thiols to the terminal dehydroamino acid. We showed that derivatives SS231 and SS234 exhibit a better antiplasmodial activity (IC_{50} = 1 µM SI > 59 and SI > 77 respectively) than thiostrepton (IC_{50} = 8.95 µM, SI = 1.7). The antiplasmodial activity of these derivatives was observed at concentrations which are not hemolytic and non-toxic to human cell lines. Thiostrepton and derivatives appeared to exhibit transmission blocking properties when administered at their IC_{50} or IC_{90} concentrations and our data also showed that they attenuate proteasome activity of *Plasmodium*, which resulted in an accumulation of ubiquitinated proteins after incubation with their IC_{80} concentrations. Our results indicate that the parasite's proteasome could be an attractive target for therapeutic intervention. In this regard, thiostrepton derivatives are promising candidates by dually acting on two independent

targets, the proteasome and the apicoplast, with the capacity to eliminate both intraerythrocytic asexual and transmission stages of the parasite.

To further support our findings, we evaluated the activity of a new class of antimalarial and proteasome inhibitors namely peptidyl sulfonyl fluorides on gametocyte maturation and analogues AJ34 and AJ38 were able to completely suppress gametocytogenesis at IC_{50} concentrations (0.23 µM and 0.17 µM respectively) suggesting a strong transmission blocking potential. The proteasome, a major proteolytic complex, responsible for the degradation and re-cycling of non-functional proteins has been studied only indirectly in *P. falciparum*. In addition, an apparent proteasome-like protein with similarity to bacterial ClpQ/hslV threonine-peptidases was predicted in the parasite. Antibodies were generated against the proteasome subunits alpha type 5 (α5-SU), beta type 5 (β5-SU) and pfhslV in mice and we showed that the proteasome is expressed in both sexual and asexual blood stages of *P. falciparum*, where they localize in the nucleus and in the cytoplasm. However, expression of PfhslV was only observed in trophozoites and shizonts. The trafficking of the studied proteasome subunits was further investigated by generating parasites expressing GFP tagged proteins. The expression of α5-SU-GFP in transgenic parasite appeared to localize abundantly in the cytoplasm of all blood stages, and no additional information was obtained from this parasite line. In conclusion, our data highlight two new tools towards combination therapy. Hybrid molecules represent promising tools for the cure of co-infected individuals, while very potent antibiotics with a wide scope of activities could be useful in ACTs by eliminating resistant parasites and limiting transmission of both, resistances and disease.

Zusammenfassung

Malaria und HIV gehören zu den wichtigsten weltweiten Gesundheitsproblemen unserer Zeit und verursachen jährlich zusammen fast drei Millionen Todesfälle. Das Verbreitungsgebiet beider Krankheit überschneidet sich in vielen Weltregionen wie Afrika südlich der Sahara, Südostasien und Südamerika, was zu einem erhöhten Risiko für Koinfektionen führt. Während der vorliegenden Arbeit stellten wir Hybridmoleküle her und charakterisierten diese in Bezug auf ihre gleichzeitige Wirksamkeit gegen *P. falciparum* und HIV mit dem Ziel einer möglichen Kombinationstherapie gegen beide Krankheiten. Diese Hybridmoleküle wurden durch kovalente Verbindung von Azidothymidin (AZT) mit Dihydroartemisinin (DHA), Tetraoxan und Chloroquin (CQ) hergestellt. Die dabei hergestellte kleine Molekülsammlung wurde auf antivirale Wirkung und Wirkung gegen Malaria getestet. In vitro ist, gemäß unserer Daten, Dihyate das wirksamste Molekül, mit einer dem DHA vergleichbaren Wirksamkeit gegen *Plasmodium* (IC_{50} = 26 nM, SI > 3000), einer mittelmäßigen Wirksamkeit gegen HIV (IC_{50} = 2.9 µM; SI > 35) und keiner Wirkung auf HeLa-Zellen bei den im Versuch verwendeten Konzentrationen (CC_{50} > 100 µM). Weiterhin ergaben pharmakokinetische Studien, dass Dihyate metabolisch instabil ist und nach einer O-Dealkylierung gespalten wird, sobald es in Kontakt mit Cytochrom P450 Enzymen kommt. Dies erklärt auch die Unwirksamkeit von Dihyate gegen dem CQ-sensitiven *P. berghei* N Stamm im Mausversuch bei oraler Gabe von 20mg/kg. Wir berichten hier von einem ersten Ansatz Hybridmoleküle gegen Malaria/ HIV zu entwickeln. Zukünftige Verbesserungen werden darauf abzielen Hybridmoleküle der zweiten Generation herzustellen um sowohl die Wirksamkeit gegen HIV als auch die Bioverfügbarkeit zu verbessern.

Auf Grund der Entwicklung von Resistenzen gegenüber sämtliche Substanzen, die zusammen mit Artemisinin in Kombinationstherapien genutzt werden, hat die Verwendung von Antibiotika bei der Behandlung der Malaria das Interesse daran neu geweckt, Antibiotika mit starker Wirksamkeit gegenüber *Plasmodium* aufzuspüren. Während der vorliegenden Studie untersuchten wir die Wirksamkeit von Thiostrepton und seinen Derivaten gegenüber *Plasmodium*. Diese Derivate wurden durch Kombinationen von Verkürzung der Seitenkette, Oxidation und der Anbringung von lipophilen Thiolen an die endständige Dehydroaminosäure hergestellt. Wir konnten zeigen, dass die Derivate SS231 und SS234 (IC_{50} = 1 µM SI > 59 und SI > 77) eine bessere Wirksamkeit gegen *Plasmodium* besitzen als Thiostrepton (IC_{50} = 8.95 µM, SI = 1.7). Diese Wirksamkeit konnte bei Konzentrationen beobachtet werden, die nicht hämolytisch sind und ungiftig gegenüber menschlichen Zelllinien. Thiostrepton und seine Derivate zeigten transmissionsblockierende Eigenschaften, wenn sie in Konzentrationen, die

ihren IC_{50}- oder IC_{90}-Werten entsprachen, eingesetzt wurden. Unsere Daten zeigen auch, dass diese Substanzen die Aktivität des Proteasoms von *Plasmodium* abschwächen, was zu einer Anreicherung von ubiquitinierten Proteinen führte, wenn die Parasiten mit den Substanzen in IC_{80}-Konzentrationen inkubiert wurden. Unsere Ergebnisse sprechen dafür, dass das Proteasom ein attraktives Ziel für therapeutische Maßnahmen sein kann. In diesem Zusammenhang sind die Derivate des Thiostreptons vielversprechende Kandidaten, da sie gleichzeitig an zwei unabhängigen Zielstrukturen angreifen, dem Proteasom und dem Apicoplasten und die Fähigkeit besitzen, sowohl die asexuellen Blutstadien als auch diejenigen Blutstadien, die für die Weitergabe des Parasiten verantwortlich sind, zu beseitigen. Um unsere Ergebnisse weiter zu untermauern, untersuchten wir die Wirkung von Peptidyl-Sulfonyl-Fluoriden, einer neuen Klasse von Substanzen mit Wirksamkeit gegen Malaria und hemmender Wirkung gegenüber dem Proteasom auf die Reifung von Gametozyten. Die Substanzen AJ34 und AJ38 unterdrückten die Bildung von Gametozyten vollständig, wenn sie in Konzentrationen, die ihren IC_{50}-Werten (0.23 µM und 0.17 µM) entsprachen, eingesetzt wurden. Dies spricht für ein starkes transmissionsblockierendes Potential dieser Substanzen. Das Proteasom, ein bedeutender proteinabbauender Komplex, der für den Abbau und die Wiedergewinnung nicht funktioneller Proteine verantwortlich ist, wurde bisher nur indirekt in *P. falciparum* untersucht. Zusätzlich wurde die Existenz eines, dem Proteasom-ähnlichen, Proteins mit Ähnlichkeiten zu bakteriellen ClpQ/hslV Threonin-Peptidasen in *Plasmodium* vermutet. Gegen die Untereinheiten alpha 5 (α5-SU), beta 5 (β5-SU) und gegen pfhslV wurden in Mäusen Antikörper generiert. Mit diesen konnten wir zeigen, dass das Proteasom sowohl in den asexuellen als auch in den sexuellen Blutstadien von *P. falciparum* exprimiert wird und im Zellkern und im Zytoplasma lokalisiert sind. Die Expression von PfhslV konnte jedoch nur in Trophozoiten und Schizonten beobachtet werden. Der Transport der Proteasomuntereinheiten wurde weiterhin durch die Herstellung von transgenen Parasiten, die GFP-markierte Proteine bilden, untersucht. Die Expression von α5-SU-GFP in transgenen Parasiten schien im Zytoplasma aller Blutstadien lokalisiert zu sein, wobei durch diese Parasiten keine zusätzlichen Informationen gewonnen werden konnten. Zusammengefasst sprechen unsere Daten für zwei neue Werkzeuge für Kombinationstherapien. Hybridmoleküle sind vielversprechende Werkzeuge zur Heilung von gleichzeitig mit Malaria und HIV infizierten Patienten. Sehr wirksame Antibiotika mit einem breiten Wirkungsspektrum könnten in Artemisinin-Kombinationstherapien nützlich werden, wenn es darum geht, resistente Parasiten zu beseitigen und die Übertragung sowohl der Resistenz als auch der Krankheit zu verringern.

1. Introduction

1.1. Generalities on malaria

Human malaria is caused by a unicellular eukaryotic protozoan parasite of the genus *Plasmodium*. Five species can infect and be transmitted to humans, among which *P. falciparum* is the most virulent species and responsible for the majority of death cases, while *P. vivax*, *P. ovale*, and *P. malariae* generally cause a milder disease that is rarely fatal. A fifth genus, *P. knowlesi* which normally infects monkeys was reported to infect humans (Jongwutiwes et al., 2011; Singh et al., 2004). Malaria is mainly transmitted to people via the bite of a female *Anopheles* mosquito and the disease is mostly threatening to pregnant women and children under the age of five living in endemic areas. In areas of stable transmission, older children slowly develop a partial immunity against mild disease while in areas of unstable malaria; both children and adults can be similarly affected by uncomplicated and severe malaria (Flateau et al., 2011).

In Africa, a better access to health care and improvement of malaria case management were the only means for durably reducing the burden of malaria (Trape, 2001). However, the widespread of resistances against available antimalarial drugs have been undermining the elimination of this scourge; a situation which prompted the WHO to recommend artemisinin based combination therapies (ACTs) as the first-line treatment for *falciparum* malaria in all endemic regions. In addition, the distribution of treated bed nets free of charge in most endemic areas has tremendously contributed to reduce transmission (Diallo et al., 2004; Müller et al., 2006; Pettifor et al., 2009). Although research for an effective vaccine against malaria over the past years has been problematic, promising results from an ongoing clinical trial (ClinicalTrials.gov number, NCT00866619) showed that the RTS, S/AS01 vaccine reduced malaria by half in children 5 to 17 months of age during the 12 months after vaccination and that the vaccine has the potential to have an important effect on the burden of malaria in young African children (Agnandji et al., 2011). A succesfull development of this vaccine would represent and extra boost for the malaria elimination program. The concerted efforts to tackle this disease so far have improved the situation over the past years and the number of deaths per year has reduced considerably. In 2010, malaria caused an estimate of 655 000 deaths of which 86 % were from African regions (WHO, 2011). On the other hand, the number of cases remained relatively high (216 million cases) in 2010; 81% of these were in the African region (WHO, 2011) where the disease remains widespread (figure 1), suggesting that efforts to limit transmission remain below the required demand.

Clinical studies and mathematical models predict that to achieve malaria elimination, combination therapies will need to incorporate drugs that block the transmission of *P. falciparum* sexual stage parasites to mosquito vectors (Adjalley et al., 2011).

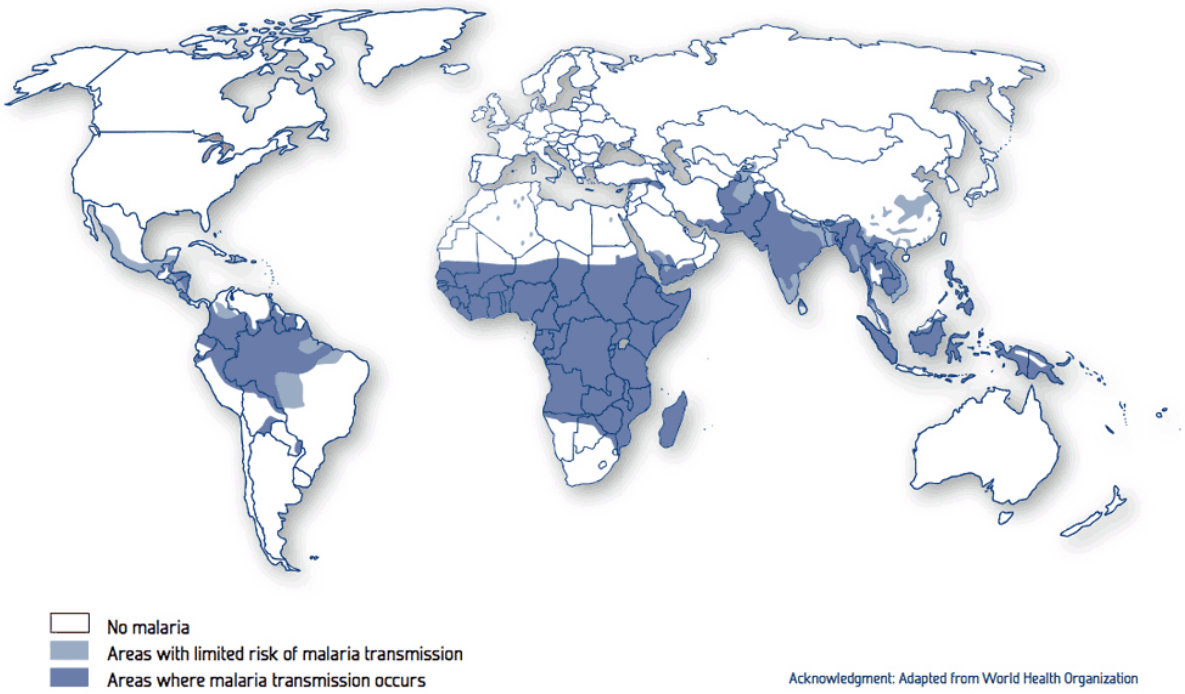

Figure 1. Malaria, countries or areas at risk of transmission.
Source: http://www.nathnac.org/pro/factsheets/images/Malaria%20YB.gif

1.2. The life cycle of P. falciparum

P. falciparum exhibits a complex life cycle involving an *Anopheles* mosquito and a human host (figure 2). Infection starts when an infected *Anopheles* species takes a blood meal and injects infective sporozoites into the peripheral circulation. These sporozoites are carried by the circulatory system to the liver where they invade hepatocytes. The sporozoite establishes in a hepatocyte and undergoes a huge asexual amplification, producing in 1 to 2 weeks, thousands of uninucleate merozoites. When the infected liver cell bursts, the merozoites enter the blood circulation, where they recognize erythrocytes, attach to, and invade them. Eventually the merozoites infect red blood cells and become an early stage trophozoite stage known as “ring stages” because of their morphology (figure 3). These

trophozoites further mature into schizonts, from which several merozoites bud and are released following the rupture of the red blood cell (RBC) membrane. Released merozoites infect more RBCs leading to clinical manifestation of the disease.

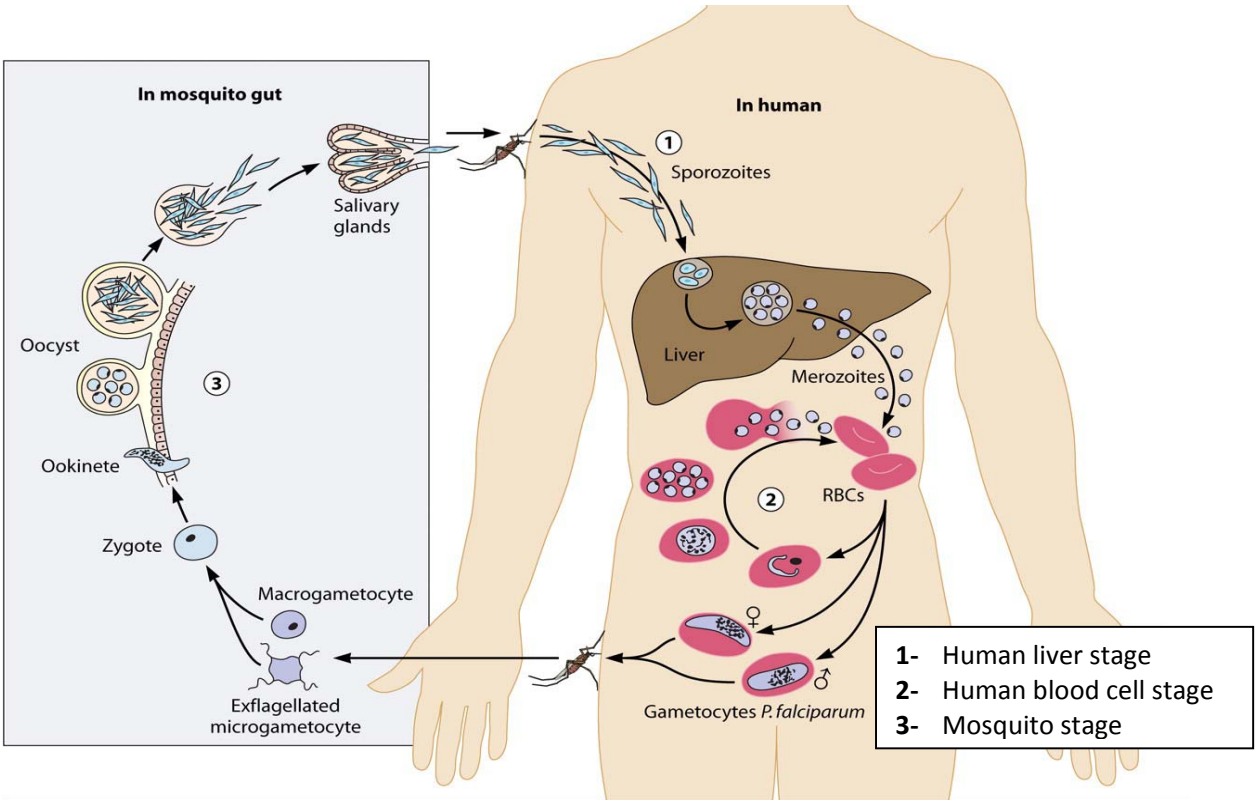

Figure 2. *P. falciparum* life cycle.
Modified from Bousema and Drakeley, 2011.

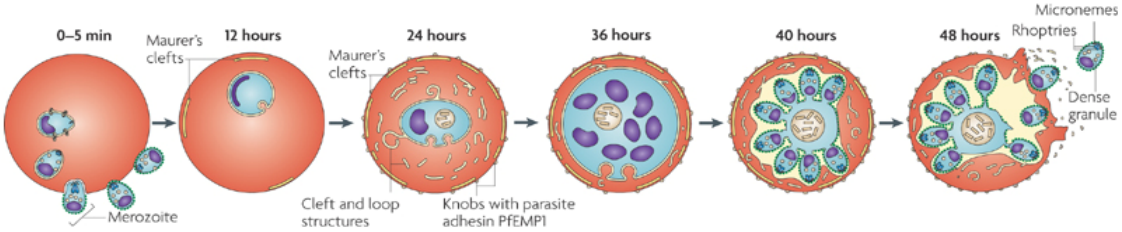

Figure 3. The different stages of *P. falciparum* asexual blood stage development. Merozoites attach to and invade mature human RBCs and the parasite develops in a parasitophorous vacuole (PV) through the ring (0–24 hours), trophozoite (24–36 hours) and schizont stages (40–48 hours). After approximately 48 hours the infected RBC ruptures, releasing 16–32 daughter merozoites. Degradation of haemoglobin results in the deposition of crystals of haemozoin in a digestive vacuole. PfEMP1: *P.falciparum* erythrocyte membrane protein 1. **Modified from Maier et al., 2009.**

Some of the trophozoites do not mature into schizonts; they instead differentiate into female (macrogametocytes) and male gametocytes (microgametocytes) through a process named gametocytogenesis (Talman et al., 2004). Gametocytogenesis is a process completed over a period of approximately 10 days in human, and encompassing five morphologically defined gametocyte stages (stage I–V). Whereas with Giemsa staining, stage I gametocytes resemble young asexual trophozoites, stages II–V are easily distinguished in a blood smear (figure 4). Ingestion of gametocytes by the mosquito vector induces gametogenesis (i.e., the production of gametes). Factors which participate in the induction of gametogenesis include: a drop in temperature, an increase in carbon dioxide, and mosquito metabolites like xanthurenic acid (XA; reviewed in Kuehn and Pradel, 2010). Microgametes, formed by a process known as exflagellation, are flagellated forms which fertilize the macrogamete to form a zygote. The zygote develops into a motile ookinete which penetrates the gut epithelial cells and develops into an oocyst .The oocyst undergoes multiple rounds of asexual replication resulting in the production of sporozoites. Rupture of the mature oocyst releases the sporozoites into the hemocoel (i.e., body cavity) of the mosquito. The sporozoites migrate to and invade the salivary glands, where they wait until the mosquito bites a host, thus completing the life cycle.

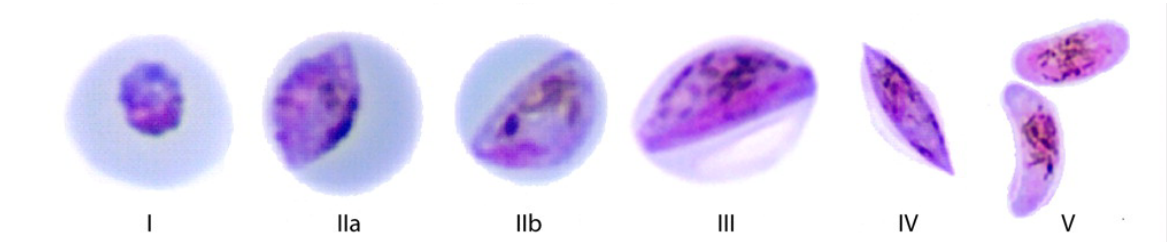

Figure 4. Formation and maturation of *P. falciparum* gametocytes
Modified from Bousema and Drakeley, 2011.

1.3. Antimalarial drugs

1.3.1. Quinolines

Quinolines are the oldest class of antimalarial drugs, and quinine the first drug in this group was isolated from cinchona tree bark and has been used to treat malaria since the early 17th century, and it is currently used for the treatment of severe malaria. Reports of resistance to quinine are rare, isolated cases have been reported from Thailand and East Africa (Jenilek et al., 1995; Pukrittayakamee et al.,

1994). Its mechanism of action has not been elucidated but appears to share common characteristics with chloroquine (CQ). CQ is a synthetic antimalarial derived from quinine and has been used for the treatment and prophylaxis of malaria. CQ efficacy started declining in the 1960s with the emergence of resistant strains (Schlitzer, 2007). The resistance to CQ is now widespread and the drug is no more recommended by the WHO for the treatment of *P. falciparum* malaria. Efforts to decipher the mode of action of CQ have led to the general consensus that it interferes with detoxification of heme, a byproduct of hemoglobin proteolysis in the *Plasmodium* food vacuole. Amodiaquine (AQ) was developed in the 1960s to counteract resistance to CQ (Burrows et al., 2011). AQ is more active than CQ and currently used for the treatment of malaria in combination with artesunate (WHO, 2010a). A certain degree of cross-resistance between AQ and CQ was observed, suggesting a similar mode of action. Other quinolines including mefloquine (MQ) and piperaquine are active against CQ-resistant strains, but resistances against both have been reported (reviewed in Schlitzer, 2007), therefore, WHO recommends their use in combination with artesunate and DHA, respectively (WHO, 2010a). Halofantrine, another quinoline like MQ, is also active against CQ-resistant *Plasmodium* strains and its mechanisms of action and resistance are most probably similar to that of MQ as cross-resistance is observed between these two antimalarial agents (Hyde, 2005).

Apart of their antimalarial activity, some quinolines have been reported to have antiviral activities. CQ was reported to have an effect on the human immunodeficiency virus (HIV) replication (Savarino et al., 2001a, b), inhibiting the production of infectious viral particles by impairing virus glycosylation (Savarino et al., 2004). CQ was also reported to exhibit an additive anti-HIV 1 effect *in vitro*, when combined with zidovudine (AZT) and hydroxyurea (Boelaert et al., 2001) and a synergistic effect on HIV suppression when administered with protease inhibitors (PIs) indinavir, ritonavir, and saquinavir at concentrations achieved with prophylaxis dosing (Savarino et al., 2004). A recent *In vitro* study reported a synergistic effect on malaria parasite growth between the PIs ritonavir and saquinavir and both CQ and MQ (Skinner-Adams et al., 2007). What remains clear is that the antiretroviral effects of CQ are modest when compared with that of combination of antiretroviral therapy.

1.3.2. Antifolate antimalarials

Antifolate agents used in the treatment of malarial infection are subdivided into two classes: inhibitors of dihydropteroate synthase (DHPS), known as class I antifolates and inhibitors of dihydrofolate reductase (DHFR), known as class II antifolates. The combination of DHFR and DHPS inhibitors is synergistic, hence their use in combination in the treatment of malaria (Nzila, 2006). The principal

antifolates used against malaria are DHFR inhibitors, pyrimethamine (PYR) and proguanil (metabolized *in vivo* to the active form cycloguanil) and the DHPS inhibitors, sulfadoxine (SDX) and dapsone. The combination sulfadoxine/pyrimethamine (SP) has been used to replace CQ as a first-line treatment of *P. falciparum* malaria in many parts of Africa (Eriksen et al., 2008). The combination has the great advantage of being a single dose treatment and inexpensive. Unfortunately, resistance usually develops within few years, facilitated by the slow elimination of SDX and PYR from the body (Barnes et al., 2006). In contrast to CQ, a study showed that the antifolate antimalarial, pyrimethamine do not inhibit HIV replication but instead promotes it (Oguariri et al., 2010).

1.3.3. Artemisinin and derivatives

Artemisinin is a potent and rapidly acting blood schizontocide, active against all *Plasmodium* species. It has an unusually broad activity against asexual parasites, killing all stages from young rings to schizonts. Furthermore, the artemisinin component of the combination reduces gametocyte carriage which reduces malaria transmission by acting particularly on young gametocytes (reviewed by Kiszewski, 2011). Although a number of potential targets have been proposed the actual mechanism of action remains ambiguous (reviewed in O'neill et al., 2010). The WHO recommendations for the first-line treatment of malaria in areas of endemicity are ACTs including: a combination of artemether plus lumefantrine, artesunate plus (AQ, MQ, or SP), or DHA–piperaquine (WHO, 2010a). It was reported that the antimalarial action of artemisinin is augmented *in vitro* when administered with HIV PIs indinavir or nelfinavir (Mishra et al., 2010). The short-acting artemisinins and their long-acting counterparts are metabolized and/or inhibit/ induce cytochrome P450 enzymes, and may thus participate in adverse drug-drug interactions with multiple drugs on the market and alterations in antimalarial drug plasma concentrations may lead to either sub-optimal efficacy or drug toxicity which may compromise treatment (German and Aweeka, 2008). The benefits of ACTs are their high efficacy, fast action and the reduced likelihood of resistance development.

1.3.4. Antibiotics

The antimalarial activity of antibiotics against human malaria was first reported for chloramphenicol, chlortetracycline and oxytetracycline. However, these antibiotics exhibited a slow acting antimalarial activity requiring up to 1 week to clear malaria infection (Pradel and Schlitzer, 2010; Nzila et al., 2011). Antibiotics were not taken into consideration when CQ and quinine were very active against malaria parasites. However, with the emergence of drug resistance to CQ in the early 1970, the use of

antibiotics in malaria therapy was re-evaluated and the combination of tetracycline with faster acting drugs (e.g. quinine) was increasingly used against CQ-resistant *falciparum* malaria (Pradel and Schlitzer, 2010). Currently, The WHO recommends the use of doxycycline, tetracycline and clindamycin in antimalarial therapy, either in combination with a rapid acting schizonticide like artemisinin derivatives or quinine as a second line antimalarial treatment (WHO, 2010a). Apart from their use as antimalarials, antibiotics are co-administered in many clinical settings to treat bacterial co-infections, taking into account that bacterial infections are a major complication of malaria. In such settings, it is crucial to know whether the co-administered antibacterial agents may have an additional antimalarial effect in order to take advantage of its dual mode of action (Pradel and Schlitzer, 2010).

Furthermore, the slow acting mechanism of antibiotics has now been well understood and it is referred as “delayed death effect” (reviewed in Pradel and Schlitzer, 2010). The delayed death effect in malaria parasites is defined by the requirement for high initial drug concentrations to achieve moderate growth inhibition after 48 h, but an approximate 10-fold increased sensitivity of the pre-treated parasites towards the same or related drugs when they have entered the next asexual replication cycle. A delayed death effect is typical for antibacterials that inhibit prokaryotic translation processes and was reported for numerous antibiotics, including azithromycin, clindamycin, telithromycin, tetracycline, doxycycline, or quinupristin-dalfopristin (summarized in figure 5; Pradel and Schlitzer, 2010). Nonetheless, the ribosome-targeting antibiotic thiostrepton is an exception to this rule, since it was shown to exhibit immediate killing of the parasite together with the antibiotic ciprofloxacin, an inhibitor of apicoplast DNA replication (figure 5).

The thiazole antibiotic thiostrepton is a natural cyclic oligopeptide derived from several strains of *Streptomyces.* Thiostrepton has been reported to block translation in bacteria by binding tightly to the GTPase-associated center of the 70S ribosome (Baumann et al., 2008; Harms et al., 2008; Schoof et al., 2009). Althought thiostrepton has never been considered for clinical use in humans because of its poor solubility, it was reported to inhibit the growth of the malarial parasite *P. falciparum* by binding to the malaria apicoplast (Clough et al, 1997*;* McConkey et al., 1997; Goodman et al., 2007) and was recently shown to induce apoptosis in cancer cells (Kwok et al., 2008; Bhat et al., 2009a, b). These findings have greatly renewed interest in the therapeutic potential of thiostrepton and the suppression of parasites growth within the first 48 h of the cycle (Goodman et al., 2007) suggests an additional mode of action in *P. falciparum*.

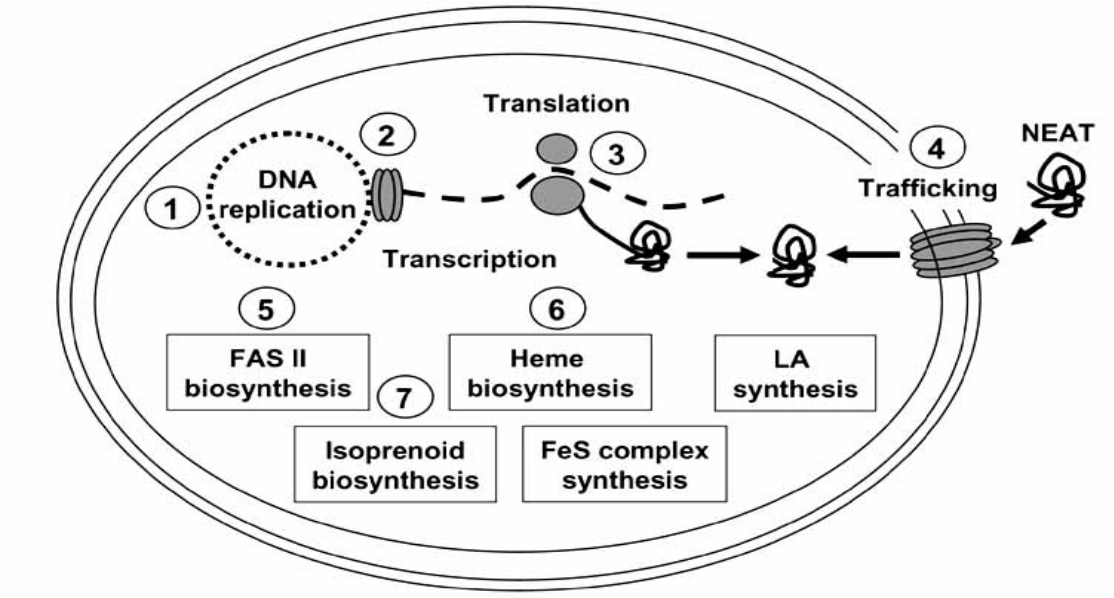

Drug	Site of action	pathway	effect	
ciprofloxacin	DNA gyrase (**1**)	replication	immediate killing (?)	[10]
rifampicin	RNA polymerase (**2**)	transcription	delayed death (?)	[9, 10, 79]
thiostrepton	LSU rRNA (**3**)	translation	immediate killing	[10, 11]
clindamycin	LSU rRNA (**3**)	translation	delayed death	[10, 79]
telithromycin	LSU rRNA (**3**)	translation	delayed death	[12]
azithromycin	LSU rRNA (**3**)	translation	delayed death	[11, 12]
chloramphenicol	LSU rRNA (**3**)	translation	delayed death	[79]
tetracycline	SSU rRNA (**3**)	translation	delayed death	[9, 10, 79]
doxycycline	SSU rRNA (**3**)	translation	delayed death	[9, 12]
quinupr.-dalfopristin	SSU rRNA (**3**)	translation	delayed death	[12]
15-DSG	HSP70 (?) (**4**)	trafficking	delayed death	[70]
thiolactomycin	Fab B/F (**5**)	FAS II	immediate killing	[82]
cerulenin	Fab B/F (**5**)	FAS II	immediate killing	[79]
triclosan	Fab I (**5**)	FAS II	immediate killing	[11, 79]
syccinyl acetone	ALAD (**6**)	heme S	immediate killing	[79]
fosmidomycin	DOXP RI (**7**)	IPS	immediate killing	[84]

Figure 5: Sites and modes of action of apicoplast-targeting drugs. Antibiotics interfere with apicoplast circular DNA replication (**1**), transcription (**2**) or translation (**3**). Other drugs target trafficking of NEAT proteins (**4**), FAS II (**5**), heme biosynthesis (**6**) or isoprenoid biosynthesis (**7**). ALAD, δ-aminolevulinic acid dehydratase; DNA, deoxyribonucleic acid; DOXP RI, 1-deoxy-Dxylulose-5-phosphate reductoiso-merase; DSG, deoxyspergualin; FAS II, fatty acid type II synthesis; HSP, heat shock protein; IPS, isoprenoid synthesis; LA, lipoic acid; LSU, large subunit, NEAT, nuclear-encoded apicoplast-targeted; RNA, riboculeic acid; SSU, small subunit**. Source: Pradel and Schlitzer, 2010.**

1.4. Malaria-HIV co-infection

Malaria treatment and control measures in endemic regions are further undermined by the co-prevalence with HIV infection. Acquired immune deficiency syndrome (AIDS) is a disease of the human immune system caused by HIV. The disease is a major health problem in many parts of the world. In 2009, WHO estimated that 33.4 million people worldwide are living with HIV/AIDS, with 2.7 million new HIV infections per year and 2.0 million annual deaths due to AIDS (UNAIDS/WHO, 2009). Malaria and HIV/AIDS, taken together are two of the most devastating diseases of our time, especially in sub-Saharan Africa (figure 1, 6).

Given the increasing number of people becoming infected with HIV, and the omnipresence of malaria in areas where the two diseases co-exist, the prevalence of co-infections might also be on the rise. Over the past ten years, research interest on malaria-HIV/AIDS co-infection has increased and data on the effect of this co-infection on patient health, implications for treatment and control programs are accumulating. HIV infection, through immunosuppression, affects the acquisition and persistence of immune response to malaria. The highest effect of HIV infection on malaria is expected in areas with a high prevalence of HIV infection and a low occurrence of malaria because natural antimalarial immunity is not acquired, thus, resulting in a high proportion of cases in adults (reviewed in Flateau et al., 2011). HIV-infected people in areas of malaria transmission have more frequent episodes of symptomatic parasitemia (Kamya et al., 2006) and higher parasitemias than those without HIV (Whitworth et al., 2000). Additionally, HIV infected people have an increase in viremia during episodes of malaria (Hoffman et al., 1999; Kublin et al., 2005), leading to a potential increased risk of HIV transmission. Finally, it appears that malaria and HIV co-infections may work synergistically, amplifying the prevalence and intensifying both in regions where they co-exist. Therefore, innovative strategies for integrated control of both diseases are needed to improve the current situation.

The WHO recommends as the first line treatment for HIV infection, the use of a non-nucleoside reverse-transcriptase inhibitor (NNRTI) plus two nucleoside reverse-transcriptase inhibitors (NRTIs), one of which should be AZT or tenofovir (TDF). Countries are encouraged to reduce the use of stavudine (d4T) in first-line regimens because of its well-recognized toxicities. The Second-line antiretroviral therapy should consist of a ritonavir-boosted PI plus two NRTIs, one of which should be AZT or TDF, based on what was used in first-line therapy. Ritonavir-boosted atazanavir or lopinavir/ritonavir are the preferred PIs (figure 7, WHO, 2010b).

A major challenge in managing malaria and HIV co-infection might come from the risk of interactions between antimalarial and antiviral drugs which remain so far poorly understood. The ability of a drug to inhibit or induce the cytochrome P450 enzymes largely contributes to the high risk of drug interaction. The risk of interactions in previous studies has been predicted based only on the metabolism of antimalarials and anti-HIV (Khoo et al., 2005).

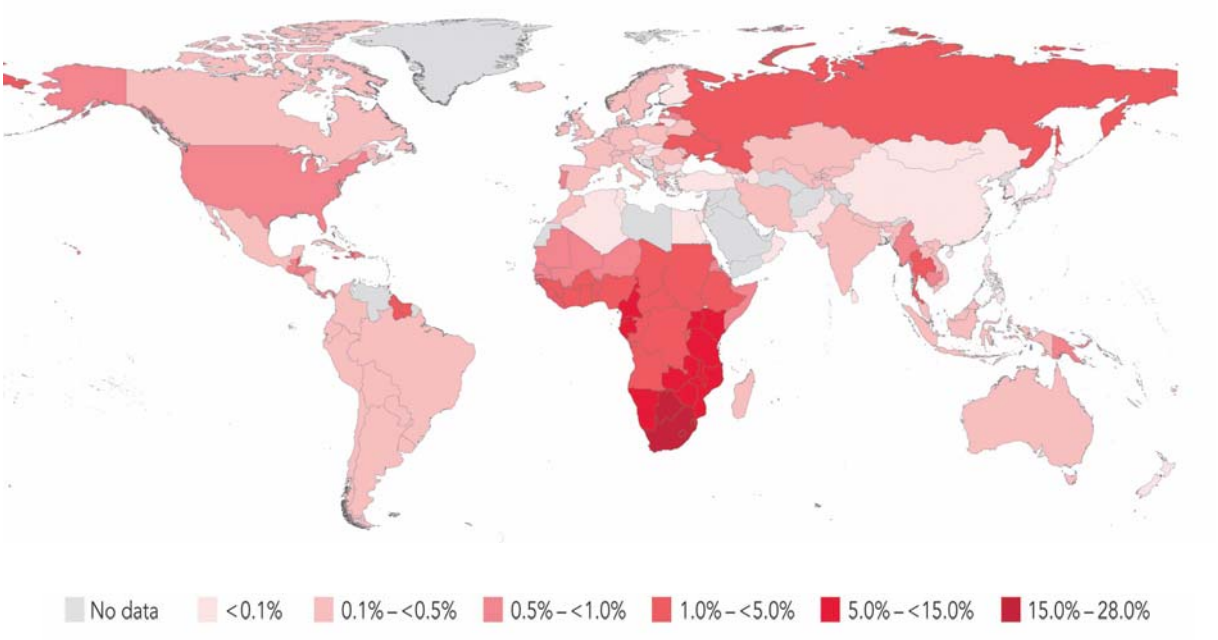

Figure 6: HIV prevalence map
Modified from: http://www.unaids.org/globalreport/HIV_prevalence_map.htm

Drug metabolism is often referred to as biotransformation, and metabolism reactions have been divided into two phases. Phase I reactions are modifications of the molecular structure by oxidation or dealkylation reactions, which occur mainly in the hepatocytes and are catalysed by enzymes called *monooxygenases*, including the cytochrome P450 family and the flavine monooxygenase (FMO) family. Phase II reactions are additions (or conjugations) of polar groups to the molecular structure. Sometimes they are considered sequential: first addition of an attachment point (e.g., hydroxyl) and then addition of a large polar moiety (e.g., glucuronic acid). However, a compound needs not to undergo a phase I reaction before a phase II reaction if it already has a functional group that is susceptible to conjugation (Kerns and Di, 2008).

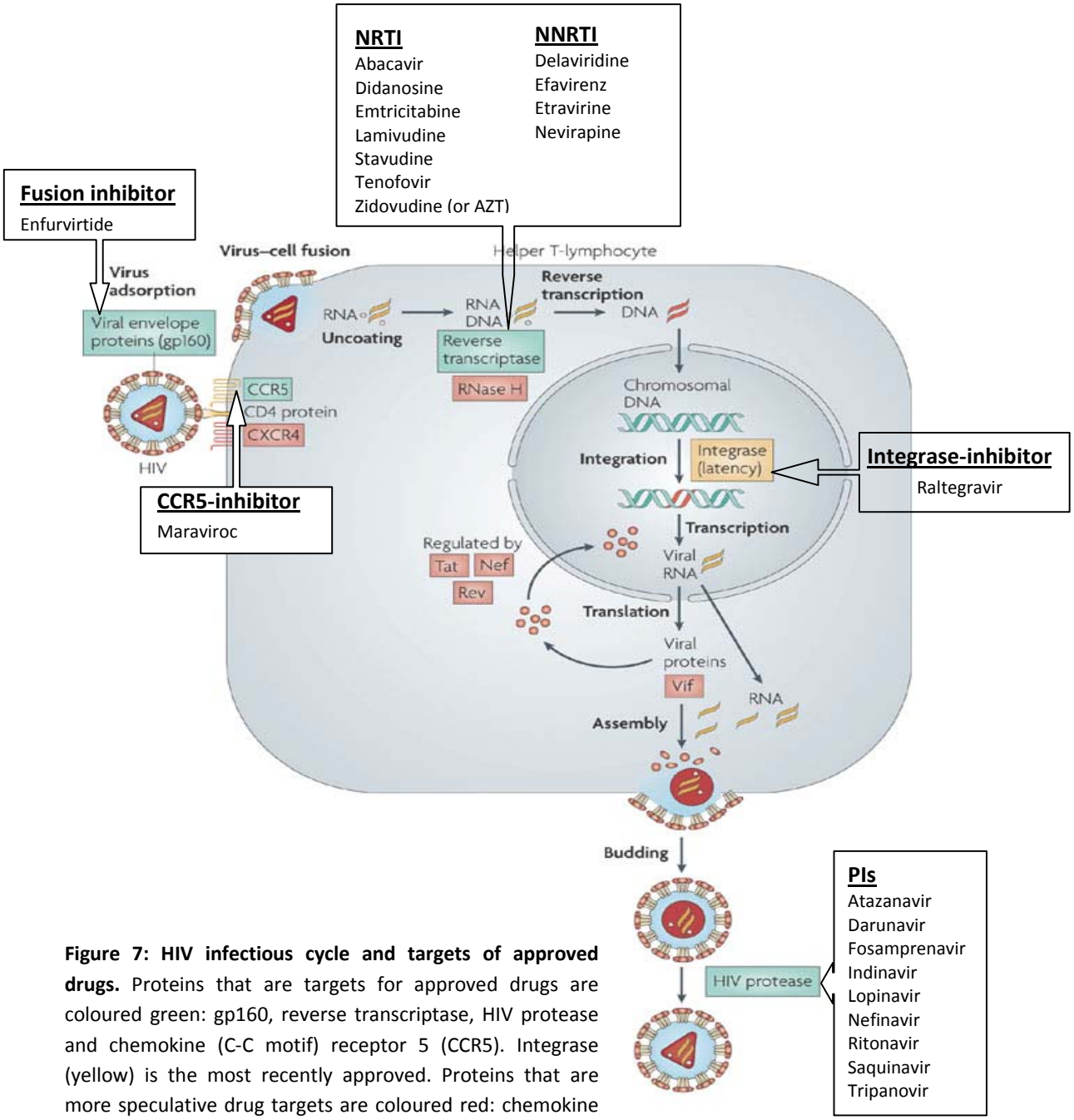

Figure 7: HIV infectious cycle and targets of approved drugs. Proteins that are targets for approved drugs are coloured green: gp160, reverse transcriptase, HIV protease and chemokine (C-C motif) receptor 5 (CCR5). Integrase (yellow) is the most recently approved. Proteins that are more speculative drug targets are coloured red: chemokine (C-X-C motif) receptor 4 (CXCR4), RNase H, tat, rev, nef and vif. FDA approved drugs used in the treatment of HIV infections were retrieved from http://www.fda.gov. **Modified from Flexner, 2007.**

Recents studies on volunteers have shed light on some clinical aspect of drug interactions. A study on 14 healthy volunteers revealed that administration of quinine plus nevirapine resulted in significant decreases in the total area under the concentration-time curve of quinine, suggesting that nevirapine significantly alters the pharmacokinetics of quinine and that an increase in the dose of quinine may be necessary when the drug is co-administered with nevirapine (Soyinka et al., 2009). In healthy volunteers, a 3-day AQ-artesunate regimen increased transaminase concentrations several weeks after treatment completion in two of five volunteers receiving efavirenz, and that was associated with large increases in the AQ area under the plasma concentration-time curve, maximum plasma concentration, and half-life (German et al., 2007). Although the information is still limited, treatment of malaria in HIV-infected patients receiving AZT or efavirenz should, if possible, avoid AQ-containing ACT regimens (WHO, 2010a). A recent study suggests that co-administration of artemisinin-lumefantrine with Lopinavir-Ritonavir can be carried out safely for patients co-infected with malaria parasites and HIV because the co-administration of lopinavir-ritonavir results in an increase in the area under the curve of lumefantrine of two to three times in healthy volunteers (German et al., 2009). The pharmacokinetics of antimalarial treatments, when co-administered with antiretroviral therapy, and the occurrence and severity of adverse events will be assessed by results from ongoing and recently completed clinical trials (www.clinicalTrial.gov; Flateau et al., 2011). A good understanding of co-infection effects on patients and the consequences on the treatment should lead to the choice of better and effective drug regimens to control mixed infections.

1.5. Antimalarial properties of anti-HIV drugs

Several peptidases of *P. falciparum*, such as plasmepsins (aspartic proteases) and falcipains (cysteine proteases), are being investigated for their potential as drug targets, both group of proteases appear to be involved in hemoglobin degradation. Antiretroviral PIs reportedly have shown effects on *Plasmodium*. Recent studies reported that antiretroviral PIs saquinavir, ritonavir, indinavir, nelfinavir, amprenavir, lopinavir, and atazanavir directly inhibit erythrocytic stages of *P. falciparum* grown *in vitro* at concentrations achieved *in vivo* (Skinner-adams et al., 2004; Parikh et al., 2005). Some antiretrovirals also seem to exert an effect on the pre-erythrocytic stages of malaria. Using the *P. berghei* model, saquinavir and lopinavir were shown to inhibit the development of extra-erythrocytic liver stages *in vitro.* Further *in vivo* studies using the rodent strain *P. yoelii* showed a reduction in liver parasite burden when lopinavir-ritonavir was administered (Hobbs et al., 2009). In the contrary, none of the 5 NRTIs is active against *P. falciparum in vitro* and only 2 NNRTIs, favirenz (22-30 µM) and etravine (3.1-3.4 µM)

showed modest activity. The fusion inhibitor enfuvirtide (6.2-7.9 µM) and entry inhibitor maraviroc (15-21 µM) also exhibit a moderate activity and raltegravir was not active. However, for all active drugs mentioned above, IC_{50}s were considerably greater than concentrations achieved with standard dosing (Nsanzabana and Rosenthal, 2011), and therefore can not eliminate the parasite. However, identifying the targets of these HIV inhibitors could lead to the discovery of new antimalarials. A new ongoing clinical trial (ClinicalTrials.gov Identifier: NCT00978068) is being carried out to evaluate HIV PIs for the prevention of malaria in Ugandan children and would certainly provide more informations on the potential of PIs as antimalarials.

1.6. Hybrid molecules

The complexicity of *P. falciparum* and the rapid emergence of resistance observed with monotherapy have prompted the WHO to implement the use of combination therapy to treat malaria, and recently fixed-dose combination (FDC) therapy where two active agents are co-formulated in a single tablet were developed to make dosing regimens simpler and thereby improve patient compliance. In contrast to FDCs, a drug hybrid is a covalent fusion of two or more existing drugs or pharmacophores to create a single molecule with multiple, but not necessarily simultaneous pharmacological targets (Corson et al., 2008). Synthesis of hybrid drugs is a relatively new concept and has shown some success in cancer therapy (reviewed in Gediya and Njar, 2009). In addition, promising hybrid antimalarials are currently under development (Walsh and Bell, 2009). Hybrid drugs can be designed using 'post hoc' or 'ad hoc' approaches. In the 'post hoc' approach, the hybrid drugs are derived from the already developed drugs. In contrast, 'ad hoc' design involves the use of lead molecules suffering from some drawback such as *in vivo* instability or lack of drug-like properties (Gediya & Njar, 2009).

Drugs or molecules used to design hybrid compounds may be incorporated based on their observed (or anticipated) synergistic or additive pharmacological activities (Guantai et al., 2010). It is also possible to exploit the active transport mechanisms of a drug by linking bioactive units to moieties that are recognized and actively transported into mammalian cells, such as amino-acids (Mishra et al., 2005) and nucleosides (Griffith et al., 1996). Like with FDCs, hybrid drugs are predicted to reduce the rate of resistances and improve patient compliance. Ultimately, no matter how familiar the building blocks may be, hybrid compounds may, at their core, become new molecules with identities independent of their precursors (Saadeh et al., 2009). Several hybrid molecules against malaria parasites have been developed. For example, the synergy between fast-acting artemisinin and slow-acting quinine has been exploited to generate a hybrid potent against a resistant and a sensitive strain of *P. falciparum* with an

activity higher than either drug alone or both drugs together in a 1:1 mixture (Walsh et al., 2007). Other artemisinin based hybrids have been described: Trioxaquines (Dechy-cabaret et al., 2000; Coslédan et al., 2008), trioxolaquine (Muregi & Ishih, 2010) trioxaferoquines (Bellot et al., 2010) and most recently a new class of hybrid called mannoxanes with outstanding oral activity profile and a potential dual mechanism has been described (Chadwick et al., 2011). A related approach is now being developed to generate anti-HIV hybrid drugs to target the virus reverse transcriptase and integrase (Wang et al., 2007; Wang and Vince, 2008a, b; Tang et al., 2011a, b).

Compared with combinations of drugs, multitarget ligands or hybrid molecules have more predictable pharmacokinetic (PK) and pharmacodynamic (PD) relationships as a consequence of the administration of a single drug (Morphy et al., 2004). However a hybrid will usually be a 1:1 fixed ratio, and may confer superior or inferior activity and safety (Walsh and Bell, 2009). The synthesis of hybrid molecules to target HIV and *P. falciparum* simultaneously has not been reported; however the intrinsic anti-HIV activity of some antimalarials and the antimalarial activity of HIV PIs already reported could be exploited within this concept.

1.7. The eukaryotic proteasome

Proteasomes are highly conserved multimeric protein complexes that are essential in all eukaryotes. Their main function is the proteolysis and recycling of nonfunctional proteins, which are tagged for degradation by polyubiquitin tails (Etlinger and Goldberg, 1977) or processing of antigens for presentation by the MHC class I pathway in eukaryotic cells (reviewed in Kloetzel, 2001). Proteasomes localize to both the cell nucleus and the cytoplasm where they are involved in a variety of cellular processes having high protein turnover rates, such as cell cycle control, stress response, and apoptosis (Peters et al., 1994). Degradation of a protein via the ubiquitin-proteasome system (UPS) involves two discrete and successive steps (figure 8). The protein substrate is first tagged by covalent attachment of multiple ubiquitin molecules. The tagging reaction is catalyzed by enzymes called ubiquitin ligases. Once a protein is tagged with a single ubiquitin molecule, this is a signal to other ligases to attach additional ubiquitin molecules. The result is a polyubiquitin chain that is bound by the 26S proteasome complex, allowing it to degrade the tagged protein. The degradion of these proteins is followed by subsequent release of free and reusable ubiquitin. This last process is mediated by deubiquitinating enzymes (DUBs; Glickman and Ciechanover, 2002). The eukaryotic proteasome has long been explored as an anti-cancer drug target (reviewed in Kisselev and Goldberg, 2001), based upon the observation

that proteasome inhibition can induce apoptosis preferentially in cancer cells. In 2003, the proteasome inhibitor bortezomib (Velcade®, PS-341) was the first approved by the U. S. Food and Drug Administration (F.D.A) for the treatment of multiple myeloma (Kane *et al.*, 2003). Since then, a stream of new proteasome inhibitors have been pursued in clinical trials (reviewed in Orlowski and Kuhn, 2008; de Bettignies and Coux, 2010).

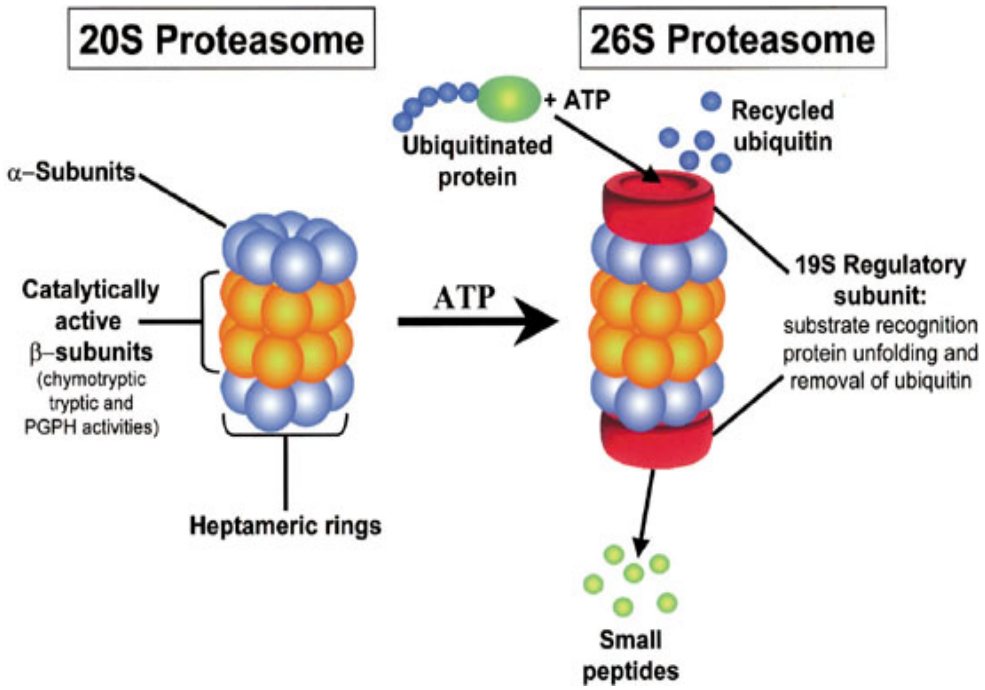

Figure 8. The UPS of eukaryotes. Protein substrates are first conjugated to multiple molecules of ubiquitin. The ubiquitinated substrate is rapidly degraded by the 26S proteasome, which is an ATP-dependent complex containing the core 20S proteasome together with two 19S regulatory subunits. **Source: Almond and Cohen, 2002**

The proteasome consists of a 19S regulatory particle (RP), involved in an ATP-dependent recognition, binding and unfolding of ubiquitinated proteins, and a proteolytic barrel-like 20S core particle (CP), which is important for proteolysis (figure 8). The CP is formed by four staged heptameric rings, i.e. two outer rings, consisting of seven α-SUs per ring, and two inner rings composed of seven β-SUs each. Substrate peptide bonds are hydrolysed by N-terminal active site threonine residues, which are embedded in the core of the CP's beta subunits (β-SUs; figure 8). Three of the seven different β-SUs are proteolytically active, namely β1, β2 and β5, displaying caspase-, trypsin-, and chymotrypsin-like

activities, respectively (Arendt and Hochstrasser, 1997; Heinemeyer *et al.*, 1997). The CP can associate with one or two of the 19S RPs. The RP recognize the ubiquitinated protein, assists in deubiquitination and unfolds the substrate, which is subsequently translocated into the CP cavity. The RP is divided into two sub-complexes, the base and the lid (reviewed in Bedford *et al*., 2010; Gallastegui and Groll, 2010).

1.8. The proteasome of malaria parasite as a target for chemotherapy

Several studies have revealed an essential role of the proteasome for the liver and blood stages of *P. falciparum* (table 1) depicting the proteasome as a promising multi-stage target in malaria therapy.

Table 1. The antimalarial effect of selected proteasome inhibitors.

	Liver stages (100% inhibition)	Blood stages (IC_{50})	Gametocytes (100% elimination)	Transmission (100% reduction)
		[μM]		
Bortezomib	n.d.	0.03-0.56[c,d]	n.d.	n.d.
Epoxomicin	n.d.	0.002[d,]	0.03[f]	0.1[f]
Lactacystin	9.0[a]	1.2-1.5[a]	n.d.	n.d.
MG-132	n.d.	0.04[e]	n.d	n.d.
MLN273	1.0[b]	0.04[b]	n.d.	n.d.
Salinosporamide A	n.d.	0.01[e]	n.d.	n.d.

n.d., not determined. [a]Gantt et *al.*, 1998; [b]Lindenthal *et al.*, 2005; [c]Reynolds *et al.,* 2007; [d]Kreidenweiss *et al.*, 2008; [e]Prudhomme et *al*., 2008; [f]Czesny *et al*., 2009.

In addition, several proteins involved in the UPS were identified in *P. falciparum*. The presence of a poly-ubiquitin encoding gene (*pfpUb*) was first reported in *P. falciparum* (Horrocks and Newbold, 2000). Later on, studies on the transcriptome of the intraerythrocytic development cycle of *P. falciparum* revealed the expression of seven α and six β subunits of the 20S CP and 16 ORFs of the 19S RP (Bozdech et al., 2003) while blast search revealed the presence of all the fourtheen subunits of the 20 S CP (Mordmüller et al., 2006). In *P. falciparum*, 8 putative E1-like enzymes, 14 putative E2-like enzymes and 54 putative E3 ligases were identified (Ponts et *al.*, 2008, reviewed in Chung and Le Roch, 2010). The *P. falciparum* genome also encodes DUBs and two independent studies identified 18 and 29 DUBs, respectively (Ponder and Bogyo, 2007; Ponts *et al.*, 2008). Due to their intrinsic protease activity, plasmodial DUBs might represent excellent targets for antimalarial drug discovery. Parasite cysteine proteases have been of interest due to their involvement in hemoglobin degradation (reviewed in

Rosenthal, 2011). However, only limited information is available on the function of the UPS in malaria parasites.

In addition to homologs of eukaryotic proteasome proteins, a predicted bacteria-like proteasomal predecessor was identified with similarity to ClpQ/hsIV threonine peptidase of *Escherichia coli*, which was termed PfhslV (Mordmüller et al., 2006). The threonine peptidase forms the CP equivalent of a primordial proteasome, comprising two hexameric PfhslV domains, and associates with one hexameric ring of the ATPase HslU, which resembles the RP base. Interestingly, in *P. falciparum*, a HsIU homolog, PfhsIU (PFI0355c), was recently identified and shown to interact with PfhsIV (Subramaniam et al., 2009). PfhsIV was originally described to localize to the cytoplasm of blood stage parasites, where it is proteolytically active, exhibiting threonine protease, chymotrypsin-like and peptidyl glutamyl peptide hydrolase activities (Ramasamy et al., 2007). A follow-up study assigned the nucleus encoded PfhsIV to the mitochondrion, to which it is transported by an N-terminal targeting sequence (Tschan et al., 2010). The attractiveness of PfhslV as a drug target is based on the absence of a homolog in the human host (Ramasamy et al., 2007). However, it is not clear whether PfhslV is essential for the blood stages or other life cycle stages of *Plasmodium* parasites.

1.9. Objective of the study

Concerted efforts to eliminate malaria are still being undermined by the development of resistances to available drugs. In addition, malaria parasites synergize with HIV in countries where they co-exist, amplifying the rate of death in these areas. The development of new drugs or new therapeutic approaches remains the standard method to fight against HIV and malaria. In areas where HIV and malaria co-exist, a combined strategy to avoid the use of drugs that may interact when treating or preventing malaria infections in HIV infected individuals is needed.

In this study we sought to evaluate hybrid molecules with dual mode of action as a potential combination therapy to treat HIV-infected individuals while protecting against or curing them from malaria infection. For this purpose, three groups of hybrid molecules were synthesized either by linking the available antimalarials DHA and CQ, or the antimalarial under development, tetraoxane, to the anti-HIV drug AZT. We intended to evaluate the hybrid compounds for their antimalarial and anti-HIV activities and potential cytotoxic effect. The best hit candidate identified should be further characterized for its drug-like properties by evaluating the bioavailability, the *in vivo* and *in vitro* metabolism as well as the antimalarial activity *in vivo*. Informations gathered from these experiments should be exploited for hit to lead optimization strategies.

While it is important to develop new therapy to replace the artemisinin derivatives in case resistances appear, the time from lead identification to licensed drug is measured in decades. In addition, resistances have been reported for all the current counterpart drugs used in combination with artemisinin derivatives. Therefore it is important to generate inhibitors targeting new pathways to design combination therapies with increased potency. The second aim of this study was to unravel the antimalarial mechanism of action of thiostrepton and derivatives and to characterize the parasite proteasome. The antibiotic thiostrepton was previously described to act on the parasite apicoplast. Recent data, however, indicated that the 26 S proteasome is the target of thiostrepton in cancer cells. Because of the poor solubility of thiostrepton, derivatives were generated to improve the properties and the activity against the parasite. We aimed at evaluating the antimalarial properties of thiostrepton and derivatives as well as their cytotoxicity.

Further investigations of the effect of thiostrepton and derivatives on the parasite proteasome should be performed by visualizing the accumulation of ubiquitinated proteins using Western blot analysis. Insight on the treated parasites phenotype could be obtained by microscopic observation and quantification of parasite treated with these inhibitors. Furthermore, the localization and function of the parasite proteasome should be investigated. Stage-specific expression and localization of selected proteasome subunits would be analyzed by diagnostic RT-PCR, Western blot as well as by immunofluorescence and immunoelectron microscopy. Characterization of these subunits would be a stepping stone in our investigation of the parasite proteasome as a potential drug target. Concomitant to the previous characterization, we further aimed to generate parasite clones expressing GFP-tagged proteasome subunits to further understand the trafficking and the subcellular localization of these proteasome subunits. Characterization of the functionality of these subunits could lay the basis for the development of new biochemical or cell based assays for the screening of plasmodial proteasome inhibitors.

2. Materials and Methods

2.1. Materials

2.1.1. Equipments

Table 2. List of equipments used in this study and their suppliers

Equipments, type	Suppliers
AccuJet® pro	Brand, Germany
Amicon® Ultra-4, Ultra-15 filter units	Millipore, Germany
Balance	Kern, Germany
BD FACSCalibur™ flow cytometer	Becton Dickinson, Germany
Bunsen burner	Schütt, Germany
Centrifuge Megafuge 1.OR	Heraeus, Germany
Chromatography column PolyPrep®	Bio-Rad, Germany
Confocal laser scanning microscope LEICA TCS SP5	LEICA, Germany
Confocal scanning microscope, LEICA TCS SP5	LEICA, Germany
Electrophoresis chamber MIDI 1, MAXI	Roth, Germany
Electrophoresis chamber mini-Protean 3	Biorad, Germany
Electrophoresis power supply	Biorad, Germany
Fluorescence microscope Axiolab HBO 50/AC	Zeiss, Germany
French® Press FA078	Heinemann, Germany
Gel documenter Gel Doc 2000	Biorad, Germany
GenePulser	Biorad, Germany
Heat Block Bio TBD-100, TBD-120	Lab-4 you, Germany
HPLC, Agilent 1200	Agilent technologies, USA
Incubator chamber	Genheimer, Germany
Incubator HERAcell	Heraeus, Germany
Incubator Model 100-800	Memmert, Germany
Life imaging microscope LEICA AF6000	LEICA, Germany
Light microscope Leica DMLS	Leica, Germany
Light microscope Leitz Laborlux 11	Leitz, Germany
Mass spectrometer, API 3200	AB Sciex, USA
Microcentrifuge Biofuge pico	Heraeus, Germany
Micropipettes	Eppendorf and Gilson, Germany
Microscope Camera Axiocam	Zeiss, Germany
Microscope Camera MP 5000	INTAS, Germany
Mini-Rocker MR1	Lab-4you, Germany

Net micrometer	Zeiss, Germany
PCR thermocycler primus 25 advanced	Peq-Lab, Germany
Phenomenex Luna PFP (50 x 2.0 mm, 5 µm) column	Phenomenex, USA
pH-Meter inoLab	WTW, Germany
Power source PowerPac HC High curent power supply	Bio-rad, Germany
Safire^2 microplate reader	Tecan, Germany
Shaker SM 30 control	Edmund Bühler GmbH, Germany
Sonication device Sonoplus HD70	Bandelin, Germany
Spectrophotometer multiskan Ascent	Thermo Electron Corporation, Finland
Sterile bench HERAsafe	Heraeus, Germany
Transmission Electron microscope, Zeiss EM10	Zeiss,Germany
Vertical electrophoresis apparatus	Biorad, Germany
Vortexer Power mix Model L46	Labinco, Breda, Netherlands
Water bath Hecht 3185 WTE	Karl Hecht KG, Germany
Water bath Typ WB20	PD Industriegesellschaft, Germany
Western blot apparatus Mini-Trans-Blot	Biorad, Germany

2.1.2. Chemicals and disposable materials

Chemicals were purchased from the following companies:

- In Germany: AppliChem, Dianova, GE Healthcare, Amersham Bioscience, Biochrom, Invitogen, Gibco, Molecular probes, Merck/Novagen, Roth, Sigma/Fluka, Thermo Scientific, WAK Chemie, Santa Cruz Biotechnology, New Englands Biolabs.
- In USA: ATCC, Santa Cruz Biotechnology.

Disposable materials or consumables were purchased from the following companies or suppliers:

- In Germany: Laborhaus Scheller, Biozym, Schubert&Weiss, BD falcon, Biorad, Greiner, A. Hartenstein, Millipore, Roth, Sarstedt.

Miscellaneous:

- Human serum and blood from A^+ group used for cell culture was purchased from Bayerisches Rotes Kreuz (BRK), Würzburg.
- Six weeks old NMRI-female mice for immunization were obtained from Charles River laboratories, Sulzfeld.

- Gas cylinders containing a mixture of 5% O_2, 5% CO_2 in 90% N_2 used as gas supplement to *plasmodium* cultures was purchased from Westfalen AG, Münster.

2.1.3. Compounds and drugs used in the study

Hybrid compounds, AZT and DHA were provided by Prof. Kelly Chibale (Department of chemistry**,** University of Cape Town**,** South Africa). Epoxomicin, thiostrepton and thiostrepton derivatives were provided by Prof. Hans-Dieter Arndt (Friedrich-Schiller-University Jena, Germany). Ciprofloxacin and derivatives were provided by Dr. Christophe Biot (Université de Lille 1, France) and new class of antimalarials with proteasome inhibitory properties namely peptidyl sulfonyl fluorides were provided by Dr. Serena Tschan (University of Tübingen, Germany). CQ and MG132 were purchased from sigma-aldrich, bortezomib was purchased from LC Laboratories, doxycycline was purchased from invitrogen, azithromycin was purchased from LKT Laboratories, WR99210 was kindly provided by Jacobus Pharmaceutical and raltegravir was kindly provided by Merck.

2.1.4. Buffers, media and solutions

Unless specified otherwise, buffers were stored at RT.

Table 3. List of solutions, buffers and media used in this study and their compositions

Buffers, medium and solutions	Ingredients, concentrations
1 M Tris-HCl pH7.5	120 g Tris, dissolve in 1l dH_2O, adjust pH to 7.5
10 % Ammonium peroxo-sulphate (APS)	10 g APS , dissolve in 100 ml dH_2O, store at 4°C
10 % Triton-X100	5 ml of 100% Triton X-100, dissolve in 50 ml dH_2O, store at 4°C
10 × Giemsa buffer	0.7 g KH_2PO_4 1.0 g Na_2HPO_4 dissolve in 1l dH_2O and adjust pH to 7.2
10 × incomplete medium *	10.43 g RPMI 1640 powder 5.94 g HEPES 0.05 g Hypoxanthine dissolve in 100 ml ddH_2O
10 × Phosphate-buffered-saline (PBS)	10.6 g Na_2HPO_4 20.1 g Na_2PO_4 x 7 H_2O 85.5 g NaCl dissolve in 1l dH_2O and adjust pH to 7.4
10 × SDS-PAGE running buffer	29 g Tris 144 g Glycerol 10 g SDS dissolve in 1l dH_2O

10 × TBS	12.1 g Tris 87.3 g NaCl dissolve in 1l dH_2O, adjust pH to 7.5
10% AlbuMax II™ stock *	10 g AlbuMax II™, dissolve in 100 ml ddH_2O
10× Giemsa buffer	7 g KH_2PO_4 18.9 g $Na_2HPO_4,7H_2O$ dissolve in 1l, adjust pH to 7.2
2 × SDS-sample Buffer	12.5 ml 0.5 M Tris-Hcl, pH 6.8 10 ml Glycerol (100%) 20 ml 10 % SDS 2.5 ml 0.1% Bromophenol blue Add dH_2O to 50 ml , store at 4°C
4% Paraformaldehyde (PFA)	4 g paraformaldehyde 90 ml dH_2O Boiled the solution to 60°C, add 2 drops of NaOH 1M to dissolve the PFA. Add 10 ml 10 x PBS. Adjust pH to 7.2, filter and place on ice. Protect from light with aluminium foil.
5% Sorbitol*	2.5 g sorbitol, dissolve in 50 ml of incomplete medium and store at 4°C
50 × TAE	242 g Tris 57.1 ml acetic acid 100 ml 0.5 M EDTA (pH 8.0) dissolve in 1l dH_2O and adjust pH to 7.5
A^+ Medium	To 500 ml RPMI 1640 (Gibco) add: 50 ml inactivated A^+ serum 550 µl Gentamycin solution 550 µl 1000 x Hypoxanthine stock
AlbuMax II™ medium	To 500 ml RPMI 1640 (Gibco), add: 25 ml 10 % AlbuMax II™ 525 µl Gentamycin solution 525 µl 1000 x Hypoxanthine stock
Ampicillin stock (100 mg/ml)	10 g of Ampicillin, dissolve in 100ml dH_2O
Blocking buffer (Immunofluorescence assay)	2 ml of 2% saponin 2 g BSA dissolve in 400 ml 1 x PBS
Cytomix buffer	2.98 g HEPES 4.47 g KCl 150 µl 0.5 M $CaCl_2$ 2 ml 0.5M EGTA 0.51 g $MgCl_2$ 0.435g K_2HPO_4 0.34 g KH_2PO_4 dissolve in 500 ml dH_2O , adjust pH to 7.6 and store at 4°C

DEPC water	Dissolve 1 g of DEPC in 1l dH_2O leave overnight with stirring at RT, then autoclave
Detergent buffer (inclusion bodies isolation)	2.42g Tris 4 ml 0.5M EDTA, pH 8.0 11.7 g NaCl 10 g deoxycholic acid 10 ml Nonidet P-40 dissolve in 1l dH_2O and adjust pH to 7.5
DMEM complete medium	To 500 ml Dulbecco's MEM (Gibco), add: 5 ml Streptomycin/Penicillin 50 ml inactivated Fetal calf serum
Elution buffer (GST-tagged protein purification)	50 ml 1 M Tris-HCl (pH 8.0) 3.07 g reduced glutathione (GSH) dissolve in 1l dH_2O. Store aliquots at -20°C
Epon	30 ml Epoxy embedding medium 24 ml DDSA (2-Dodecenylsuccinic anhydride) 21 ml MNA (Methylnadic anhydride) 1.5 ml accelerator homogenize and prepare 10 ml aliquots, store at -20°C
Equilibration buffer	12.1 g Tris 5.8 g NaCl 10.2 g $MgCl_2$ dissolve in 1l dH_2O and adjust pH at 9.5
Giemsa staining solution	3.5 ml Giemsa solution (Roth) dissolve in 70 ml 0.5 x Giemsa buffer
Glycerolytes 57	26.66 g Sodium lactate 570 g Glycerol 300 mg KCl 517 mg Na_2PO_4,H_2O (Monobasic sodium phosphate) 1242 mg (dibasic Sodium Phosphate) add ddH_2O to nearly 1000 ml, adjust pH to 6.8 with HPO_4 and adjust volume to 1 l. Store at 4°C
Luria Bertani-agar medium	10 g Tryptone 5 g Yeast extract 5 g NaCl 12 g Agar dissolve in 1l dH_2O and autoclave
Luria-Bertani (LB) medium	10 g Tryptone 5 g Yeast extract 5 g NaCl dissolve in 1l dH_2O and autoclave
Lysis buffer (protein purification)	20 ml 50 mM Tris-HCl/10 % Glycerol pH 8.0 1.4 ml 5 M NaCl 216 µl 1M Imidazol

	216 µl 20% (v/v) IGEPAL 20 µl β-mercaptoethanol
Lysis buffer (inclusion bodies isolation)	6.1 g Tris 2.5 g Sucrose 2 ml 0.5 M EDTA , pH 8.0 dissolve in 1l dH_2O and adjust pH to 8.0
Lysis buffer (infectivity assay)	5 ml of 10 % triton X-100 was diluted in 495 ml 20 mM HEPES (pH 7.4). Mix the solution and store at 4°C. Before use, DTT was added at a final concentration of 1 mM from a 1M DTT.
Lysis buffer (preparation of cell lysate)	20 µl 1M Tris-HCl pH 8.0 20 µl 0.5 M EDTA, pH 8.0, 80 µl 5 M NaCl, 10 µl 1M PSMF, 10 µl 1M β-glycerophosphate, 10 µl 1M NaF, 5 µl 1x PIs cocktail 25 µl 10 % triton X-100 dissolve in 1ml dH_2O, prepare fresh prior to lysis
Lysozyme solution	Dissolve 10 mg lyzozyme in 1 ml ddH20 prior to lysis
Ketamin/Xylazin	To 1000 µl 10% Ketamin (dissolved in H_2O), add 150 µl 2% Xylazin (dissolved in methanol)
Malstat reagent	1 ml 10% Triton X-100 1 g L (+) Lactate 0.33 g Tris 0.033 g 3-Acetylpyrimidin-adenine dinucleotide (3-APAD) dissolve in 100 ml dH_2O and adjust pH to 9
SOC medium	20 g Tryptone 5 g Yeast Extract 2ml of 5M NaCl. 2.5 ml of 1M KCl. 10 ml of 1M $MgCl_2$ 10 ml of 1M $MgSO_4$ 20 ml of 1M glucose dissolve in 1l dH_2O and autoclave
Solubilization Solution (MTT assay)	45ml Isopropanol 5 ml 10% Triton X-100 1 drop 37% HCl (12M)
Stop buffer (Western blot)	1.2 g 0.4 g EDTA dissolve in 1l dH_2O, adjust pH to 8
TBST buffer solution	990 ml 1x TBS 10 ml 10% Tween 20
TE buffer	10 ml 1M Tris-Cl pH 7.5

	2 ml 0.5 M EDTA (pH 8.0)
Transfer buffer	3.03 g Tris 14.4 g Glycerin 200 ml Methanol dissolve in 1l dH_2O
Trypan blue	0.4 g Trypan blue 80 ml 1 × PBS bring to a slow boil, cool to RT add PBS 100 ml
Washing buffer (inclusion bodies isolation)	5 ml 100% Triton X-100 2 ml 0.5M EDTA dissolve in 1 l dH_2O
Xanthurenic acid 1 mM	Dissolve 0.05 g of xanthurenic acid in 2 ml of 0.5 M NH_4OH Add 243 ml of dH_2O, store at 4°C
X-Gal staining solution	1 ml X-Gal stock 5 ml 100 mM $K_4Fe(CN)_6$ 5 ml 100 mM $K_3Fe(CN)_6$ add wash buffer to 25 ml and use immediately
Wash buffer (X-gal staining solution)	19 mg $MgCl_2$ dissolve in 100 ml mixture of: 5.3 ml 100 mM NaH_2PO_4 + 94.7 ml 100 mM Na_2HPO_4
X-Gal stock (25mg/ml)	Dissolve 250 mg of X-Gal in 10 ml N, N-Dimethylformamide, vortex and protect from light with aluminium foil. Store at 4°C.
1000 × Hypoxanthin stock (0.4M) *	0.5 g hypoxanthin dissolve in 100 ml ddH_2O

*solutions were sterile filtered either using syringe filter (0.22µm) or via bottle-top filter (Millipore) before use.

2.1.5. Enzymes and commercial kits

Table 4. List of commercial kits used in this study and their suppliers

Enzymes and Kits	Suppliers
Epoxy Embedding Medium Kit	Fluka
NucleoBond® Xtra Midi	Machery-Nagel
nucleospin® Plasmid quick pure	Machery-Nagel
QIAamp Blood Mini kit	Qiagen
QIAprep® Spin Miniprep Kit	Qiagen
QIAquick PCR purification kit	Qiagen
Superscript™ First Strand Synthesis System for RT-PCR	Invitrogen
Restriction endonucleases and buffers	New England Biolabs
PHUSION polymerase and buffer	New England Biolabs
GOTaq polymerase and buffer	New England Biolabs
T4-DNA-ligase and buffer	New England Biolabs

2.1.6. Antibodies and antisera

Table 5. List of antibodies used in this study and their suppliers

Antibodies	Type	Origin	Working dilution		Suppliers
			Western Blot	IFA	
Anti-alpha tubillin	primary	mouse	/	1:500	Sigma
Anti-GFP	primary	rabbit	1:500	/	Santa Cruz
Anti-mouse, Alexa Fluor® 488	secondary	Goat	/	1:1000	Molecular Probes
Anti-MSP-1	primary	rabbit	/	1:500	ATCC
Anti-Pf39	primary	Mouse	1:500	/	AG Pradel
Anti-pfhslv	primary	Mouse	1:50	1:50	In this study
Anti-rabbit, AlexaFluor® 594	secondary	Goat	/	1:1000	Molecular Probes
Anti-ubiquitin (P4D1)	primary	mouse	1:500	/	Santa Cruz
Anti-α5-SU	primary	Mouse	1:100	1:50	In this study
Anti-β5- SU	primary	Mouse	1:50	1:20	In this study
Neutral goat serum	blocking	Goat	1%	/	Sigma
Neutral mouse serum	control	Mouse	same as tested antibody	Same as tested antibody	AG Pradel

2.1.7. Plasmids

psPAX2: (http://www.addgene.org/12260/)

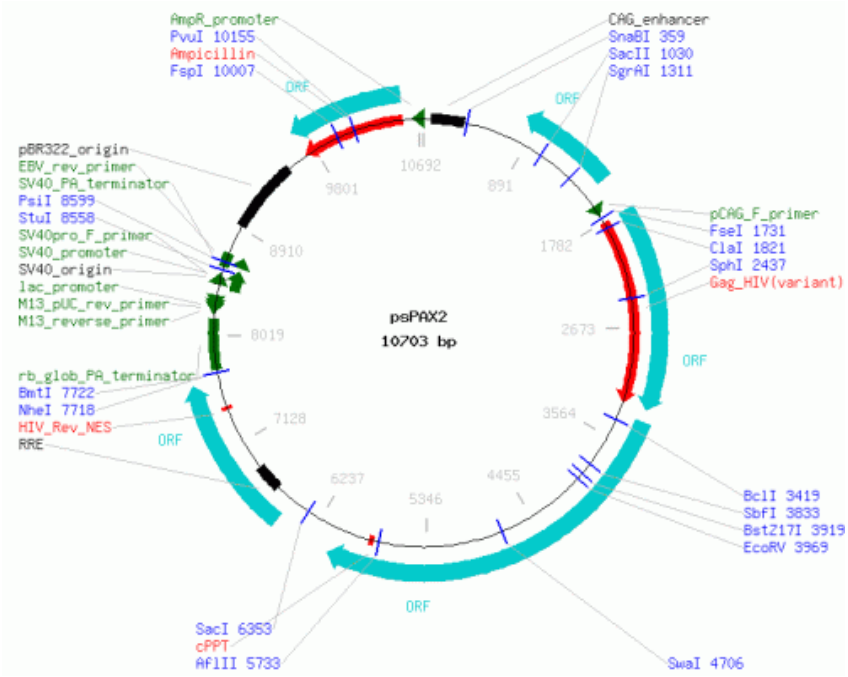

pMD2.G : (http://www.addgene.org/12259)

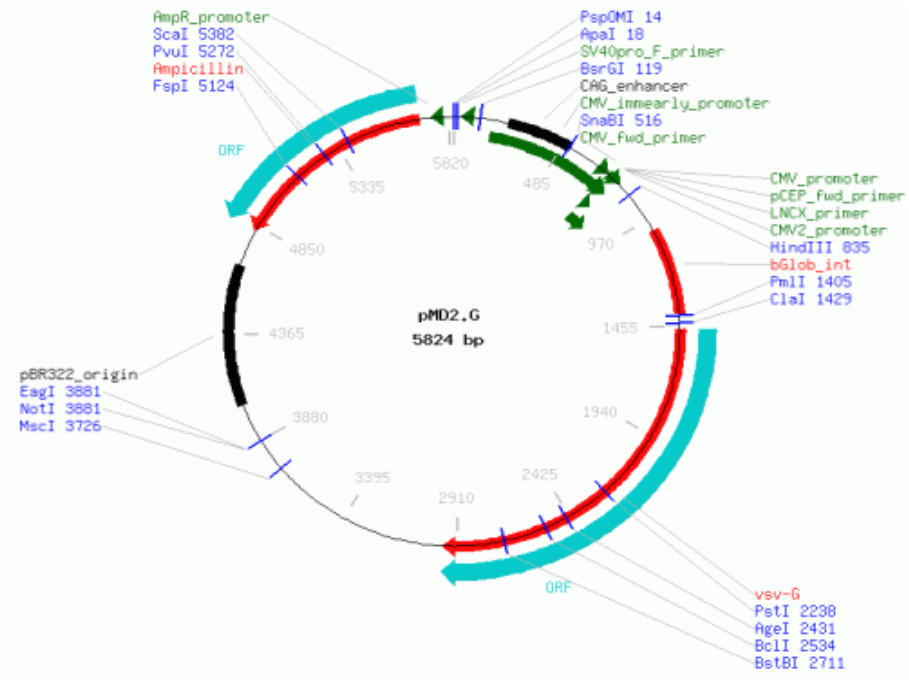

pWPXL: (http://www.addgene.org/12257)

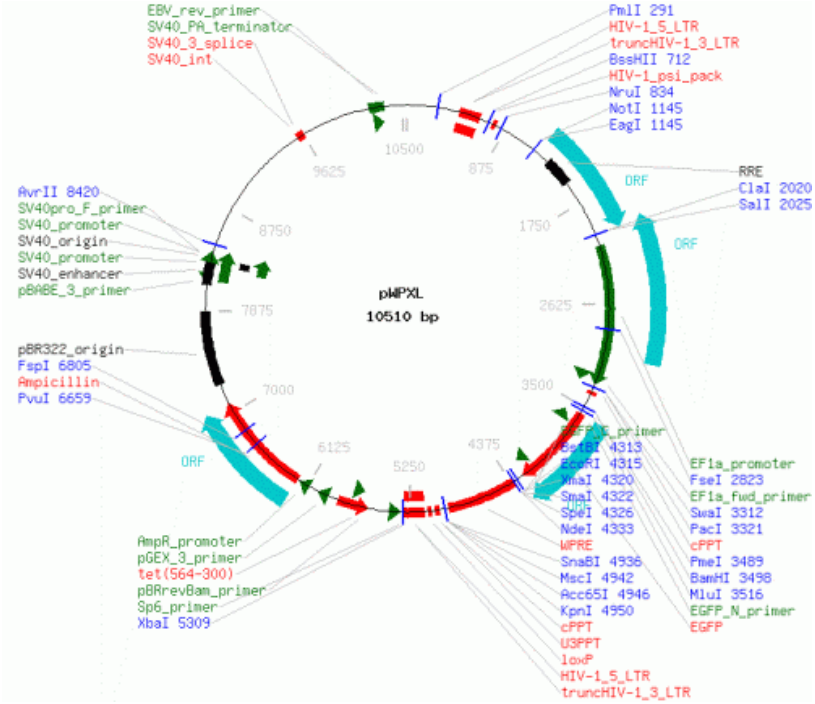

pARL2-GFP:

(https://www.lablife.org/lab?a=shared_view&oid=g1764.e8a00d4fa783a183e0149cbde5b271ab9c87fee5)

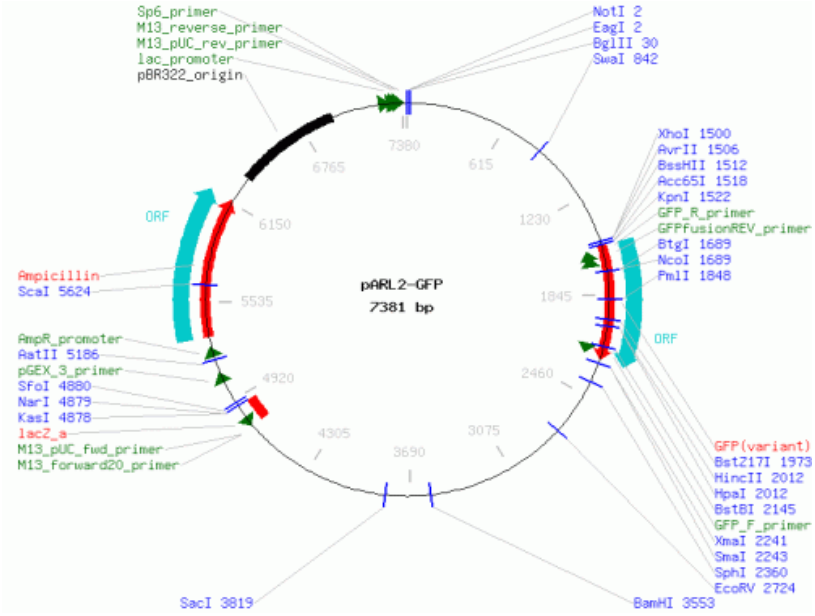

pGEX-4T1: (http://www.biovisualtech.com/bvplasmid/pGEX-4T-1.htm)

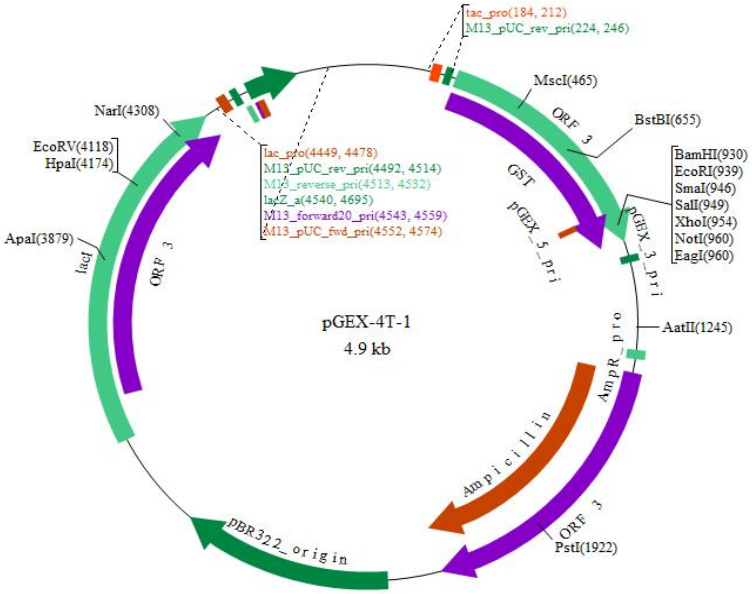

2.1.8. Oligonucleotides

Table 6. List of primers used in this study and their annealing temperature

Application	Names	5'→ 3' sequence	Annealing temperature (°C)
Episomal expression	α-SU EP AS	5'-ATGGTACCTGCTGTCATGTCT-3'	40
Episomal expression	α-SU EP S	5'-ATCTCGAGATGTTTTCAACAAG-3'	
Episomal expression	β-SU EP AS	5'-ATGGTACCCATAACATATTGATC-3'	40
Episomal expression	β-SU EP S	5'-ATCTCGAGATGGTAATAGCAA-3'	
Recombinant protein	β-SUrp1 AS	5'-TAGCGGCCGCTCACATAACATATTG-3'	42
Recombinant protein	β-SUrp1 S	5'-TAGGATCCATGGTAATAGCAAG-3	
Recombinant protein	α-SUrp1 AS	5'-TAGCGGCCGCCTATGCTGTCATG-3'	42
Recombinant protein	α-SUrp1 S	5'-GCAGGATCCATGTTTTCAACAAG-3'	
Recombinant protein	Pfhslv AS	5'-TAGCGGCCGCATTACAATGTTTCACAAATA-3'	40
Recombinant protein	Pfhslv S	5'-TAGGATCCATGTTTATCAGAAACTTTG-3'	
RT PCR	PfCCP1 RT3 S	5'-CTGGTATGGACCATTATGTTGGG-3'	50
RT PCR	PfCCP1 RT3 AS	5'-CGAAATTACAGAAGAATCAACACCATG-3'	
RT PCR	PfAMA-1 AS	5´-GATCATACTAGCGTTCTT-3´	42
RT PCR	PfAMA-1 S	5´-GGATTATGGGTCGATGGA-3´	
RT PCR	α-SU type 5 AS	5´-GAT TACACTCGACTCTTG-3´	35
RT PCR	α-SU type 5 S	5´-AGTTGAATATGCCTTAGG-3´	
RT PCR	β-SU type 5 AS	5´-CTAGCTGCACGTACTGAT-3´.	42
RT PCR	β-SU type 5 S	5´-TTGCAGTAGATTCCCGAG-3´	
Sequencing	pARL2GFP AS	5'-TTGTGCCCATTAACATCACC-3'	Seqlab
Sequencing	pARL2GFP S	5'-TCCGTTAATAATAAATACACGCAGTC-3'	
Sequencing	pGEX AS	5'-ACGTGACTGGGTCATGGC-3'	Seqlab
Sequencing	pGEX S	5'-TGGACCCAATGTGCCTGG-3'	

2.1.9. Bacterial, human and plasmodia cell lines

***E.coli* BL21 (DE3) RIL** : Chemically competent *E. coli* cells suitable for protein expression.

***E.Coli* Nova Blue:** Chemically competent *E.coli* cells suitable for cloning.

HeLa cells: immortal cell line used in scientific research, it is derived from cervical cancer cells taken from Henrietta Lacks, who died from her disease in 1951. HeLa cells have been routinely used for HIV studies (Garcia et al., 2009).

MT4 cells: immortalized helper/inducer T-cell clone obtained by cloning a normal T4 cell line in the presence of tumor cells derived from a patient with adult T-cell leukemia (Balzarini et al., 1989).

HEK293 T cells: cell line originally derived from human embryonic kidney cells grown in tissue culture. HEK 293 cells are very easy to grow and transfect very readily and have been widely-used in cell biology research for many years.

TZM-bl cells: HeLa-cell derivatives that express high levels of CD4 and both co-receptors CXCR4 and CCR5, and are stably transduced carrying a LTR-driven firefly luciferase as well as a LTR-driven β-galactosidase cassette. Challenging these indicator cells with HIV-1 and HIV-2 isolates results in the induction of luciferase and β-galactosidase allowing easy detection of infection and titration (Kaumanns et al., 2006).

***P. falciparum* 3D7 (MRA 102):** originally cloned from NF54 isolate (MRA-1000) by limiting dilution. Applications: Genome sequencing strain, CQ sensitive (www.mr4.org).

***P. falciparum* Dd2 (MRA 150)**: Derived from W2-Mef, which was selected from clone W2 for resistance to mefloquine. Applications: CQ-resistant (intermediate), pyrimethamine-resistant, mefloquine-resistant. (www.mr4.org).

***P. falciparum* NF54 (MRA-1000):** NF54 derived from patient isolate near Schipol Airport, Amsterdam; parasite presumed of West African origin (Delemarre BJM & Van der Kaay HJ, Ned. T. Geneesk 123(1979). Applications: Gametocyte and mosquito stages, vaccine studies, drug studies (www.mr4.org).

***P. berghei* N (CQ sensitive):** Rodent malaria parasite isolated from *Grammomys surdaster* caught in forest gallery River Kisanga, near Lubumbashi by Vincke and Lips (1948). (source: http://ebookbrowse.com/p-berghei-isolates-clones-pdf-d700308)

2.1.10. Genes investigated in the study

Table 7. The following gene identifiers are assigned to the proteins investigated in this study. Gene Ids and names were retrieved from plasmoDB website (www.plasmodb.org).

Gene IDs	Gene name
PF07_0112	Proteasome alpha5 sub-unit
PF10_0111	20S proteasome beta subunit, putative
PF11_0098	Endoplasmic recticulum-resident calcium binding protein (Pf 39)
PF11_0344	Apical Membrane Antigen 1 (AMA1)
PF14_0723	LCCL domain-containing protein (PfCCP1)
PFL1465C	Heat shock protein hslV
PF10_0075	Transcription factor with AP2 domain(s), putative

2.2. Methods

2.2.1. Cell biology methods

2.2.1.1. Compounds stock solution preparation

Compounds were dissolved in DMSO or dH_2O at a final concentration of 20 mM and stored at - 20°C in several aliquots of 10-20 µl to reduce freeze-thaw cycles. For all our assays, serial dilutions were first prepared in DMSO, then in medium to achieve the required concentrations. The final DMSO concentration in our assay was 0.5 % for Malstat assays and 1% for HIV infectivity, MTT assays, exflagellation and gametocytes toxicity assays.

2.2.1.2. Cultivation and maintenance of human cell lines

a. Thawing cells

To start a fresh culture from a stock, cryotubes were retrieved from the liquid nitrogen tank and immediately placed in a water bath set at 37°C until the ice melted. Then the cell suspension was immediately transferred into a 15 ml falcon tube containing 10 ml pre-warmed DMEM. To wash away

the cytotoxic DMSO, cells were centrifuged at 800 g for 5min at RT, resuspended in fresh medium and seeded into a 75 cm^2 cell culture flask.

b. Passaging cells

Human cells were passaged every 2-3 days, preferably when the cells reached 80-90 % confluence. Before starting, DMEM and Trypsin/EDTA were warmed to 37°C in the water bath. To passage cells, old medium was aspirated from the flask and adherent cells were washed twice with 10 ml PBS, afterwards 1 ml Trypsin/EDTA solution was added to detach cells from the flask. Cells were incubated and monitored for 1-5 min at 37°C until detachment was observed. A long 2 ml pipette was then used to gently resuspend cells and break down cell clumps. About 10 ml of fresh medium was added and cells were resuspended and transferred to a 15 ml centrifuge tube. An aliquot of the suspension was diluted 10 times with fresh medium to achieve a confluence of about 10% and transferred back into the culture flask.

c. Cell counting using a Neubauer haemocytometer

Cell counting was performed when seeding cells for transfection, infectivity assay or MTT assay. The number of cells in a suspension was calculated by counting cells in a Neubauer haemocytometer. Ten (10) µl aliquot of cell suspension prepared as described above was mixed with 10 µl trypan blue to count viable cells. Non-viable cells were stained blue while viable cells were not. The mixture was used to fill one side of the haemocytometer chamber and viable cells were counted in each of the four corner squares of the haemocytometer omitting cells lying on the bold lines (see figure 9A, B). The mean count of viable cells per four corner squares was calculated and viable cells concentration per ml was calculated using the following formula:

C (number of cells/ml) = M ×d × 10000

C = Initial cell concentration

M = mean count of the 4 squares

d = Trypan blue dilution (always = 2, 10 µl culture + 10 µl trypan blue)

10000 = conversion factor for counting chamber

Finally, the initial volume (V) necessary to prepare the working dilution was calculated using the following formula:

$$V = \frac{C' \times V'}{C}$$ Where, C' = final concentration and V'= final volume

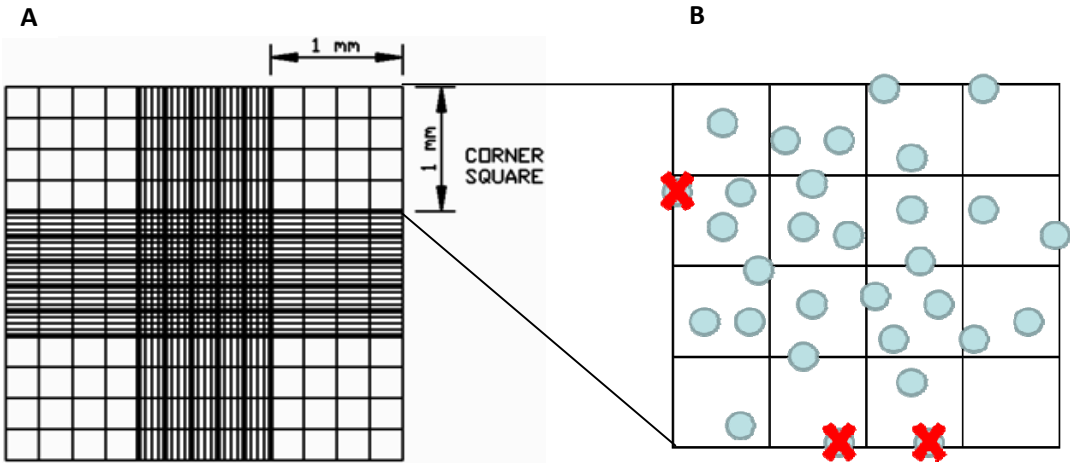

Figure 9. A) The counting grid pattern of a Neubauer chamber; **B)** illustration depicting cells counted on the square. **Source of A**: http://www.nexcelom.com/Products/DisposableHemacytometer.html

d. Freezing cells

To prepare culture stocks, adherent cells were detached and resuspended in DMEM and centrifuged at 800 g for 5 min at 4°C to pellet the cells. The cell pellet was resuspended in ice cold freezing medium DMSO/HBSS (1:9, v/v), the volume of freezing medium added was approximately 5 × the volume of the pellet; aliquots of approximately 1.5 × 10^6 cells per cryotube were prepared and frozen at -80°C. For long storage, cells were transferred into liquid nitrogen after 24 h incubation at - 80°C freezer.

2.2.1.3. Production and concentration of pseudotyped HIV-1 based lentiviral vectors

Pseudotyped HIV-1 lentiviral vectors or HIV-1 (VSV-G) were used for inhibition assays because they are safer and can be handled in biosafety level 2 laboratories. They were generated by co-transfection of 293T cells with the packaging plasmid psPAX2, the transfer vector plasmid (pWPXL) and the glycoprotein expression plasmids (pMD2.G). Twenty-four hours before transfection, 10x10^6 293T cells were seeded in 25ml DMEM into a 175 cm^2 flask and incubated at 37°C, 5% CO_2 overnight. The next day, a 2 ml plasmid DNA solution was prepared by mixing the equivalent volumes of 16 µg of pWPXL, 12 µg psPAX2 and 4.8 µg of pMD2.G in HBSS. Similarly, 2ml PEI solution at a final concentration of 1mg/ml were prepared in HBSS. Plasmids solution and PEI solution were mixed and the 4 ml resulting mixture was vigorously mixed and incubated at RT for 30 min. Before adding the transfection mixture

to cells, the old medium was replaced by 21 ml fresh DMEM and 4 ml of transfection medium was added to cells and incubated at 37°C. Eighteen to twenty hours later, expression was induced with sodium butyrate at a final concentration of 10 mM to boost the viral particle expression. Six hours after induction, the medium was replaced and incubated at 37°C overnight. After 20-24 h, medium containing lentiviral vectors was collected and stored at 4°C (first harvest) and fresh medium was added to cells. Cells were further incubated for 20-24 additional hours. Afterwards, the medium was collected (second harvest); the two harvested media containing lentiviral vectors were pooled and filtered through a 0.45 µm filter to remove cells and cell debris. The filtered supernatant was then transferred to Amicon 100000 MWCO filter tubes and centrifuged at 3500 g at 4°C for 15 min to concentrate the lentiviral vectors. The goal was to make a 10 fold concentrate viral suspension. When higher, the virus suspension was slightly diluted with HBSS to adjust the concentration. 500 µl aliquots were prepared and stored at -80°C.

2.2.1.4. Transduction of HeLa cells and titration of HIV-1 (VSV-G) suspensions

HIV-1 (VSV-G) suspensions were titrated to estimate the dilution necessary to obtain a good signal in the 96 well plates and to guide the choice of our dilution factor. For transduction, approximately 2×10^5 HeLa cells were transfered into each well of a 24 well plate, then centrifuged at 1000 g for 10 min to pellet the cells. The plate was then incubated at 37°C for about 1h. During that time, lentiviral vectors stock was diluted from 2 to 1000 times. After incubation, different concentrations of HIV-1 (VSV-G) suspension were added to HeLa cells in duplicate. After 48 h, cells were analyzed by fluorescence activated cell sorting (FACS) and the percentage of green fluorescent cells for each dilution was recorded.

2.2.1.5. Fluorescence activated cell sorting

FACS analysis was used to sort cell populations for GFP-expression. For this purpose, adherent cells were washed twice with PBS and detached by incubation with 0.5 ml Trypsin-EDTA solution per well. Approximately 1×10^5 to 5×10^5 cells in suspension were transferred into glass tubes and centrifuged at 500 g, 4°C for 10 min. The resulting supernatant was discarded and cells were resuspended in 3-5 ml PBS. The apparatus was set to analyze 2×10^4 cells per sample and the percentage of GFP labeled cells was recorded.

2.2.1.6. Inhibition assay

This assay was used to evaluate the activity of compounds against HIV-1 (VSV-G). Eighteen (18) to 24h before the assay**,** HeLa cells were counted and re-suspended in fresh medium. 100 µl of culture containing approximately 1.2×10^4 HeLa cells were seeded in a 96-well plate and incubated overnight at 37°C. The next day, two hours before the assay, the virus stock was removed from -80°C freezer and thawed on ice. During the thawing, compounds were first diluted in DMSO, then in medium. Virus stock was diluted in DMEM to prepare the working virus suspension and 90 µl were seeded in a 96-well plate. To the virus suspension, 10 µl of compound were added, the old DMEM from plate containing HeLa cells was then replaced by the viral suspension containing different concentrations of tested compounds ranging from 100 µM to 1 nM and incubated for 48 h at 37°C. After 48 h incubation, the plate was removed from the incubator and the medium containing lentiviral vectors was discarded and 100 µl ice cold PBS was added to rinse the cells. The washing step was performed twice. Afterward PBS was replaced by 110 µl of lysis buffer and one freeze-thaw cycle was performed to break cells membrane. The plate was allowed to rest at RT with gentle shaking until the cell suspension was completely thawed. Plates were then centrifuged at 800 g for 10 min at 4°C to pellet cell debris. 100 µl of supernatant was then transferred to a black plate for fluorescence measurement. Fluorescence intensity was measured using *Safire*^{2} plate reader with the following settings, Measurement mode: from the top, excitation wavelenght/bandwidth: 488 nm/10 nm, emission wavelenght/bandwidth: 509 nm/10 nm, gain (manual): 100, Temperature: RT.

2.2.1.7. Infectivity assay using infectious wild type HIV-1 virus

For the most active compound, the anti-HIV activity was evaluated on the replication of a wild type infectious virus in a biosafety level 3 laboratory. A fresh co-culture was prepared by diluting a co-culture of NL43 virus (kindly provided by the Bodem Lab, institute of Virology, University of Würzburg) with uninfected MT4 cells in a 1:10 ratio (5 ml NL43 co-culture, 5 ml MT4 culture, 40 ml RPMI culture), the co-culture was assayed in a 48 well plate at a final volume of 500 µl of diluted co-culture per well. After 4 h incubation at 37°C, 5 µl of inhibitors dissolved in DMSO were added to each well and plates were incubated for 48 h. Fourty eight (48) hours after incubation, 1×10^4 TZM cells were seeded in a 96 well plate and incubated at 37°C to allow the cells to attach at the bottom and the 48-well plate containing co-culture was centrifuged at 800 g for 10 min. One hundered (100) µl of MT4 cell-free supernatant from each concentration was used to infect TZM cells in triplicate, which enables to

determine the amount of infectious particles that have been produced in the presence of inhibitor. After 2 days post infection, cells were fixed with Aceton: Ethanol (1:1), washed three times with PBS. The infected TZM cells were further incubated with X-Gal (5-bromo-4-chloro-3-indolyl-β-D-galactopyranoside) staining solution for 2 - 4 h. After incubation, the number of blue cells in each well was counted under bright field illumination and the mean number of blue cells in each well and for each concentration was calculated.

2.2.1.8. Evaluation of compounds cytotoxicity on HeLa cells

The cytotoxicity of compounds was evaluated using MTT assay. This assay was first described by Mosmann et al., (1983). MTT (3-(4, 5-Dimethylthiazol-2-yl)-2, 5 Diphenyltetrazoliumbromid) is taken up by living cells and converted by mitochondrial dehydrogenases to a violet formazan that can not diffuse through cell membranes and crystallizes in viable cells. HeLa cells were plated in 96-well microtiter plates and incubated overnight at 37 °C. The next day, the old medium was replaced by 90 µl of fresh medium, serial dilutions of compounds were prepared in DMSO and added in corresponding wells at final concentrations ranging from 200 µM to 1 nM and the culture was further incubated for 48 h. After incubation, medium containing drugs was replaced by 100 µl fresh drug-free medium supplemented with 25 µl MTT (5 mg/ml) in each well and incubated for 3-4 h at 37 °C. After 3-4 h, a formazan precipitate was observed at the bottom of the wells where all or a fraction of cells was still viable. The MTT preparation was then removed from wells and replaced by 100 µl solubilization solution. Plates were then rotated at about 500 rpm at RT until the formazan precipitate was totally resuspended and the optical density was measured at 450 nm.

2.2.1.9. *In vitro* cultivation and maintenance of *Plasmodium* parasites cultures

a. Thawing

Cryotubes containing frozen cultures were collected from the freezer and thawed at RT. Parasite cultures were transferred into a 15 ml centrifuge tube and 200 µl of 12% NaCl solution were added drop wise. The mixture was incubated at RT for 2 min and afterwards 10 ml of a 1.6 % NaCl solution were slowly added with gentle shaking. The mixture was then centrifuged for 5 min at 800 g; the resulting supernatant was discarded and 10 ml 0.2 % Dextrose, 0.9 % NaCl solution was added drop wise. The mixture was centrifuged at 800 g for 5 min and the supernatant was discarded. The red blood cell pellet was finally resuspended in 5 ml RPMI medium and transferred to a 25 cm^2 flask.

b. Freezing

Red blood cells were resuspended in a 25 cm^2 culture flask and transferred to 15 ml centrifuge tube. The culture was centrifuged at 800 g for 5 min and the supernatant was discarded. The pellet was resuspended in glycerolyte (approximately 5× the volume of the pellet), aliquots were transferred to 2ml cryotubes and stored at -80°C until needed.

c. Blood smear preparation

To perform a blood smear, an aliquot of 100 µl of the culture was collected in a 1.5 ml eppendorf tube and centrifuged at 3500 g for 1 min at RT. About 50-70 µl of the supernatant was discarded and the pellet was resuspended. Approximately 5 µl was placed on a slide. The RBCs were smeared across the slide with the help of another slide, to get a thin film (figure 10) and the slide was dried at RT. Slides were then fixed by immersing in methanol for 30 seconds and allowed to dry. The slides were then stained with Giemsa stain for 10-15 minutes and washed with water to remove excess stain. Slides were dried and observed under the 100 × objective (under oil immersion) of a light microscope.

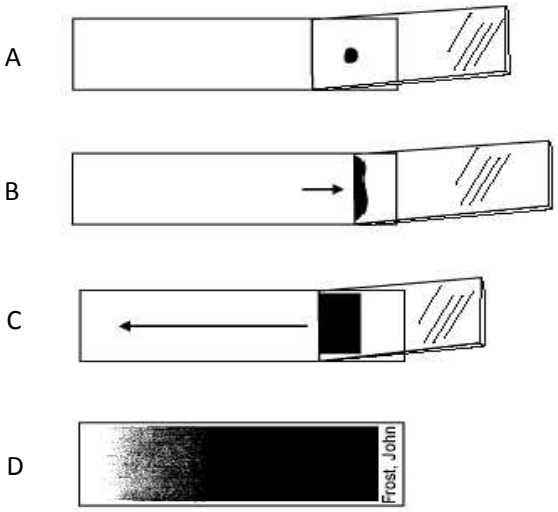

Figure 10. Making a blood smear. **A)** Placing second slide at 45 degree angle, **B)** Blood distributing itself along second slide's edge, **C)** Drawing blood across surface of slide to make the smear, **D)** Example of a properly prepared blood smear.
Modified from http://medical.tpub.com/14295/css/14295_286.htm

d. Estimation of the percentage of infected erythrocytes

Estimation of the percentage of infected erythrocytes was done prior to Malstat assays, before and after *in vivo* antimalarial activity studies and after gametocytes toxicity test. An area of stained thin blood film where the erythrocytes were evenly distributed was observed using 100 × objectives with the help of a net micrometer. Erythrocytes in a specific area were counted without moving the slide; the number of infected erythrocytes amongst the erythrocytes was also counted. The slide was moved randomly to adjacent fields and counting was continued as mentioned above. An equivalent of 500-750 erythrocytes was counted in total examination of at least five different parts of the slide. The percentage of infected RBCs (parasitemia) was estimated as following:

A = sum of infected erythrocytes

B = sum of total erythrocytes (Infected + Non-infected)

$$\text{Percent infected erythrocytes (\% parasitaemia)} = \frac{A}{B} \times 100$$

If one erythrocyte contained ≥ 2 parasites, it was still counted as one infected erythrocyte.

e. Splitting and feeding

To maintain continuous culture and avoid stress, cultures were splitted every 48 h to maintain the parasitemia lower than 3%. Parasites were either counted or estimated by looking at a good blood smear. Then an aliquot was removed from the culture and transferred to new flask containing fresh medium and fresh erythrocytes (5% haematocrit). Gametocytes were fed everyday by removing the old medium and replacing by fresh medium.

f. Synchronization of parasite cultures

Parasites where synchronized using 5% sorbitol. Initially, the culture was transferred into a 15 ml centrifuge tube and centrifuged at 800 g for 2 min to remove old medium. Then the pellet was resuspended in 5 times pellet volume of 5% sorbitol and was incubated at RT for 10 min. After incubation, the culture was centrifuged as previously and the sorbitol supernatant was discarded. The infected red blood cells were rinsed once by resuspending them in 5 ml of complete medium and centrifuging as previously. After rinsing, infected red blood cells were resuspended again in complete medium and the culture was transferred to a new 25 cm^2 culture flask and incubated at 37°C under appropriate gas mixture.

2.2.1.10. Determination of antimalarial drug susceptibility *in vitro*

Malstat assay described by Makler and others (Makler et al., 1993, Makler and Henrichs, 1993) was used to assess the *in vitro* activity of compounds on *P. falciparum* sensitive (3D7) and resistant (Dd2) strains. Non treated parasitized red blood cells were used as negative control; CQ, MG132 or DHA were used as internal control. Infected red blood cells were plated in flat-bottomed 96-well microtiter plates at ring stages, in a volume of 190 µl, 5% hematocrit and 1% parasitemia.

Compounds and controls were first diluted in DMSO then in medium to a final DMSO concentration of 10%. Compounds final concentrations ranging between 100 µM and 1nM were achieved by adding 10 µl of the above described compounds dilutions to each well. Plates were placed in a sealed jar and flushed with a gas mixture of (5% O_2, 5% CO_2, and 90% N_2); plates were incubated at 37°C for 72 h. After incubation, NBT (1mg/ml) and diaphorase (1mg/ml) were prepared and mixed at 1:1 ratio. The culture in each of the wells of the original plate was resuspended by pipetting up and down with a multichannel pipette. Thereafter, 20 µl of culture from each well was tranfered to a new 96-well microtiter plate. One hundred (100) µl of Malstat reagent was added to initiate the formation of pyruvate from parasite lactate dehydrogenase (LDH) and the release in the reaction of reduced APAD (APADH). The colorimetric reaction was initiated when 20 µl of the mixture NBT/Diaphorase solution was added to each well of the replica plate. In wells containing viable parasite, NBT and APADH reacted to form a purple coloration which absorbance was measured at 630 nm after 30 min of incubation at RT. Optical density (OD) values were generated at various concentrations of the drug as raw data. OD values from control wells represent the maximum amount of LDH that is produced by parasites. OD values were then plotted against corresponding logarithmic concentrations of the drug using GraphPad Prism (GraphPad version 5, http://www.graphpad.com/prism/prism.htm) to generate log dose–response curves from which IC_{50} values were automatically estimated by the software. For the "delayed-death" experiment, the Malstat assay was carried out as described above at 48, 72, 96, and 120 h after drug treatment with an initial parasitemia of 0.5%, and the respective IC_{50} concentrations were calculated.

2.2.1.11. Red blood cells pre-treatment

Erythrocytes pre-treatment was used to investigate the effect of compounds on the RBCs. A volume of 1 ml of uninfected spin washed erythrocytes was incubated for 3 h at 37°C in the presence of 5 µM of compounds. After incubation, erythrocytes were washed twice with incomplete medium, and rinsed

once with Albumax II medium by centrifuging cultures at 500 g for 5 min. Ring stages culture was diluted 10 × in pre-treated erythrocytes at a final concentration of 0.5% parasitemia and cultured for 72 h. Parasite viability was subsequently measured using the Malstat assay.

2.2.1.12. Gametocyte toxicity test

This test was used to evaluate the ability of a compound to inhibit gametocytes at their early stages, therefore preventing the formation of mature gametocytes which is necessary for transmission. *P. falciparum* NF54 parasites were cultured at high parasitemia to favor gametocytes commitment. Upon appearance of stage II gametocytes, 1 ml of culture was aliquoted in triplicate in a 24-well plate in the presence of compounds IC_{50} or IC_{90} concentrations. The gametocyte culture was cultivated in the presence of compounds for 48 h, medium was replaced daily. After 48 h treatment, gametocytes cultures were subsequently maintained for 5 additional days to allow healthy gametocytes to mature to stage IV and V. During these 5 additional days, 750 µl of medium was removed and replace by 800 µl fresh compound-free medium. After 7 days, Giemsa-stained blood smears were prepared and the gametocytemia was evaluated by counting the numbers of gametocyte stages IV and V in a total number of at least 500 erythrocytes.

2.2.1.13. Hemolysis test

To evaluate the effect of compounds on the RBC integrity, a volume of 1ml of spin washed uninfected erythrocytes was resuspended in regular medium at a final haematocrit of 5 % and plated in quadruplicates in a 96- well plate at a final volume of 200 µl per well in the presence of 10 µM of compounds. Medium supplemented with 0.15% saponin was used for lysis control and 0.5% DMSO was used for no lysis control. After 48 h of incubation at 37°C, the plate was centrifuged at 500 g for 2 min and a volume of 100 µl of the resulting supernatant was carefully transfered to another plate and the optical density was measured at 550 nm.

2.2.1.14. Exflagellation assay

Exflagellation of the microgametocyte in the life cycle of malarial parasites occurs in the stomach of mosquitoes following an infective blood meal. The exflagellation assay was used to evaluate compounds activity on gametes formation**.** Prior to the assay, an aliquot of 100 µl culture was collected from culture flask, activated by incubating with XA (1:10) for 15 min, then centrifuged at 3500 g. The

pellet was resuspended in about an equal volume of supernatant, and a small drop of 10 µl of this suspension was placed on a glass slide and covered with a coverslip. The number of exflagellation centers per field was counted using a light microscope at 40 x magnification. If a minimum of 5 centers were observed per field, the culture was ready for the assay. To perform the assay, two aliquots of 100 µl per compound were prepared, in the first tube, the compound was added and in the second only DMSO to a final concentration of 1% (control). The cultures were incubated for 15 min with compounds or DMSO and were immediately activated using (1:10) for another 15 min, for each compound a DMSO control was prepared. After incubation, the preparation was centrifuged and the resulting pellet was resuspended as described above and a drop was placed on the Neubauer chamber as previously described. On the first cuvette of the chamber, the compound treated preparation was added and on the second one the DMSO-treated. Exflagellation centers were counted in 16 fields. The experiment was repeated twice.

2.2.1.15. Purification of asexual blood stages

To extract DNA material or to prepare parasite lysate, RBCs were lysed to release parasites. The culture was first transferred from culture flasks to falcon tubes and centrifuged at 800 g for 5 min. The medium was then aspirated and the pellet was resuspended in 10 ml ice cold 1 x PBS to wash the red blood cells. The mixture was centrifuged again at 800 g for 5 min and the supernatant was discarded. To lyse red blood cells, pellets were resuspended in 0.15% saponin solution by gently pipetting up and down until the blood turned dark-red and incubated on ice for 10 min. When lysis was completed, the tubes were centrifuged at 3500 g for 10 min and the supernatant containing RBCs proteins were discarded. The black parasite pellet on the bottom of the tube was resuspended in PBS to wash the residual RBCs lysate, and centrifuged again at 3500 g for 10 min. Parasite pellets were directly stored at –20°C or immediately resuspended in 5 x pellet's volume of lysis buffer and incubated for 15 min on ice to obtained parasite lysate for SDS-PAGE.

2.2.1.16. Purification of gametocytes using Percoll®

Gametocytes were purified as previously described by Kariuki et al (1998). To purify DNA or parasite lysate from gametocytes, a culture containing mostly gametocyte at stages IV and V was transferred into a 50 ml falcon tube, centrifuged at 3500 g for 5 min and resuspended in 1ml incomplete medium (ICM). Percoll was diluted by addition of one volume of 10 × ICM to nine volumes of stock Percoll

solution to prepare a 90% Percoll solution. This solution was then diluted with 1 × ICM to make 80%, 65%, 50% and 35% Percoll solutions. Two milliliters (2 ml) of each of these diluted solutions were run slowly down the side of a tilted 15-ml test tube, starting with the heaviest (80%), to form the layered gradient. The 1 ml blood suspension was layed on the above gradient and the falcon tube was centrifuged for 10 min at 800 g. The interface between the first and the second layer was collected and resuspended in 5-10 ml incomplete medium to wash the red blood cells, then centrifuged at 800 g for 5 min, and the gametocyte pellet was obtained for further experiments.

2.2.1.17. Transfection of *P. falciparum*

a. Generation of plasmids

The full size of *P. falciparum* proteasome subunits α-type 5, β-type 5 were amplified using corresponding primers (see table 6) as described below and inserted into pARL-2-GFP plasmid using the restriction site Xho I and Kpn I to obtain pARL-α5-GFP and pARL-β5-GFP. Recombinant plasmids were then used to transform *E. coli* Nova blue cells and a midi preparation of the plasmids was carried out to generate enough material for the transfection of *P. falciparum* NF54.

b. Preparation of RBCs for transfection

For transfection experiments, fresh A^+ blood was collected in sodium citrate (0.106 M) into a 50 ml centrifuge tube. The collected blood was centrifuged at 800 g for 5 min at RT. Plasma and buffy coat were removed with sterile Pasteur pipette. To wash RBCs, incomplete medium was added and centrifuged at 800 g for 5 min and the supernatant was removed. The washing procedure was repeated until the entire buffy coat was removed. The resulting pellet was diluted with imcomplete medium (1:1) and stored at 4°C.

c. Transfection procedure

P. falciparum NF54 infected erythrocytes cultures were transfected with plasmids for episomal expression of proteins fused to GFP. For this purpose, parasites were synchronized and cultured in 75 cm^2 cell culture flasks to achieve a highly synchronal culture. Once parasitemia was between 5-10 % with the majority being ring stages, transfection was performed with 5 ml culture, and a control without plasmid was included. On the day of transfection, the culture medium was replaced and a blood smear was prepared. After 2 h of culture in the fresh medium, the culture was centrifuged at 500 g for 5 min and the pellet was resuspended in 400 µl of cytomix buffer containing 50-80 µg of

plasmid**.** The parasite suspension in transfection medium was transferred into a cooled Gene Pulser cuvette (0.2 cm electrode gap) and cells were electroporated using the following conditions: voltage; 0.31 KV, capacity; 975 µFD, Time constant; 10-13s (Fidock and Wellems, 1997). The electroporated infected erythrocytes were then transferred to a 25 cm^2 cell culture flask containing fresh RBCs prepared for the purpose and diluted to 5% haematocrit in 3 ml. The remaining sample was rinsed from the cuvette by washing it once with 1 ml A^+ medium and transferred to the corresponding flask. Drug selection was started 4-6 h post-transfection by replacing A^+ medium with A^+ medium supplemented with 10 nM WR99210. Twenty four (24) hours later, blood smears were prepared and parasites were cultured in medium supplemented with inhibitors. This introduces a drug pressure in which only parasites containing the plasmid with human DHFR resistance cassette would survive. As a control, parasites were electroporated only with cytomix buffer and cultured for the same length of time. The parasites disappeared in 2-3 d after transfection and about 100 µl of fresh A^+ erythrocytes was added per week until parasites reappeared. Parasites were maintained at 2% parasitemia and a stock was prepared every 4 weeks.

2.2.1.17. Indirect immunofluorescence assay

Indirect immunofluorescence assay (IFA) was used to study the localization of proteasome in *P. falciparum*. Aliquots (100 µl) of synchronized *P. falciparum* 3D7 parasite cultures at ring, trophozoite and schizont stages and non-activated NF54 gametocyte were obtained from culture flasks, centrifuged at 3500 g for 1 min and most of the supernatant was discarded. RBCs were resuspended and thin smears were carefully prepared by placing a drop of the culture in each well of the slide, the excess culture was aspirated using a pipette and the specimen was air dried. After drying, specimens were fixed for 10 min in -80°C cold methanol. Slides were incubated in blocking buffer for 30 min at RT, and further blocked in blocking buffer supplemented with neutral goat serum (1%) for another 30 min. After blocking, slides were incubated with primary antibodies diluted in blocking buffer for 2 h at 37°C. Thereafter, specimens were washed three times with 0.01% saponin in PBS and incubated with fluorochrome-coupled goat anti-mouse or anti-rabbit secondary antibodies for 1 h at 37°C. After the incubation with secondary antibodies, specimens were washed twice in PBS for 10 min. During this procedure the slides pot was protected from light. After washing, when appropriate, counterstaining of erythrocytes was performed using 0.05% Evans Blue in PBS for 1 min. The slides were rinsed twice in PBS and finally stained with Hoechst 33342 for 1 min. Specimens were mounted on a cover slip with

anti-fade mounting media. Labelled specimens were examined by confocal laser scanning microscopy using a LEICA TCS SP5 or a Zeiss Axiolab fluorescence microscope in combination with a Zeiss AxioCam ICc1 camera. Digital images were processed using Adobe Photoshop CS software.

2.2.1.18. Immunoelectron microscopy

Immunoelectron microscopy (IEM) was used to further investigate proteasome localization in asexual parasites**.** Asexual parasites of *P. falciparum* NF54 specimens embedded in LR White were prepared by Shruti Agarwal (Agarwal, 2010). Ultra thin sections of specimens were then subjected to post-embedding; sections were rinsed in PBS for 5 min and blocked with 1% BSA/0.1% Tween20 for 5 min. The sections were further incubated with primary mouse antibody anti-proteasome β5-SU (1:50) for 1h. After incubation, ultra thin sections were rinsed two times with 1% BSA/0.1% Tween20 and two times with 0.1% BSA/0.1% Tween20. After washing, sections were incubated with 12 nm gold-conjugated goat anti-mouse secondary antibodies. After incubation, sections were rinsed two times with 0.1% BSA/0.1% Tween20 and one time with PBS, then fixed in 1.25 % glutaraldehyde for 2 min and washed three times for 5 min with distilled water. Ultra thin sections were subsequently post-stained with 2% uranylacetate. All solutions used for IEM were dissolved in PBS. Photographs were taken with a Zeiss EM10 transmission electron microscope and scanned images were processed using Adobe Photoshop.

2.2.2. Molecular biology methods

2.2.2.1. Isolation of parasite genomic DNA

Genomic DNA (gDNA) was isolated from purified asexual or sexual blood stages of *P. falciparum* using QIAamp Blood Mini Kit. Parasites were initially purified with 0.15% saponin as described above **(2.2.1.15)** and DNA was purified following the manufacturer instructions. For DNA elution, 50 µl of buffer AE were used instead of 200 µl to increase the final DNA concentration in our eluate. The DNA concentration was determined photometrically by measuring absorption at 260 nm.

2.2.2.2. Plasmid DNA preparation

The purification of low amounts of plasmid DNA was performed with the QIAprep® Spin Miniprep kit. Three (3) ml LB medium supplemented with ampicillin were inoculated with one bacteria colony and

incubated overnight at 37°C. The next day, bacteria were harvested at 16000 g for 2 min at RT. The resulting pellet was used for the preparation of plasmid DNA according to the manufacturer's instructions. For the purification of high amount of plasmid DNA, The NucleoBond® Xtra Midi kit was used. First, a starter culture was prepared by inoculating 5 ml of LB medium with a colony from a freshly streaked agar plate and incubated overnight at 37°C, the next day the starter culture was diluted 1:1000 in 400 ml LB medium and incubated for 12 to 16 h. DNA was then purified following the instructions of the manufacturer and the concentration of the isolated plasmid DNA was determined photometrically by measuring absorbance at 260 nm.

2.2.2.3. Transformation of competent bacteria

To transform chemically competent *E. coli* bacteria, cells were thawed on ice and approximately 100 ng of plasmid DNA or 2-3 µl of a ligation reaction were added to one aliquot of 20-50 µl of competent cells and mixed thoroughly on ice. Samples were incubated on ice for 30 min and after incubation bacteria were heat shocked at 42°C for 45-60 sec. After heat shock, 600 µl of S.O.C. medium were added to the sample and incubated for 1h at 37°C on a bacterial shaker at 220 rpm. After incubation, the sample was centrifuged at 3000 g for 3 min. Approximately 500 µl of the supernatant were discarded and bacteria were resuspended in the remaining medium and spread on a LB agar plate supplemented with ampicillin and incubated at 37°C over night. The next day, colonies were picked either for a colony PCR, a mini-plasmid preparation or a mini-expression.

2.2.2.4. Isolation of parasite total RNA

RNA was isolated from asexual and sexual stages using the TRIzol® method. Harvested parasites or purified gametocytes pellet was resuspended in 1 ml prewarmed TRIzol by pipetting carefully up and down. Two hundred (200) microliters chloroform was added and mixed using a vortex until a white solution appeared. The mixture was subsequently incubated at RT for 10 min on a rocker. After incubation, the mixture was centrifuged at 12000 g at 4°C for 15 min. Centrifugation separates the mixture into lower red phenol-chloroform phase containing DNA and protein, a white interphase containing DNA and the upper colorless aqueous phase containing RNA which was transferred carefully into a new tube. To this aqueous solution, 500 µl isopropanol was added, mixed by inverting the tube and incubated at RT for 10 min. The centrifugation at 12000 g was repeated and the supernatant was discarded carefully to avoid disturbing the RNA pellet at the bottom of the tube. The pellet was

subsequently washed by resuspension in 1 ml 75% ethanol (prepared with DEPC water), and centrifugation at 8000 g for 5 min at 4°C. The ethanol was discarded and residual ethanol was carefully aspirate with a Pasteur pipet without disturbing the pellet and the RNA sample was air dried for about 10 minutes, then resuspend in DEPC water and heated for 10 min at 60°C. RNA purity was determined by measuring the ratio A260/A280. A ratio higher than 1.8 was indicative of a good RNA preparation. The sample was stored at -20°C until needed.

2.2.2.5. Removal of genomic DNA and RNA clean up

To obtain a good quality RNA deprived of genomic DNA and other RNA contaminants, 2.5 µl DNase I stock solution and 10 µl of buffer RDD was added to 2-3 µg of RNA. The reaction volume was adjusted to 100 µl with DEPC water and incubated at RT for 40 min. RNA was further treated to remove all contaminating salts and proteins. The purified RNA (free of DNA) was mixed with 250 µl of DEPC-water, 150 µl of phenol and 150 µl of chloroform. The mixture was incubated on the rocker for 5 min and centrifuged for 5 min at 12000 g. The aqueous phase (top) was then transferred to a new tube and 300 µl of chloroform were added to it. The mixture was again incubated on a rocker and centrifuged as previously. The aqueous phase was transferred to a new eppendorf tube and mixed with 30 µl of 3M NaOAc and 1 ml of ethanol. The resulting mixture was incubated on ice for 50 min and centrifuged at 12000 g for 20 min at 4°C. The precipitated RNA was washed once with 1 ml of ice-cold RNAse free 75% ethanol, mixed using a vortex and finally centrifuged at 10 000 g for 5 min at 4°C. The supernatant was carefully removed and RNA pellet was briefly air-dried and resuspended in 50 µl DEPC-water. The concentration was measured as described above.

2.2.2.6. Agarose gel electrophoresis

Agarose gel electrophoresis was used to analyze PCR and digestion products. A 1% agarose gel was used for the analysis of plasmids digestion. Proteasome subunits and pfhsIV have a lenght of less than 1000 bp and were separated using a 1.5% agarose gel. All RT-PCR products were separated using a 2% gel. To prepare the gel, agarose powder was weighed and the adequate amount of TAE buffer was added and boiled until the gel was totally dissolved, the gel was allowed to cool down at RT and poured in a gel tray. Combs were placed on the gel tray to create loading pockets. After gel solidification, the combs were removed and the tray was placed in a clean gel tank filled with 1 x TAE buffer. Samples were mixed with loading dye (1 µl loading dye per 4 µl DNA sample) and loaded in appropriate wells.

Molecular weight marker and controls were also loaded into separate wells of the same gel. Electrophoresis was performed at 100 V for approximately 45 min. Afterwards the fragments were photographically documented under UV light. For protein expression, DNA fragments encoding for the protein of interest were isolated from the gel as described below.

2.2.2.7. Isolation of DNA fragments from agarose gels

The DNA fragment of interest was excised out of the gel using a clean scalpel and transferred into a 1.5 ml eppendorf tube. Purification of DNA fragments from excised agarose gels was performed using NucleoSpin® Gel and PCR Clean-up kit. A buffer solution (provided with kit) was added to each tube containing excised gel and gels were melted by heating at 50°C for 10 min to release DNA into the buffer. This kit is based on the binding of DNA to silica gel membranes in the presence of a high concentration of chaotropic salt. The rest of the procedure was performed following manufacturer's instructions and DNA was resuspended in dH_2O.

2.2.2.8. Polymerase chain reaction

Polymerase chain reaction (PCR) was used to amplify proteasome subunits sequences and pfhsIV sequence for protein expression and purification as well as diagnostic PCR to identify proteasome subunits transctripts in the parasite. Two distinct polymerases were used during this study. Production of recombinant proteins usually requires a high fidelity copy of the gene of interest. Go-Taq polymerase was initially used to set the better reaction conditions, after which the PHUSION polymerase was used because of its 3'5' exonuclease activity that reduces the error rate.

a. Amplification from plasmid and genomic DNA

For PCR amplification, a PCR mix of 25 µl containing the following ingredients was used:

GoTaq reaction:

50-100 ng DNA (for colony PCR, one colony was diluted in 10 µl distilled water)

1.25 U GoTaq polymerase enzyme

5 µl 5× GoTaq buffer

1.5 µl $MgCl_2$ (25 mM)

0.5 µl dNTPs (10 mM each)

0.5 µl forward primer (100 pM)

0.5 µl reverse primer (100 pM)

Add volume to 25 µl bi-distilled water.

Conditions of the reaction:

Initial denaturation:	95°C	2 min	
Denaturation:	95°C	30 s	35 Cycles
Annealing: **See section 2.1.8** for all primer pairs			
Elongation:	72°C	(1min/1000bp)	
Final Elongation:	72°C	5 min	

PHUSION polymerase reaction:

50-100 ng DNA

5 U PHUSION polymerase enzyme

2.5 µl 10 x PHUSION buffer

0.5 µl dNTPs (10 mM each)

0.5 µl forward primer (100 pM)

0.5 µl reverse primer (100 pM)

Add volume to 25 µl with bi-distilled water.

Conditions of the reaction:

Initial denaturation:	98°C	30s	
Denaturation:	98°C	10 s	35 Cycles
Annealing: **See section 2.1.8** for all primer pairs			
Elongation:	72°C	(30s/1000bp)	

b. Reverse-transcriptase PCR

Reverse-Trancriptase PCR was performed using superscript First strand synthesis system for RT-PCR. The cDNA synthesized here was used for proteasome alpha type 5 subunit protein expression. cDNA samples used to amplify the transcripts of proteasome subunits at different stages were provided by Nina Simon and Shruti Agarwal. Total RNA was extracted from a saponin lysed mixed culture of *P.falciparum* 3D7 as described above.

A master mix was prepared as follow:

RNA	(up to 5 µg)
Random hexamers (50 ng/ µl)	1 µl
10 mM dNTP mix	4 µl
Add volume to 24 ml with DEPC-H2O	

The mixture was incubated for 5 min at 65°C, then on ice for at least 1 min. Two aliquots of 10 µl were prepared in two separate tubes; one was labeled as “sample “and the other as ”no RT” control. During incubation time, a primer mix was prepared as follow:

10 × RT Buffer	5 µl
50 mM $MgCl_2$	5 µl
0.1 M DTT	5 µl
RNAse OUT inhibitor	2.5 µl

Seven (7) µl of this solution were added to 10 µl of master mix, gently mixed and incubated for 2 min at 25°C. 1 µl (50 U) of superscript II RT was added only to the sample tube and the two tubes were incubated for 10 min at 25 °C. Afterwards the mixture was transferred to 42°C and incubated for 50 min. To stop the reaction the tubes were heated at 70°C to inactivate the enzyme. Samples were finally treated with 1 µl RNAse H and incubated for 20 min at 37°C. The resulting cDNA was amplified using a standard PCR reaction with the PHUSION polymerase enzyme as described above.

Conditions of the reaction:

Initial denaturation:	95°C	2 min	
Denaturation:	95°C	30 s	25 Cycles
Annealing: **See section 2.1.8** for all primer pairs			
Elongation:	72°C	30s	
Final Elongation:	72°C	1 min 30 s	

2.2.2.9. Restriction digestion and ligation of plasmid DNA

Standard restriction reaction:

0.5 - 2 µg DNA

20 U of each restriction enzyme

5 µl of 10 × buffer (NEB buffer 3 or 4, depending on the used restriction enzymes)

5 µl 10 × BSA

Add volume to 50 µl with distilled water

The restriction sample was incubated for 3 h or overnight at the optimum temperature of the used restriction enzyme. In case of a double digest with restriction enzymes needing different NEB buffers, the optimal buffer for the double digest was chosen. After incubation, the restriction sample was separated on a 1% agarose gel and the desired DNA fragment was purified from the gel.

2.2.2.10. Ligation of DNA fragments

DNA ligation is the process of joining together two DNA molecules ends. Specifically, it involves creating a phosphodiester bond between the 3' hydroxyl of one nucleotide and the 5' phosphate of another. This reaction is usually catalyzed by a DNA ligase enzyme. This enzyme will ligate DNA fragments having blunt or overhang, complementary, 'sticky' ends. Recombination of DNA was performed by ligation of two double-stranded DNA molecules exhibiting blunt ends.

The following reaction mixture was used:

Approximately 0.1 µg vector DNA

Insert DNA (molar ratio of vector to insert = 1:5)

2 µl 10 × ligase buffer

400 U T4-DNA-ligase

Add volume to 20 µl with distilled water

The reaction mix was incubated at RT for 2 to 3 hours or overnight at 15°C. The ligated DNA was directly used for the transformation of *E.coli.*

2.2.2.11. Nucleic acid sequencing

Genes of interest inserted in expression plasmids were sequenced to verify that the gene coding for the protein of interest is inserted in the right frame. Mini-plasmid preparations were performed using nucleospin® Plasmid quick pure following the manufacturer's instructions. To submit samples for sequencing, a mixture of 600 - 700 ng plasmids DNA plus 20 pmol of one primer (sense or antisense) in a total volume of 7 µl was prepared and sent to Seqlab (http://www.seqlab.de) for sequencing.

2.2.3. Protein biochemistry methods

2.2.3.1. Preparation of cell lysates

P. falciparum asexual cultures were harvested and transfer to a centrifuge tube and centrifuged at 800 g for 5 min. The pellet was washed once in 10 ml PBS and centrifuged at 800 g for 5 min. Asexual stage parasite were treated with 0.015% saponin solution and incubated for about 15 min to release parasite from RBCs. Parasite pellets were washed once in 10 ml PBS and centrifuged at 800 g for 5 min. Gametocytes were enriched from mixed gametocyte cultures by Percoll gradient purification as described above. Pellets were resuspended in lysis buffer and incubated on ice for 15 min. The lysate containing parasite proteins were used immediately for western blotting or kept at -20°C until needed.

2.2.3.2. Mini-expression of fusion proteins

For protein expression, *E.coli* BL21 (DE3) RIL cells were transformed with pGEX-4T1 as described above. 4-5 colonies were picked randomly and grown in LB medium. After 2 h, temperature was shifted to 30°C and the expression was induced by adding isopropyl-β-thiogalactopyranoside (IPTG) with a final concentation of 0.075 mM. After 5 hours, cells were collected and mixed with 2 × SDS buffer (1:1 ratio), boiled for 10 min at 95°C and loaded on a 10% SDS gel.

2.2.3.3. Purification of inclusion bodies

Inclusion bodies were prepared to produce antibody against the parasite proteasome beta subunit type 5 (β5-SU). A starter culture of 100 ml *E.coli* BL21 (DE3) RIL cells transformed with the appropriate recombinant DNA was incubated overnight at 37°C. The next day, fresh medium was added to a final volume of 1500 ml and incubated for 1h at 37°C. The temperature was decreased to 30°C and 1500 µl

of 0.75M IPTG were added to the culture and incubated for 5 h at 30°C. Afterwards, the culture was centrifuged at 3500 g for 5 min at 4°C and the pellet resuspended in 80 ml ice cold lysis buffer containing lysozyme (10 mg/ml) and incubated on ice for 10 min and sonicated for another 10 min on ice. Then 200 ml of detergent buffer was added to the lysate and centrifuged at 5000 g for 10 min, the supernatant was discarded and the pellet was resuspended in 250 ml wash buffer and centrifuged at 5000 g for 10 min. The washing was repeated until a tight pellet was obtained. The pellet was then resuspended and washed in 70% Ethanol by centrifugation at 5000 g for 10 min and the pellet was allowed to dry on ice. Once ethanol was evaporated, pellet were resuspended in a small volume (2-5ml) of sterile PBS and sonicated until the suspension was able to pass a 23 gauge needle. To estimate protein concentration a 12 % SDS gel was prepared and 6-8 dilutions of the protein suspension were separated on the gel. A serial dilution of bovine serum albumin (BSA; from 10-0.1 µg) was separated on a 12 % SDS-gel and used as a standard. The fusion protein band was compared by eye to BSA bands at different concentrations. A BSA band with comparable amount of protein on the gel was used to deduce the concentration of our fusion protein.

2.2.3.4. Purification of recombinant proteins

Recombinant proteins were prepared to generate antibodies against parasite proteasome alpha subunit type 5 (α5-SU) and PfhsIV. A starter culture of 100 ml *E. coli* BL21 (DE3) RIL transformed with the appropriate recombinant DNA was incubated overnight at 37°C. The next day, fresh medium was added to a final volume of 1500 ml and incubated for 1 h at 37°C. The temperature was decreased to 25°C and 1500 µl of 0.75M IPTG was added to the culture and incubated for 4-5 h at 25°C. After incubation the culture was centrifuged at 9000 g at 4°C for 10 minutes. Afterwards, the supernatant was discarded and bacteria pellet was drained to remove most of the residual LB medium. Pellet and lysate were kept on ice during the whole procedure. To lyse bacteria, the pellet was totally re-suspended by adding 40 ml of ice cold lysis buffer per 1 l of culture. The bacteria lysate was then transferred to a clean 50 ml conical tube and the mixture was rotated for 1 h at 4°C. To ensure the total disruption of the cell wall, samples were processed using a FRENCH press, and then sonicated. The total lysate was centrifuged at 33000 g at 4°C for 1.5 h. The resulting supernatant (approximately 40 ml) was filtered through a 0.22 µm filter and transferred to a falcon tube containing 1 ml washed glutathione. The mixture was rotated at 4°C for 2 hours or overnight to allow the 26 kDa GST-tagged protein to bind. After binding the mixture was transferred to a polyprep chromatography column containing a resine that bind to gluthatione. Recombinant protein in the column was rinsed 5x with ice cold PBS and

the protein was eluted from the column by collecting 8 fractions of 1 ml each. Purified proteins were analysed for purity using a 12% SDS-PAGE and the fractions with the highest amount of proteins were mixed and filtered through an Amicon filter tube 30000 MWCO to exchange the buffer and to concentrate the protein. Proteins were resuspended in sterile PBS.

2.2.3.5. Production of polyclonal antisera

Recombinant proteins were used for raising antibodies in 6-8 weeks old NMRI white female mice. A volume of recombinant protein equivalent to 100 µg protein of interest was diluted in 1 x sterile PBS to a final volume of 200 µl. For immunization of one mouse, 200 µl the recombinant protein was mixed with 200 µl of Freund's incomplete adjuvant and the mixture was administered sub-cutaneously to each of the three mice. Four weeks later, mice were boosted by administering 75 µg of the same recombinant protein in incomplete Freund's adjuvant and 10 days after the first boost, a second boost similar to the first was administered to maximize antibody production. Two weeks after the second boost, each mouse was anaesthetized by intra peritoneal injection of 150 µl mixture Ketamin/Xylazin. Blood was collected by cardiac puncture and transferred in 5 ml blood collection tube and blood was allowed to coagulate by incubating at RT for 30 min, then centrifuged at 2000 g for 15 min. Several aliquots of the serum were then prepared in 1.5 ml Eppendorf tubes and stored at -20°C until use.

2.2.3.6. SDS – Polyacrylamide gel electrophoresis (SDS-PAGE)

a. Gel preparation

During the study the following gel concentrations were used and the volumes in the table were used for the preparation of 2 gels.

Table 8. Polyacrylamide gels composition for SDS-PAGE

Reagents	Resolving gels		Stacking gel
	10 %	**12%**	**5%**
H_2O	4.0 ml	3.3 ml	2.08 ml
30% acrylamide	3.3 ml	4.0 ml	0.5 ml
1.5 M Tris pH 8.8	2.5 ml	2.5 ml	0.38 ml
10% SDS	0.1 ml	0.1 ml	0.03 ml
10% ammonium persulfate (APS)	0.1 ml	0.1 ml	0.03 ml
TEMED	0.004 ml	0.004 ml	0.003 ml

b. Sample preparation and SDS-PAGE

Cell lysates or purified proteins were mixed in 1:1 ratio (v/v) with 2 x SDS-sample buffer and boiled at 95°C for 10 min. Inclusion bodies and cell lysates used for the detection of ubiquitinated proteins by Western blot were separated on a 10 % gel, purified proteins and cell lysates used for other Western blot analysis were separated on a 12 % gel. The gels were placed into mini-protean II electrophoresis cells, and the chamber was filled with 1 x running buffer. Afterwards, samples and PAGE rulers were loaded into corresponding wells and a current was applied at a voltage of 100 V at RT.

2.2.3.7. Protein staining

GelCode® Blue Stain Reagent was used to visualize proteins separated by SDS-PAGE, to monitor the expression of recombinant protein or to check for equal loading. After protein separation was completed, gels were washed twice with distilled water by shaking on a rotator, about 50 ml of staining solution, necessary to cover the gels was applied and proteins were stained at RT until bands became visible. After staining, gels were destained with distilled water, and then transferred in a solution of 20% ethanol/10 % Glycerol for 30 min at RT, thereafter the gel was sealed in a plastic foil and allowed to dry at RT.

2.2.3.8. Western blot analysis

Parasite proteins separated by SDS-PAGE were transferred to Hybond ECL nitrocellulose membrane. Gels, membranes, pads and whatman paper were first soaked in the transfer buffer, then "sandwisches" were assembled in a holder cassette in the following order: pad, 2 sheets of filter paper, gel, membrane, 2 sheets of filter paper, pad. The holder cassettes were then placed in a transfer chamber containing transfer buffer and ice. Proteins were transferred on the nitrocellulose membrane at 25 V for 2 h or 15 V overnight. After blotting, the membranes were briefly rinsed in 1 x TBS and tranfered to a dish containing a blocking solution and incubated for 1 h at RT or overnight at 4°C. After blocking, membranes were washed twice with 1 x TBS and incubated with primary antibody for 2 h at RT or overnight at 4°C. The appropriate primary antibodies were diluted in 3% milk/TBS. After incubation with the primary antibodies, the membranes were washed once with 3% milk/TBS for 5 min and twice with 3% milk/0.1% Tween 20 /TBS for 10 min and washed once again with 3% milk/TBS for 5 min. After washing, the membranes were incubated for 1 h at RT or overnight at 4°C with secondary antibody conjugated to alkaline-phosphatase and diluted 1:5000 in 3% milk/TBS. After incubation with

secondary antibody, membranes were washed once with 1 x TBS for 10 min, twice with 0.1% Tween 20/TBS for 15 min and washed once again with 1 x TBS for 10 min. Membranes were finally incubated in equilibration buffer for 3 min and developed in NBT/BCIP solution for 5-30 min. The reaction was stopped with stop buffer and blots were scanned and processed using Power point.

2.2.4. Pre-clinical pharmacology methods

2.2.4.1. *In silico predictions*

These following software packages are available from Molecular Discovery (http://www.moldiscovery.com/software.php).

a. MetaSite

MetaSite analyses were used to predict metabolic transformations related to cytochrome-mediated reactions in phase I metabolism. Two-dimensional structures of the compounds were generated from SMILES files and submitted to the MetaSite program, which is a fully automated procedure.

b. VolSurf+ predictors

VolSurf+ includes number of models that have been developed using both public and pharmaceutical data, including passive intestinal absorption (Caco-2 cells), blood-brain barrier permeation, solubility, protein binding, volume of distribution, and metabolic stability. This software was used to predict these properties.

2.2.4.2. Compound administration and blood collection

A stock solution of Pheroid™ vesicules containing dihyate were prepared at the Unit for Drug Research and Development (North-West University, South Africa) and were dissolved in NO_2-water for the assay. Dihyate was also dissolved in 10 % DMSO, and the two formulations were compared. Dihyate was administered to two groups of male mice (C57/BL6) at 20 mg/kg by oral gavage and blood was collected from mice by tail bleeding at different time points. The blood collected was transferred to heparanized tubes and immediately centrifuged at 3000 g for 10 min at 4°C. The plasma was separated from red blood cells and stored at −80°C until analysis. The study and all procedures were approved by the Ethics Committee of the University of Cape Town (REC REF: 010/026). Dihyate dissolved in DMSO-water (1:9) formed a white precipitate and was resuspended prior to administration. The total volume

per administration was 200 µl and 20-25 µl of blood were collected at 30, 120, 240, 480 min after drug administration (dihyate dissolved in DMSO). For mice treated with dihyate entrapped in Pheroid vesicles, blood was collected from one mouse at a time at 10, 20, 30, 40, 60, 90, 120, 180, 240, 300, and 360, 420 min after drug administration to maximize the number of samples collected and to reduce the gap between times of collection.

2.2.4.3. Quantification of plasma level of dihyate, AZT and DHA

a. Calibration standard

Stock solutions of test compounds (dihyate, AZT and DHA) were prepared in acetonitrile at a concentration of 1 mg/ml. Ten (10) microliters of the stock solutions were diluted in human plasma to obtain standard (S) 1 at a concentration of 10 µg/ml. S2 (5 µg /ml), S3 (2.5 µg /ml), S4 (1.25 µg /ml), S5 (0.625 µg /ml), S6 (0.313 µg /ml), S7 (0.156 µg /ml), S8 (0.0781 µg /ml) and S9 (0.0391 µg /ml) were prepared by serial dilution. S4 to S9 were used to obtain calibration curves (for dihyate, AZT and DHA) between 39.1 and 1250 ng/ml. The calibration standards were briefly vortexed and used immediately or stored at −20°C. The calibration standards were analysed in duplicate in each study sample batch. The accuracies (%Nom) of the calibration standards of dihyate, AZT and DHA were between 88.2% and 111.1%, and the precision (%CV) were between 1.4 and 13.9% during study sample analysis.

b. Compounds extraction

To extract drugs from plasma samples collected from mice, 20 µl of standards and plasma samples were thawed on ice and mixed with 80 µl of internal standard solution (100 ng/ml of deoxythymidine in acetonitrile). The samples were vortexed for 1 minute, and sonicated for 5 min, then centrifuged at 1500 g for 5 minutes at RT. The supernatant (approximately 60 µl) was transferred to a clean tube and evaporated under vacuum in a rotor evaporation system at 30° C for 45 min or until the samples were completely dried. The residue was reconstituted in 100 µl of mobile phase (10 mM ammonium acetate: methanol, 85:15, v/v).

2.2.4.5. Chromatography and Mass spectrometry

Dihyate, DHA and AZT were quantified using an Agilent 1200 HPLC connected in tandem to an AB Sciex API 3200 mass spectrometer equipped with a turbo ion spray (ESI) source. The software Analyst 1.5.1 was used to control both, the liquid chromatogram and the mass spectrometer. The Phenomenex Luna

PFP (50 x 2.0 mm, 5 µm) column was used for compounds separation. The mobile phase consisted of a gradient of methanol and 10 mM ammonium acetate. The system operated at a flow rate of 0.5 ml/min and the volume of injection was 20 µl. The ESI interface was used in positive mode and the turbo ion spray source was heated to 450°C. The AB Sciex API 3200 mass spectrometer was operated at unit resolution in the multiple reaction monitoring (MRM) mode, monitoring the transition of the protonated molecular ions at m/z 534.1 to the product ions at m/z 126.9 for dihyate, the protonated molecular ions at m/z 268.1 to the product ions at m/z 127.0 for AZT, the ammonium adduct at m/z 302.2 to the product ions m/z 267.1 for DHA, and the protonated molecular ions at m/z 227.1 to the product ions at m/z 127.0 for the internal standard.

2.2.4.6. *In vivo* efficacy studies of dihyate

a. Donor mice infection

To start an infection, a cryotube containing frozen *P. berghei N* (CQ sensitive) parasites was quickly thawed at RT, then mixed with an equal volume of PBS and 200 µl of the resulting mixture was injected immediately intra-peritoneally into a naive recipient C57/BL6 male mouse. After 3-4 days, parasites were monitored in peripheral blood by Giemsa staining, and when parasitemia was higher than 10 %, blood was obtained by cardiac puncture and diluted in an equal volume of PBS.

b. The Peters' four day suppression test

The parasitemia in blood collected from the donor mice was determined as described above and the number of red blood cells per ml of blood suspension was estimated using a haemocytometer as decribed above. In our experiment, we infected mice with 10^7 parasitized RBCs/mouse.

Calculation of number of parasitized RBCs/ml (C1):

$$C1 = \frac{\text{Parasitemia (\%)} \times \text{total erythrocytes (RBCs/ml)}}{100}$$

Knowing the concentration (C1), we prepared a suspension of 5 x 10^7 parasitized RBCs /ml by diluting the stock solution with PBS. At this point 200 µl of our working suspension contained 10^7 parasitized RBCs. The four day suppression test was performed as described (Peters, 1975). Animals were inoculated intraperitoneally with 200 µl of this blood suspension. The test drug dihyate entrapped in pheroid vesicles (20 mg/Kg), the standard drug CQ (10 mg/kg) and PBS control were administered to

parasitized mice 30 minutes after administration of infected erythrocytes on day zero. The same dose was repeated on days 1, 2 and 3 after infection. Blood was collected by tail bleeding and smears were prepared and stained with Giemsa. Parasitemia was assessed to qualitatively assess the activity of the compound at the tested dose. A dose resulting in survival times greater than that of infected non treated mice was considered active. Death occurring before day 6 of infected and treated mice was regarded as toxic death.

2.2.4.7. *In vitro* metabolism studies

In vitro metabolism studies were performed to confirm metabolism observations made *in vivo*. A final concentration of 1 µM of dihyate was incubated at 37°C with mice liver microsomes. The incubation mix consisted of dihyate (1 µM), 0.2 mg/ml mice microsomal protein, and 100 mM KPO_4 in 200 mM phosphate buffer, pH 7.4. The reaction was initiated by the addition of NADPH (1 mM). The mixture was rotated at 37°C. Aliquots were collected before initiating the reaction. At varying time points 200 µl of incubation mixture were removed and added to 100 µl ice cold acetonitrile to stop the reaction. The rate of loss of parent compound was determined at 0, 15, 30, and 45 min by LC-MS/MS analysis. The amount of compound in the samples was expressed as a percentage of remaining compounds compared to time point zero (100%).

2.2.5. Computational methods

- The molecular weight of studied proteins was calculated using the Compute pI/Mw, a tool which allows the computation of the theoretical pI (isoelectric point) and Mw (molecular weight) of proteins (http://web.expasy.org/compute_pi/).

- In order to identify parasite homologs to proteasomal SUs, we performed a BLAST search using human proteasome SU proteins (http://www.uniprot.org) as queries against the *P. falciparum* 3D7 genome (http://plasmodb.org; Aurrecoechea et al., 2009). Predicted homologs of proteasome precursor or SU sequences were ranked as having high score segment pairs and low P-values. PlasmoDB (www.plasmodb.org) was also used to retrieve coding sequences (DNA and cDNA) for the cloning of *P. falciparum* 3D7 proteins.

- Multiple sequence alignment of proteaome β5-SU was generated using ClustalW2 (www.ebi.ac.uk/clustalW).

- The IC_{80} and IC_{90} concentrations of compounds were generate by GraphPad Prism web calculator online (http://graphpad.com/quickcalcs/ECanything2.cfm).

- To identify potential ubiquitylation sites *in Silico*, the translated coding sequence for PF10_0075 was downloaded from PlasmoDB and analyzed for the presence of putative ubiquitylation sites using *UbPred* (http://www.ubpred.org/). Predictions with *UbPred* were classified by level of confidence, from low (score ranging from 0.62 to 0.69) to medium (score ranging from 0.70 to 0.84) to high (score equal to or higher than 0.85), according to the software instructions (Radivojac et al., 2010).

3. Results

3.1. Hybrid molecules as potential candidates for a Malaria/HIV combination therapy

3.1.1. Optimization of HIV assay

An existing *in vitro* cell-based screening assay was optimized resulting in the generation of a method in which GFP expression can be quantified in a 96-well format. Several experimental parameters were found to affect the readout, including the number of seeded cells and concentrations of pseudo-particles. Minor parameters like timing of each step (reagent additions, infection/incubation) were optimized while running the first assays. For active compounds, screening was repeated at least three times. The production of good virus stock was an important step in our assay. Therefore the amount of virus needed to achieve an acceptable signal to background ratio in a 96-well plate format was determined. A stock of virus was diluted and used to infect HeLa cells in a 24 well plate. After 48 h incubation cells were collected and sorted using flow cytometry and the percentage of fluorescent cells was recorded for each virus dilution (figure 11).

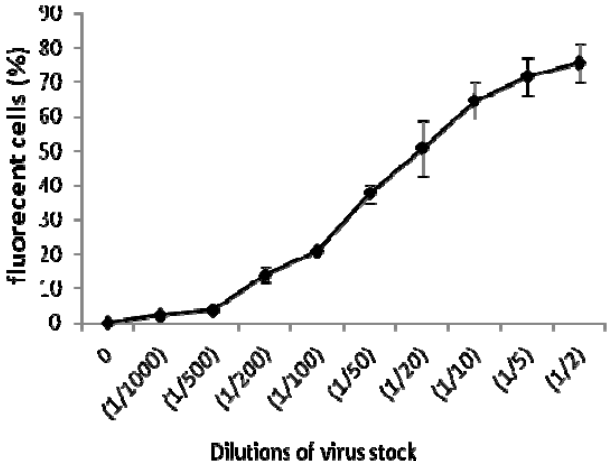

Figure 11. Virus stock titration. Parasites were diluted 2 to 1000 times, added to HeLa cells cultures and incubated for 48 h. Fluorescent cells were counted post-transduction and the percentage of fluorescent cells per virus dilution was recorded.

To evaluate the suitable virus dilution to be used in the assay, three virus dilutions were assessed (figure 12A). The virus stock diluted 10 times generated fluorescence intensity up to 5000 RFU after

48 h incubation with 2 × 10^4 HeLa cells. To evaluate the suitable cell confluence for the assay, a dose-response curve of AZT using 1:10 dilution virus stock at different cells confluences (1 × 10^4 to 4 × 10^4) was generated. Fluorescence was monitored after 48 h incubation and quantified. The strongest signal was observed in wells where 1 × 10^4 cells were seeded (figure 12B). For subsequent anti-HIV assays we chose to count 1.2 × 10^4 cells considering errors during counting. For a suitable assay it was therefore necessary to seed between 1 × 10^4 and 1.5 × 10^4 cells to achieve a good signal.

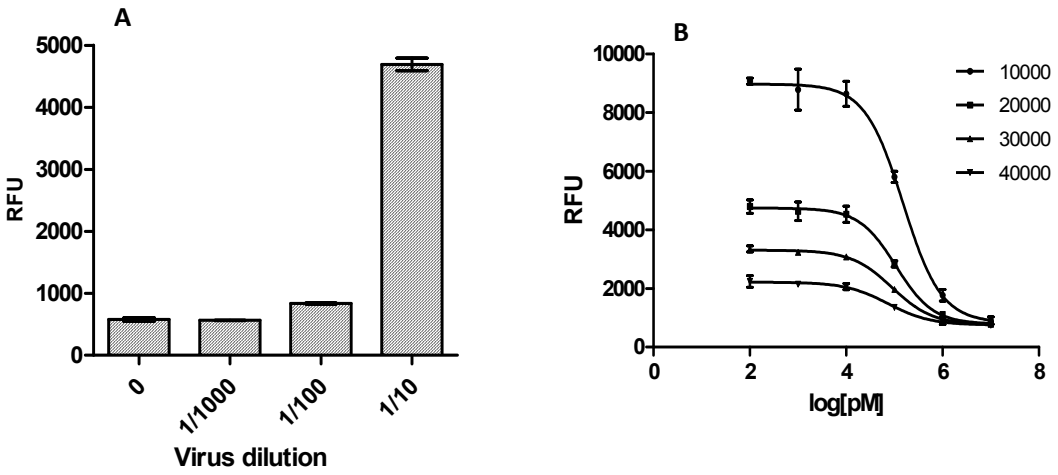

Figure 12. Parameters optimization. The kinetic of infection was monitored at various cell densities and pseudotyped particle dilutions as specified. Optimal results were achieved for all conditions at 48h post-infection. Signal is expressed in Relative Fluorescence Unit (RFU).

3.1.2. Compound screening for cytotoxicity, antiplasmodial and anti-HIV activity

A small library of generated hybrid molecules was evaluated for their inhibitory activity against pseudotyped HIV-1, *P. falciparum* 3D7 and *P. falciparum* Dd2. Upon receipt, compounds were pre-screened for 3 concentrations (50, 5 and 1 µM) to establish their activity and cytotoxicity (table 9). Compounds found toxic to HeLa cells at 5 µM were considered highly toxic and were remove from the study. Compounds with no activity on HIV and *P.falciparum* at 50 µM (i.e with IC_{50} > 50 µM for both) were not further screened since the exact IC_{50} could not be determined. Compounds with acceptable activities were further evaluated for their cytotoxicity on HeLa cells. Compounds with IC_{50} > 15 µM for anti-HIV activity and IC_{50} > 10 µM for antiplasmodial activity were classified as not effective in our study. The selectivity index (SI; table 10) was also used as cut-off parameter to prioritize the most

potent and selective compounds. Therefore a compound with a SI < 100 in both assays was considered not effective (NE; table 9).

Precursor drugs

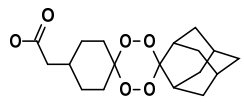

Tetraoxane

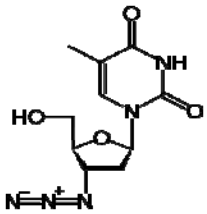

AZT

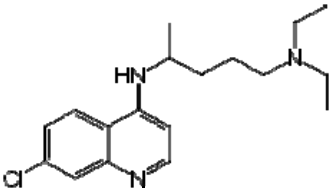

CQ

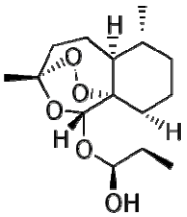

DHA

AZT-CQ hybrids

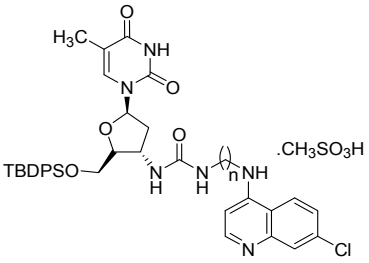

VAK 92 (n=2)
VAK 93 (n=5)
VAK 87 (n=4)

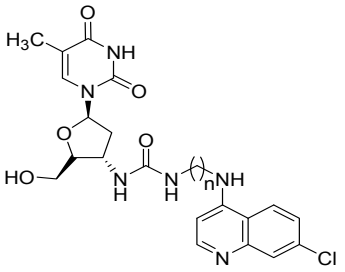

VAK 41-DS (n=2)
VAK 37-DS (n=5)
VAK 59-DS (n=4)

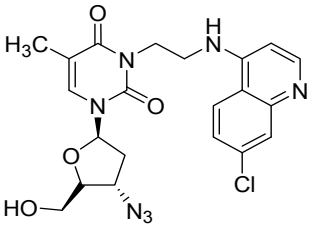

AKAZTQ

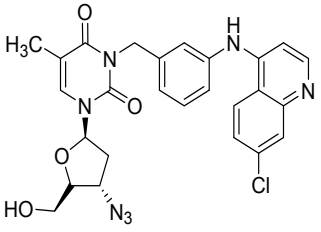

AKAZTBQ

Figure 13. Structures of precursor drugs and hybrid molecules.

AZT-DHA hybrids

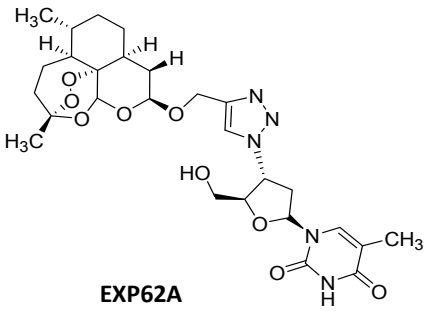

EXP62A

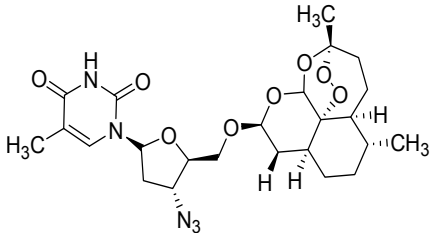

DIHYATE

AZT-tetraoxane hybrids

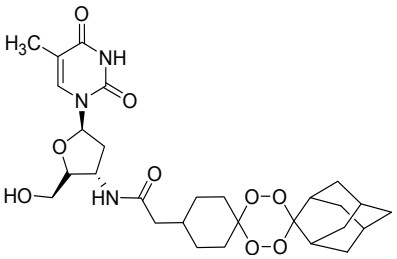

AKTXAZ

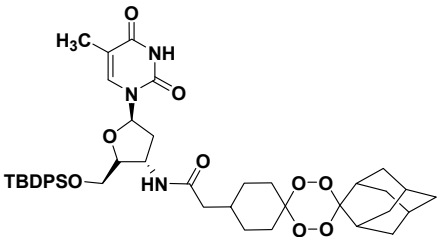

AKTXAZ -DS

Intermediates

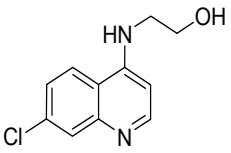

CQOH

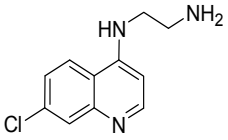

A 102

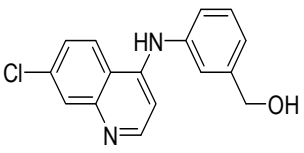

AK-04

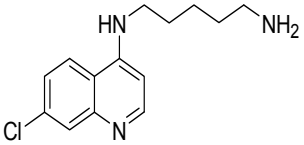

A 105

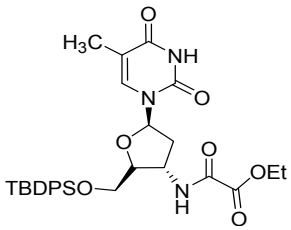

VAK49

Figure 13. Structures of precursor drugs and hybrid molecules.

Table 9. Estimation of IC_{50} (concentration resulting in 50 % inhibition of cell growth or viral replication) obtained after inhibition of *P. falciparum* sensitive strain(3D7), resistant strain (Dd2), HIV-1(VSV-G) and HeLa cells with serial dilution of hybrid molecules. IC_{50}s and standard deviations were calculated using the software GraphPad prism**.**

	IC_{50} (µM)			
Compounds	***P. falciparum* 3D7**	***P. falciparum* Dd2**	**HIV-1(VSV-G)**	**HeLa cells**
	IC_{50} ± SEM	**IC_{50} ± SEM**	**IC_{50} ± SEM**	**CC_{50} ± SEM**
A102	0.03 ± 0.02	0.23 ± 0.04	NE	63.44 ± 6.28
A105	0.13 ± 0.10	0.23 ± 0.12	NE	56.64 ± 17.88
AK-04	1.42 ± 0.28	1.46 ± 0.30	NE	>100
AKAZTBQ	0.16 ± 0.06	0.22 ± 0.06	1.76 ± 0.46	>100
AKAZTQ	0.46 ± 0.01	0.65 ± 0.14	7.15 ± 2.57	>100
AKTXAZ	0.27 ± 0.09	0.19 ± 0.08	NE	>100
AKTXAZ DS	0.22 ± 0.17	0.10 ± 0.08	NE	23.38 ± 4.97
CQOH	2.20 ± 0.14	1.72 ± 0.04	NE	>100
Dihyate	0.03 ± 0.01	0.01 ± 0.00	2.86 ± 0.39	>100
EXP62A	0.27 ± 0.06	0.10 ± 0.03	11.10 ± 0.46	>100
Vak31-DS	3.53 ± 0.56	31.60 ±14.71	NE	>100
VAK37-DS	5.18 ± 0.42	8.02 ± 2.43	NE	>100
VAK49	11.12 ± 2.77	12.10 ± 1.43	NE	63.97 ± 11.07
VAK59 DS	1.94 ± 0.49	10.57 ± 4.95	NE	>100
VAK-87	0.38 ± 0.22	0.08 ± 0.02	0.90 ± 0.11	28.65 ± 5.09
VAK-92	0.37 ± 0.15	0.34 ± 0.20	NE	23.78 ± 1.70
VAK-93	0.58 ± 0.17	0.08 ± 0.02	7.92 ± 2.34	36.13 ± 1.43
Control drugs				
Raltegravir	NE	/	0.01 ± 0.00	>100
AZT	NE	/	0.04 ± 0.02	>100
CQ	0.03 ± 0.01	0.71 ± 1.19	12.48 ± 2.45	>100
DHA	0.03 ± 0.01	0.01 ± 0.01	NE	>100
Tetraoxane	0.32 ± 0.28	0.12 ± 0.03	NE	>100

Seventeen (17) compounds (figure 13) exhibited strong to moderate inhibition against HIV-1 (VSV-G) and *P. falciparum* (table 9). The integrase inhibitor raltegravir and the reverse transcriptase inhibitor AZT were used as positive controls in HIV assay while CQ and DHA were used as positive controls in Malstat assays. Eleven (11) compounds had IC_{50} values in both strains of *P.falciparum* in the nanomolar range. Among these, three compounds VAK87, VAK92 and VAK 93 showed significant reduction in HeLa cells growth. Nonetheless, VAK 87 showed high activity against pseudotyped HIV-1 (IC_{50} = 0.9 µM;

SI=31.8) while VAK 92 showed no effect and VAK 93, a moderate effect (IC_{50} = 7.92; SI=4.6). These data suggest that the high activity of VAK 87 might not be linked to its cytotoxicity against HeLa cells. All compounds with an antiplasmodial IC_{50} value higher than 1 µM exhibited no effect against HIV and 16 out of the 22 inhibited *P. falciparum* with IC_{50} values lower than 1 µM. Interestingly, dihyate demonstrated an antiplasmodial activity comparable to reference antimalarial drugs CQ and DHA and was considered our priority since a moderate activity against HIV was also observed (IC_{50} = 2.86 µM; SI > 35). Dihyate was not toxic to HeLa cells at 100 µM. For further characterization, we decided to focus only on the compound with the most optimal profile.

Table 10. Selectivity index values (SI= *CC_{50}/IC_{50}) of active hybrid molecules.

Selectivity index (CC_{50}/IC_{50})			
Compounds	***P.falciparum* 3D7**	***P.falciparum* Dd2**	**HIV-1(VSV-G)**
A102	2114,7	275,8	ND
A105	>435,7	>246,3	ND
AK-04	>70,4	>68,5	ND
AKAZTBQ	>625	>454,5	>56,8
AKAZTQ	>217,4	>153,8	>14
AKTXAZ	>370,4	>526,3	ND
AKTXAZ DS	106,3	233,8	ND
CQOH	>45,5	>58,1	ND
Dihyate	>3333,3	>10000	>35
EXP62A	>370,4	>1000	>9
Vak31-DS	>28,3	>3,2	ND
VAK37-DS	>19,3	>12,5	ND
VAK49	5,75	5,3	ND
VAK59 DS	>51,5	>9,5	ND
VAK-87	75,4	358,1	31,8
VAK-92	64,3	69,9	ND
VAK-93	62,3	451,6	4,6
Raltegravir	ND	/	>10000
AZT	ND	/	>2500
CQ	>3333,3	140,8	>8
DHA	>3333,3	10000	ND
Tetraoxane	>312,5	>833,3	ND

*CC_{50} = IC_{50} on HeLa cells: cytotoxic concentration 50, which is concentration resulting in 50 % inhibition of HeLa cells growth. ND: Not determined

Dihyate and VAK 87 appeared to be the most active compounds, but VAK 87 was discontinued due to higher cytotoxicity (CC_{50} = 28.6 µM) and weaker antiplasmodial activity compared to dihyate. Since DHA is reported to have an additional effect on young and mature gametocytes (Adjalley et al., 2011), gametocytocidal activity of dihyate was also evaluated and it appeared that the activity of dihyate on developing gametocytes is moderate and comparable to that of DHA in our assay, but less active than primaquine, a known gametocytocidal drug used as control (figure 14).

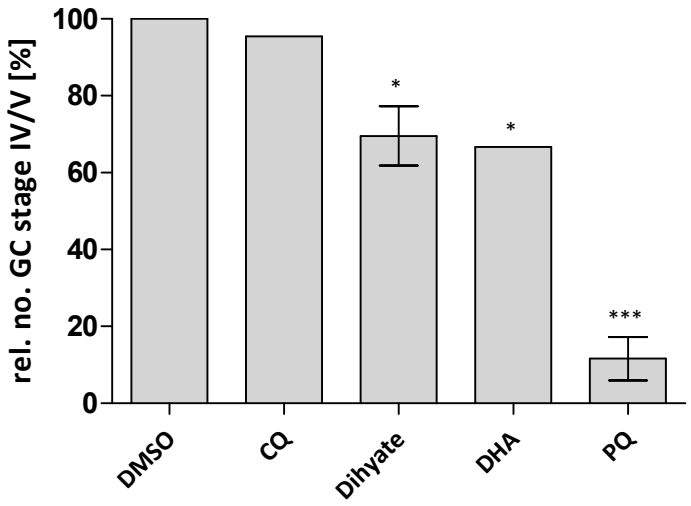

Figure 14. Inhibition of gametocytes maturation. Compounds at IC_{50}s or a 0.5% volume of DMSO were added to stage II gametocyte cultures for 2 days. The numbers of stage IV and V gametocytes were counted after 7 days and correlated to the gametocytemia of the DMSO control (normalized to 100 %). The graph represents results of two independent experiments in triplicate for PQ, dihyate, CQ (mean ± SEM) and a single experiment for DHA (mean ± SD). Statistical analysis was performed using one way ANOVA followed by a *Tukey* test and mean gametocytemia of compounds tested once were compare with mean gametocytemia in DMSO control using t-test (GraphPad Prism 5). Asterisks represent a significant difference between tested compounds and DMSO control (annex), where *** correspond to P < 0.001; **correspond to 0.001 < P <0.01; * correspond to 0.01< P < 0.05 and for p > 0.05 the difference in not considered significant and there is no asterisk.

Since HIV-1 (VSV-G) enter cells through the endocytic pathway and can be inhibited by compounds that block endosomal acidification (Aiken, 1997), dihyate activity was further evaluated on a full replicative wild type NL43 HIV-1. Dihyate was 72 × and 600 × less potent than AZT against pseudotyped viruses and the wild type NL43 HIV-1 respectively (table 11 and figure 15). Viral infection was measured in the presence of drugs tested at six different concentrations and compared to AZT, non-

infected TZM cells and non treated-infected TZM cells were used as 100% activity and 0% activity controls, respectively.

Table 11. IC_{50}s values of dihyate obtained from the two HIV *in vitro* assays

	IC_{50} (nM)	
	HIV-1 (VSV-G)	Wild type (NL43)
AZT	40 ± 20	0.8 ±0.7
Dihyate	2860 ± 390	485.5 ± 16.5

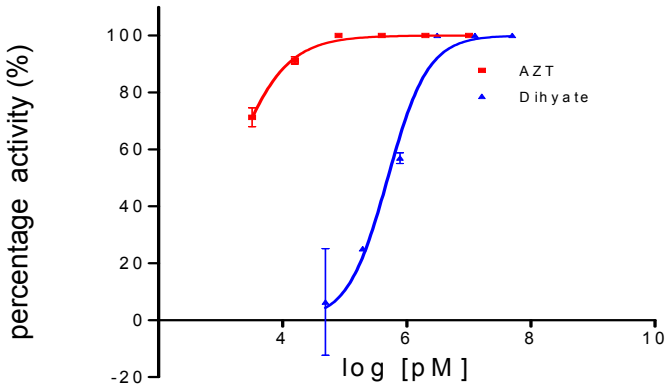

Figure 15. Inhibition of wild type HIV replication. NL43 virus co-culture was maintained in the presence of different concentrations of AZT and dihyate for 48 h and the supernatant was used to infect TZM cells to quantify the amount of particles formed in the presence of inhibitors. The mean count of wells with "no drug and no virus" was normalized to 100% activity and the mean count of wells "no drug and with virus" was normalized to 0 % activity. Percentage activities were deducted for treated wells.

3.1.3. *In silico* prediction of pharmacokinetic properties of dihyate

We evaluated the pharmacokinetic (PK) properties of dihyate *in silico* using VolSurf and MetaSite predictors. Molecules were projected on pre-calculated models: Caco-2 cell absorption, plasmatic protein binding, solubility, metabolic stability and volume of distribution. AZT and DHA were used as control drugs since they are dihyate precursor drugs. From the plots (figure 16), AZT and DHA were predicted to have higher solubility compared to dihyate, with AZT being the more soluble. When projected to the plasma affinity model, dihyate showed moderate affinity to plasma protein while DHA and AZT were predicted to have less affinity. AZT was further predicted to be highly stable, while DHA was anticipated to have an intermediate metabolic stability. The control drugs were predicted to be

more stable than dihyate which was predicted to have the lowest stability. When projected on the Caco 2 permeability model, DHA was predicted to have the highest permeability while dihyate was predicted to have intermediate permeability. Finally we predicted the volume of distribution; AZT and dihyate were predicted to have an intermediate volume of distribution while DHA was predicted to have a low volume of distribution.

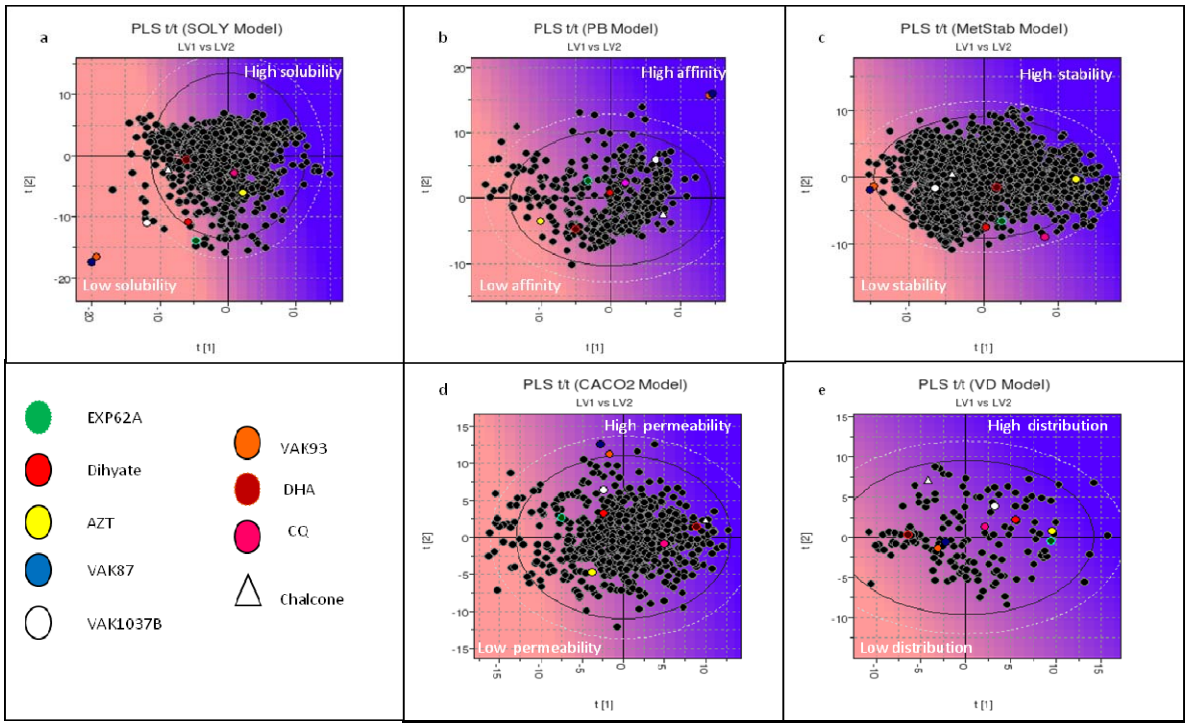

Figure 16. Projection of the studied compounds. The precalculated VolSurf models a) solubility, b) protein binding, c) metabolic stability, d) Caco-2, e) volume of distribution were used to predict PK properties of dihyate (red dot).

In silico metabolism prediction of dihyate was further characterized using MetaSite software. MetaSite predicted two types of biotransformations for dihyate in its top 5 predictions, and the main route of metabolism for dihyate was predicted to be O-dealkylation at the oxygen linking AZT to DHA moieties and the predicted metabolites were DHA and an oxidized analog of AZT (figure 17A). The software also predicted aliphatic hydroxylations at several sites of the DHA moiety of dihyate. AZT and DHA were also used as controls and the software predicted an alcoholic oxidation of AZT and an aliphatic hydroxylation of DHA as the main metabolic biotransformation reactions (figure 17B, C). Phase II metabolism was not predicted in this study.

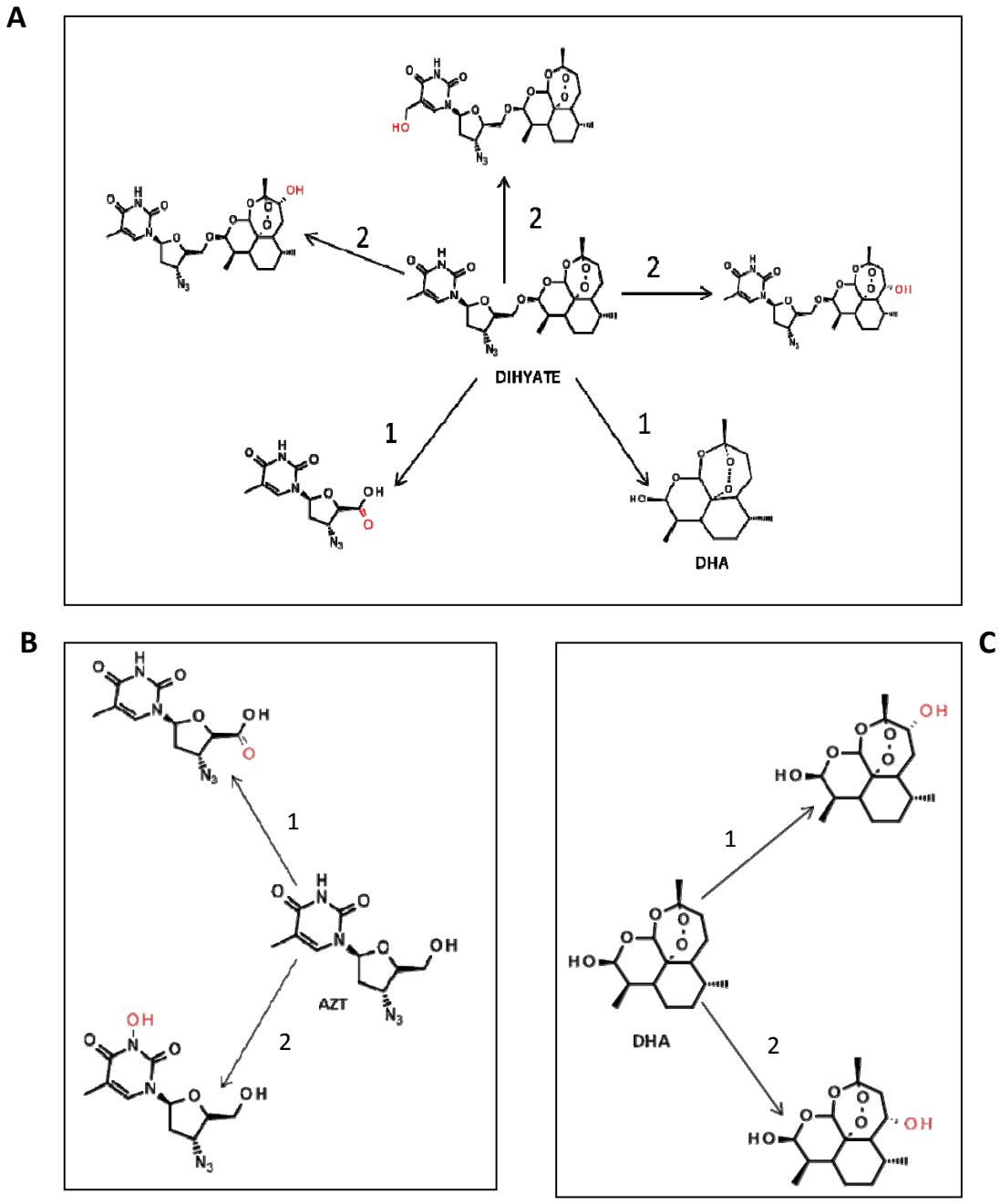

Figure 17. Metabolites prediction with MetaSite. **A)** Metabolites of dihyate released after being metabolize in the liver by Cytochrome P450. (1) Indicates O-dealkylation followed by the oxidation of AZT resulting in a release of DHA and an oxidized analog of AZT. (2) Indicates aliphatic hydroxylation of dihyate resulting in a release of different forms of hydroxylated products of dihyate. **B)** Metabolites of AZT. (1) Alcoholic oxidation and (2) aliphatic hydroxylation. **C)** Metabolites of DHA. (1, 2) aliphatic hydroxylations.

3.1.4. *In vivo* antimalarial efficacy studies

Dihyate formulated into pheroid vesicles was evaluated *in vivo* using the *P. berghei* mouse model. Infected mice were treated for 4 days and the parasitemia was monitored on days 2, 4 and 7. The parasitemia (%) was calculated for each mouse and mean parasitemias and standard deviations were calculated (Table 12).

Table 12. *In vivo* activity of dihyate against the erythrocytic forms of *P. berghei N*

Compounds	Dose (mg/Kg per day)	Parasitemia D2 (%)	Parasitemia D4 (%)	Parasitemia D7 (%)
Dihyate	20	4.24 ± 0.6	11.43 ± 2.6	35.2 ± 3.6
CQ	10	<1%	<1%	<1%
Untreated control	0	3.2 ± 1.3	9.9 ± 1.8	33.1 ± 3.4

***D:** day*

Dihyate treatment did not reduce parasitemia at the administered concentration 7 days after the beginning of the treatment. These data suggest that dihyate doesn't suppress parasite growth *in vivo* after oral administration. Dihyate appeared not to be toxic to mice as mice in the dihyate treated group became distressed at the same time as mice from the untreated group. For a drug to be effective, enough of the active form must reach the target to elicit the desired effect. We therefore sought to understand why the molecule was not active *in vivo*.

3.1.5. Evaluation of dihyate bioavailability *in vivo*

To verify data obtained from *in silico* predictions, dihyate was administered to mice in two different formulations: the first group of mice received dihyate dissolved in DMSO/H_2O (1:9, v/v) and the second group received dihyate formulated into pheroid vesicles. We found no trace of dihyate in the plasma from the group of mice treated with dihyate dissolved in DMSO/ H_2O (figure 18A), but after being formulated into pheroid vesicles, a maximal concentration of approximately 40 ng/ml was measured in mouse plasma (figure 18B). This suggests that the absorption of dihyate is enhanced by pheroid formulation, but the peak-like shape indicate a rapid clearance of the parent drug (figure 18B). The 2

precursor drugs were further quantified in the same plasma samples collected from our two groups of mice, AZT was present in the blood (figure 19A, C) of both groups of mice but not DHA (Figure 19B, D).

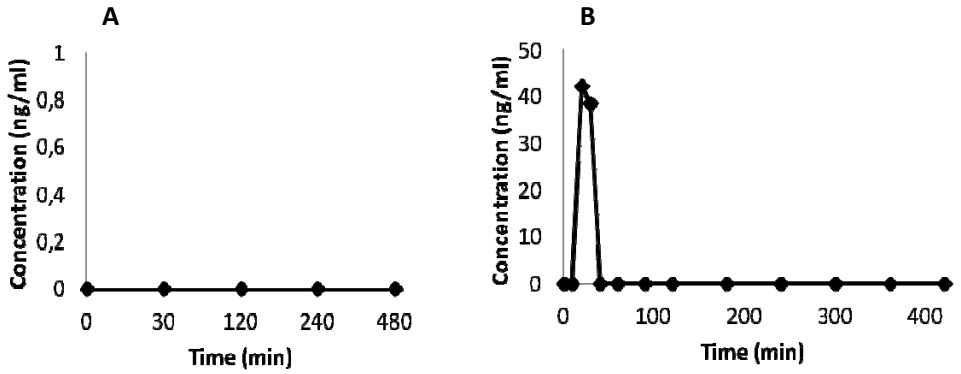

Figure 18. Plasma concentration–time profiles of dihyate. A) Plasma concentration of dihyate in mice treated by oral administration of 20 mg/kg dissolved in 10% DMSO; **B)** Plasma concentration in mice treated by oral administration of 20 mg/kg dissolved in Pheroids formulation.

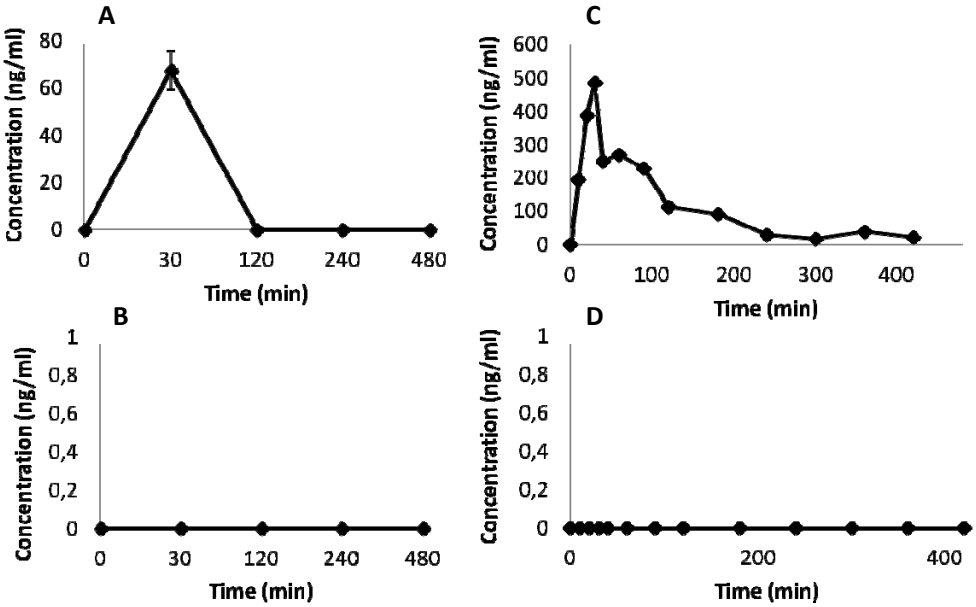

Figure 19. Plasma concentration–time profiles of AZT and DHA. **A)** Plasma concentration of AZT in mice treated by oral administration of 20 mg/kg dissolve in 10% DMSO **B)** Plasma concentration of DHA in mice treated by oral administration of 20 mg/kg dissolved in 10% DMSO **C)** Plasma concentration of AZT in mice treated by oral administration of 20 mg/kg dissolved in Pheroids formulation and **D)** Plasma concentration of DHA in mice treated by oral administration of 20 mg/kg dissolve in Pheroids formulation.The experiments were performed once.

3.1.6. *In vitro* metabolism of dihyate

To further investigate the metabolism of dihyate and to verify observations made *in vivo*, we carried out an *in vitro* study, taking into consideration that no elimination would occur and we would probably be able to identify DHA presence. The presence of AZT in buffer was detected after 15 min incubation while more than 90 % of dihyate was already metabolized. DHA was still not detected as previously observed *in vivo* (figure 20).

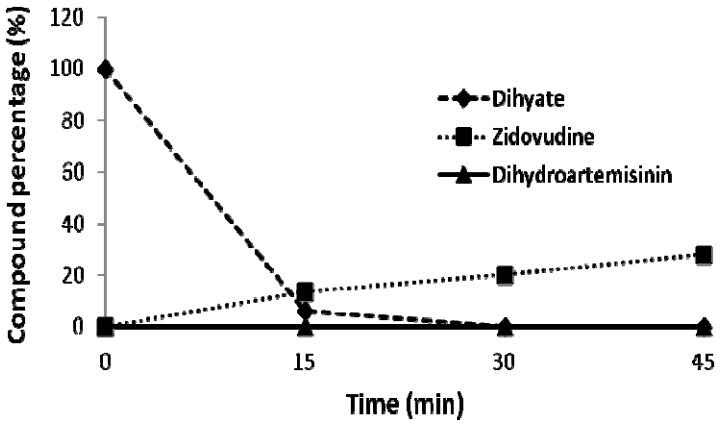

Figure 20. Dihyate metabolism in mice liver microsomes.

3.2. Thiostrepton activity and mode of action

3.2.1. Antimalarial activity of thiostrepton and derivatives

A number of thiostrepton derivatives were generated by selective oxidization of the thiazoline residue to improved chemical stability, and a small focussed library of candidate compounds was synthesized using combinations of tail truncation, oxidation, and addition of lipophilic thiols to the terminal dehydroamino acid to improve antiplasmodial properties (Schoof et al., 2010). Thiostrepton and derivatives were evaluated for their antimalarial activity in the CQ-sensitive 3D7. Compounds with IC_{50} < 5 µM, i.e. exhibiting a better IC_{50} concentration than thiostrepton, were considered for further evaluations on CQ-resistant strain of *P. falciparum* (strain Dd2).

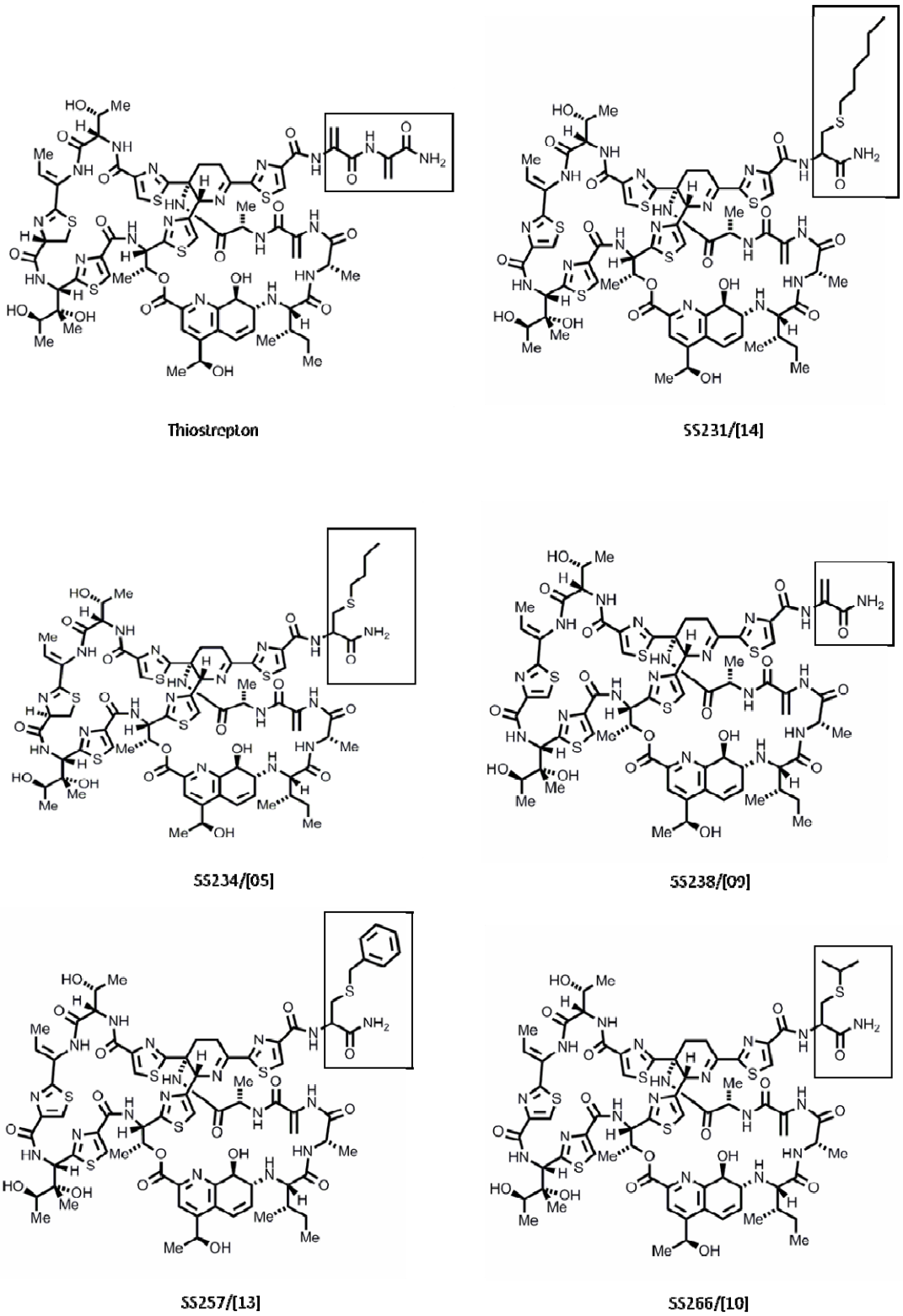

Figure 21. Chemical structures of thiostrepton and most active derivatives. black frame: appendage

Table 13. Antimalarial activities of the compounds, cytotoxicity and selectivity index of thiostrepton and derivatives.

Compounds	IC_{50} (µM)				Cytotoxicity
	Antimalarial activity				
	3D7	Dd2	SI_1	SI_2	
Thiostrepton	8.9 ± 1.7	16.7 ± 3.3	3.1	1.7	27.8 ± 10.9
SS231	1.0 ± 0.4	1.7 ± 0.3	>100	>59	> 100
SS234	1.0 ± 0 .1	1.3 ± 0.2	>100	>77	> 100
SS238	2.9 ± 0.3	2.3 ± 1.1	7.2	9.2	21.1 ± 10.3
SS257	1.4 ± 0.4	0.8 ± 0.1	>71.4	>125	> 100
SS266	3.5 ± 0.4	1.3 ± 0.2	>29	>77	> 100
Epoxomicin	0.03 ± 0.001	/	/	/	/
MG132	0.05 ± 0.02	0.04 ± 0.001	/	/	/
CQ	0.027 ± 0.002	0.45*	>3000	>200	>100

**Tested once in this assay*

SI_1 represent the selectivity index for sensitive strain (3D7) and SI_2 for resistant strain (Dd2)

Thiostrepton exhibited a modest antimalarial activity with an IC_{50} value of 8.89 µM in our assay. Some thiostrepton-based derivatives revealed an increased activity (figure 21; table 13); with an 8-fold higher activity for derivatives SS231 and SS234 (table 13). No differences were observed between the activities of compounds against CQ-sensitive and CQ-resistant malaria parasites. Furthermore, the proteasome inhibitors epoxomicin and MG132 were tested in our assay (table 13). Epoxomicin and MG132 were previously shown to exhibit highest antiplasmodial activities among proteasome inhibitors in various laboratory strains (Kreidenweiss et al., 2008) and exhibited growth inhibition with IC_{50} values of 0.03 µM and 0.05 µM, respectively, in our study (table 13).

Compound cytotoxicity was tested by MTT viability assay on HeLa cells, which measures the activity of the human mitochondrial dehydrogenase. Among thiostrepton derivatives, only SS238 showed a moderate cytotoxic effect on HeLa cells (IC_{50} = 21.07 µM) (Table 13). Moderate cytotoxicity was also observed for thiostrepton (IC_{50} = 27.76 µM). The cytotoxic effect of thiostrepton on human cancer cell lines has previously been reported (Bhat et al., 2009 b).

3.2.2. Quantification of blood stage parasites after treatment with thiostrepton derivatives

To gain phenotypic insight into the mode of action of thiostrepton and derivatives, we investigated the stage of growth inhibition via blood stage quantification. Compounds were added to synchronized parasites at IC_{80} concentrations either at the ring, trophozoite or early schizont stage (figure 22). Blood smears were taken at seven time points between 0 and 48 h of drug treatment, stained with Giemsa, and the number of different blood stages, i.e. ring stages, trophozoites, early schizonts and mature schizonts, were counted under the microscope. The two most active compounds, SS231 and SS234, as well as thiostrepton and MG132 were chosen for these experiments and results were compared to DMSO-treated control parasites.

While parasites in the control wells completed the 48-h replication cycle, the growth of MG132-treated parasites was stopped immediately when MG-132 was added to the ring or trophozoite stage, thus prior to DNA replication (figure, 22 left and center panels). When added to the early schizont stage, MG132 was not able to eliminate all parasites within the first replication cycle, and a fraction escaped the immediate killing and entered the second cycle (figure 22, right panel). Similarly, thiostrepton and derivatives were able to eliminate the majority of parasites in the ring and trophozoite stages when the inhibitors were added to these stages (figure 22, left and center). A minority of parasites, however, escaped the immediate killing and entered the second replication cycle. When added to the early schizont stage, the compounds were not able to eliminate all parasites within the first cycle, which was particularly obvious for SS231 and SS234 treated cultures (figure 22, right). Here, the majority of parasites entered the second replication cycle and were present as ring stages at 48 h of drug treatment.

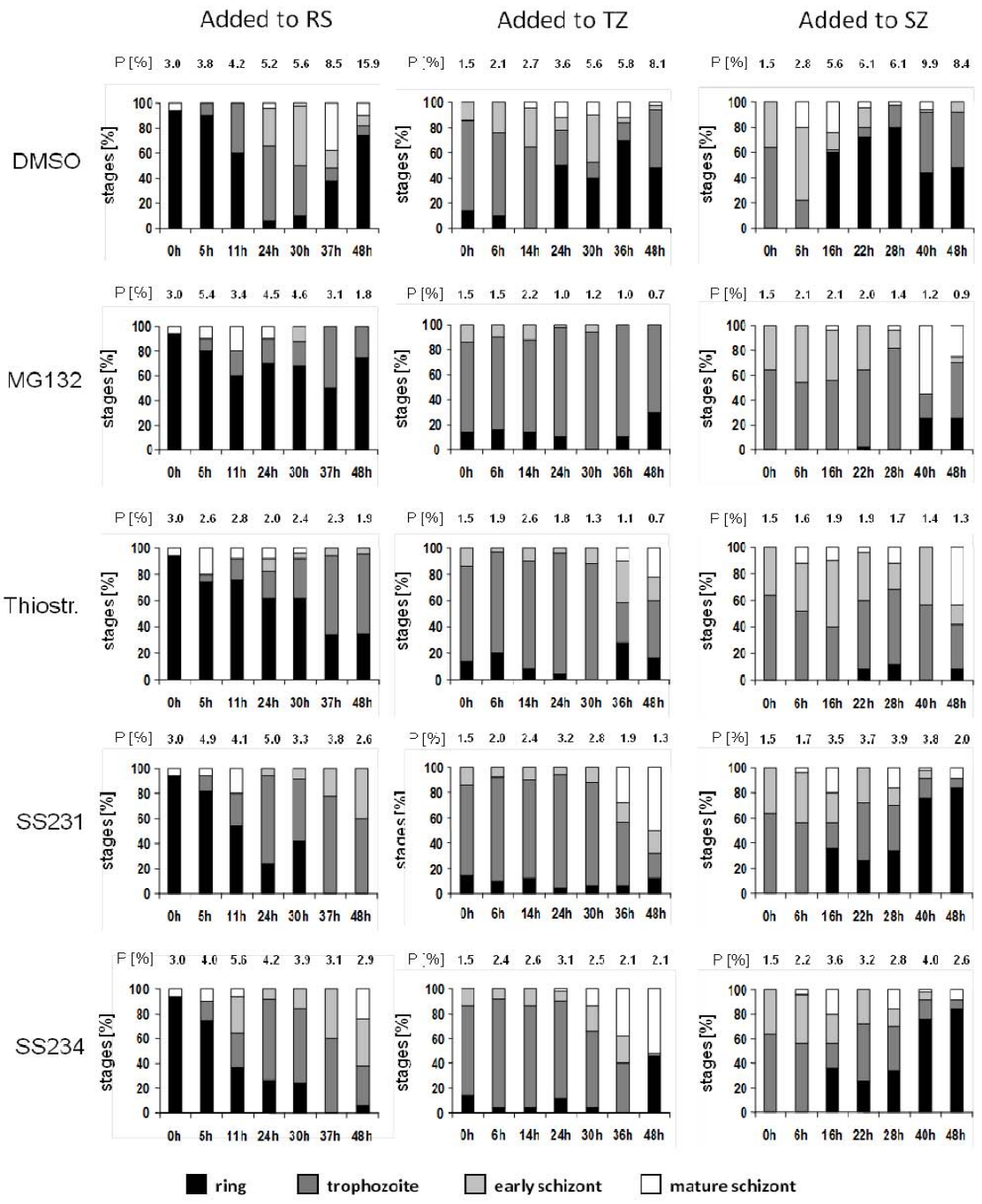

Figure 22. Stage of growth inhibition of *P. falciparum* during 48 h of compound treatment. Compounds at IC_{80} or in a 0.5% vol of DMSO were added to synchronized parasites at the ring, trophozoite, or early schizont stage. Histograms indicate the percentages of developmental stages present in the respective blood smears. The respective parasitemia (P) is indicated above each column. Fifty parasites were counted for each condition. In samples with low parasite numbers, 20 parasites were counted. RS, ring stage; SZ, schizont; TZ, trophozoite (Leubner, 2010).

To investigate the fate of the parasite fraction that had escaped the immediate killing and entered the second replication cycle, we applied a delayed-death test and determined parasite growth inhibition at 48, 72, 96, and 120 h of drug treatment. The ribosome-targeting antibiotics doxycycline and azithromycin were used as positive controls. These antibiotics were previously reported to induce the typical delayed-death phenotype (Barthel et al., 2008, Dahl et al., 2006, Sidhu et al., 2007). As expected, treatment with doxycycline SS234 also resulted in a decrease of the respective IC_{50}s during the incubation time and azithromycin showed a more than 10-fold decrease in IC_{50}s between 48 and 96 h of incubation (table 14). The treatment of parasites with thiostrepton, SS231, and SS234 also resulted in a decrease of the respective IC_{50} values during the incubation time. However, only approximately 3-fold decrease in the IC_{50}s was observed between 48 and 96 h of drug treatment. At 120 h of incubation time, compounds SS231 and SS234 exhibited antimalarial activities with IC_{50}s of 0.46 and 0.26 µM, respectively.

We then quantified the stage of growth inhibition for compound-treated parasites screened in the delayed-death test (figure 23). Parasites were treated with compounds at IC_{50}s. CQ was used as an immediate killing control and azithromycin as a delayed-death control in the tests. The DMSO treated parasites developed normally throughout the 48-h replication cycle, and ring stages were observed at 0, 48, and 96 h of culturing (figure 23). Treatment with CQ resulted in a strong reduction of parasite numbers during each replication cycle, while a minor fraction of parasites continued to grow (figure 23). In parasites treated with thiostrepton, SS231, or SS234, parasite numbers decreased drastically during the first replication cycle.

Table 14. Antimalarial activities of the compounds over time (delayed-death test)*

Compounds	**IC_{50} (µM) at:**			
	48 h	**72 h**	**96 h**	**120 h**
Doxycycline	17.6	5.4	3.1	0.52
Azythromycin	18.3	2.1	4.1	0.12
Thiostrepton	8.2	4.7	2.8	2.1
SS231	1.6	0.62	0.52	0.46
SS234	2.0	0.46	0.57	0.26

**experiment was performed once*

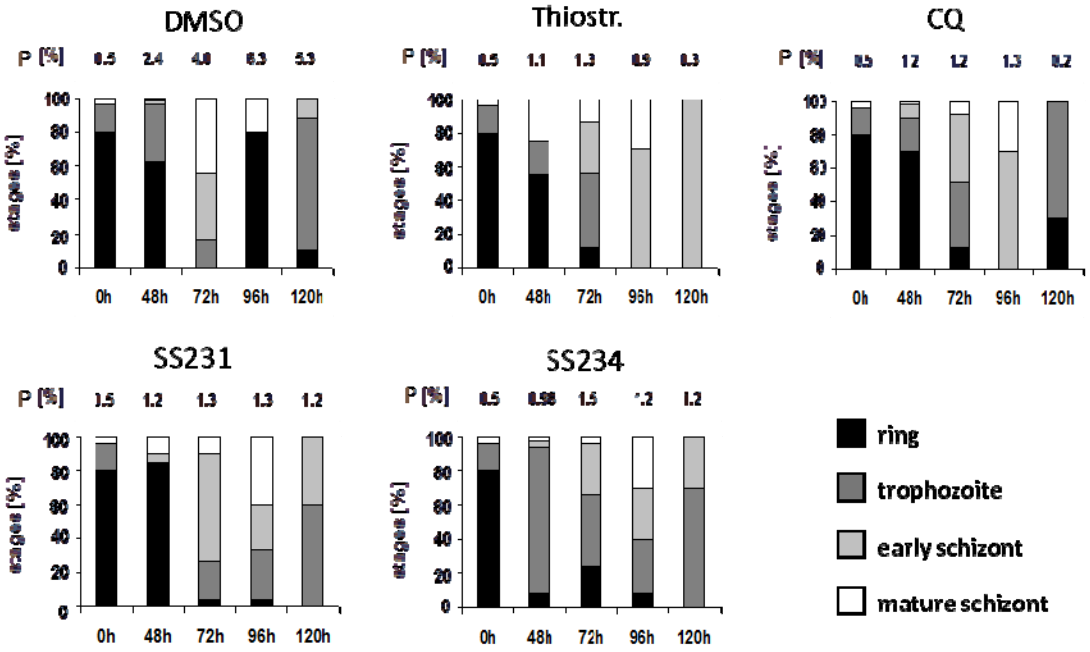

Figure 23. Delayed-death effect. Compounds at IC_{50}s or a 0.5% volume of DMSO was added to synchronized ring-stage parasites. Giemsa-stained blood smears were made at 0, 48, 72, 96, and 120 h of incubation with inhibitor, and the developmental stages were quantified as described in figure 19. The respective parasitemia (P) is indicated above each column. A total number of 50 parasites were counted for each condition. In samples with low parasite numbers, 20 parasites were counted.

3.2.3. Toxicity of thiostrepton and derivatives to red blood cells

We investigated the potential effect of thiostrepton and derivatives on erythrocyte integrity to rule out the fact that our inhibitors may have an effect on the proteasome of red blood cells instead. Fourty eight hour incubation of red blood cells with 10 µM of compounds did not increase the amount of free hemoglobin in the medium, when compared to controls treated with medium alone or with 0.5% DMSO (figure 24). Erythrocyte-lysis with saponin, which was used as positive control, resulted in an approximate 26-fold increase in OD_{550}-values of the supernatant.

We also exposed uninfected erythrocytes to 5 µM thiostrepton and derivatives as well as with MG132 (10 µM and 200 nM), epoxomicin (100 nM) and CQ (100 nM) for 3h. Pre-treated erythrocytes were then used to culture parasites, and growth inhibition was quantified by Malstat assay. No growth inhibition was observed for any of the drug-treated parasites after 72 h, when compared to untreated control parasites (figure 25), indicating that pre-treatment of erythrocytes with compounds has no

effect on parasite viability. However a reduced parasite growth was observed when erythrocytes were pre-treated with 10 µM MG132.

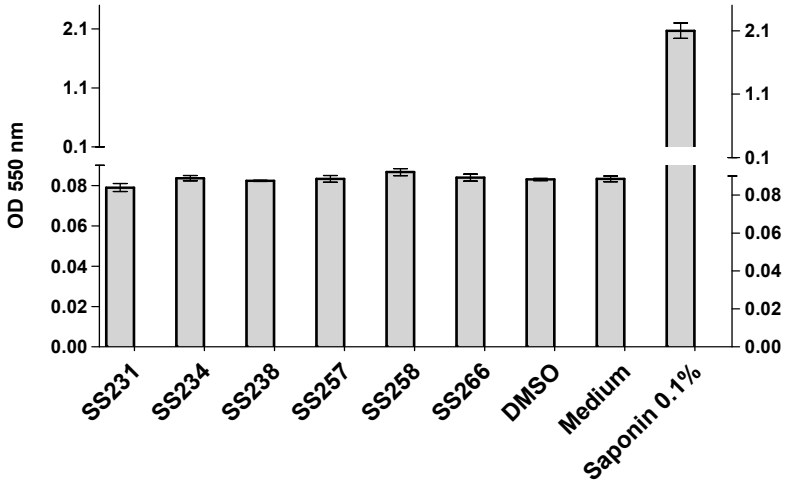

Figure 24. Effect of compounds on red blood cells integrity. RBCs were treated for 48 h in the presence or absence of 10 µM of each compounds, lysis of RBCs with 0.1 % saponin was used as positive control. The hemoglobin content of the supernatant was determined photometrically as an indication of cell integrity**.** Experiments were done in quadruplicate.

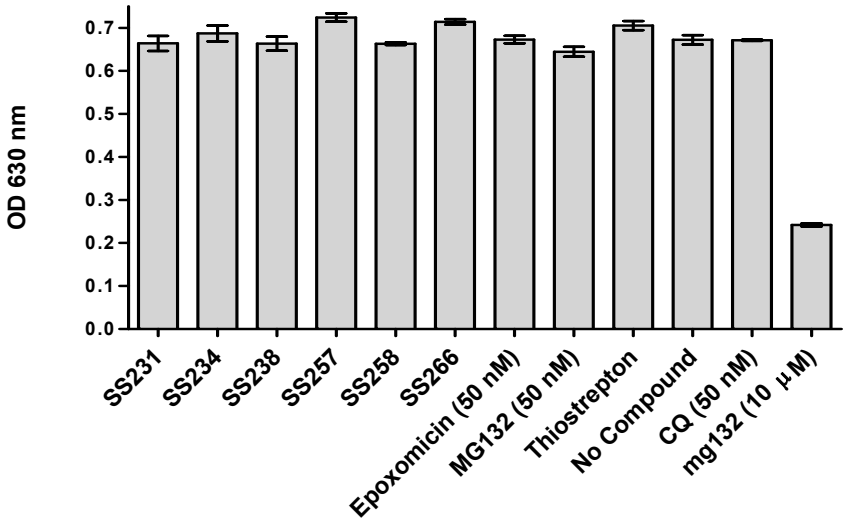

Figure 25. Effect of compound on RBCs. RBCs were pre-incubated with 5 µM of compounds for 3h and subsequently used for parasite culture. No significant difference compared to no compound control was detected in parasite development after 72 h incubation. MG132 and Epoxomicin are known proteasome inhibitors and were used as controls. Experiments were done in quadruplicate. Mean ± SD.

3.2.4. Gametocytocidal activity of thiostrepton and derivatives

We investigated the toxic effect of the thiostrepton-based compounds on gametocyte maturation. Gametocytes are intraerythrocytic sexual precursor cells, which are formed by the parasite in response to stress and which mediate the transition of the parasite from the human to the mosquito (reviewed in Kuehn and Pradel, 2010; Pradel, 2007). The gametocytocidal effect of a compound would block further transmission of parasites that escaped the blood stage killing and thus counteract further spread of drug resistance. Thiostrepton and derivatives SS231 and SS234 were added to young gametocyte cultures at stage II. The numbers of gametocytes of stages IV and V were counted seven days later and compared to DMSO-treated control gametocytes. For positive control, gametocytes were treated with epoxomicin and primaquine, while azithromycin-treated gametocytes were used as negative control (figure 26). The gametocyte toxicity assay revealed that epoxomicin and thiostrepton fully eliminated gametocytes in the cultures at IC_{50} concentrations, while primaquine resulted in a reduction of gametocyte numbers of 62 % (figure 26). Treatment with MG132, SS231 and SS234 did not result in a significant reduction of gametocytes, when added at IC_{50} concentrations, while a significant decrease in gametocyte numbers was observed, when these compounds were added at IC_{90} concentrations. Azithromycin treatment had no significant effect on the development of gametocytes (figure 26).

3.2.5. Effect of thiostrepton and derivatives on the parasite proteasome

The rapid elimination of malaria parasites treated with thiostrepton and derivatives leads to the assumption that the compounds have an additional target besides the apicoplast. All compounds have previously been shown to inhibit human proteasome *in vitro* (Schoof et al., 2010), and one of the active derivatives exhibited a modest inhibition of HeLa cells growth. Therefore, an effect on the parasite proteasome can be expected. We then investigated the effect of thiostrepton and derivatives on the parasite proteasome by monitoring the accumulation of ubiquitinated proteins. Synchronized parasites at the early trophozoite stage were treated with the compounds IC_{80} for 6 h, harvested and parasite extracts were investigated by Western blot using mouse anti-ubiquitin antibody. Treatment with MG132 was used as positive control and CQ-treatment as negative control in the assays. The effect of ciprofloxacin on the proteasome was also investigated as a non-proteasome inhibitor control. A number of ciprofloxacin derivatives bearing a ferrocenyl-, a benzyl- or an adamantyl substituent at C (7) of the quinolone ring were generated (table 15). In parallel, to enhance the hydrophobic capacity

of these products, a prodrug strategy consisting of the ethyl esterification of the carboxylic acid was adopted (Dubar et al., 2009).

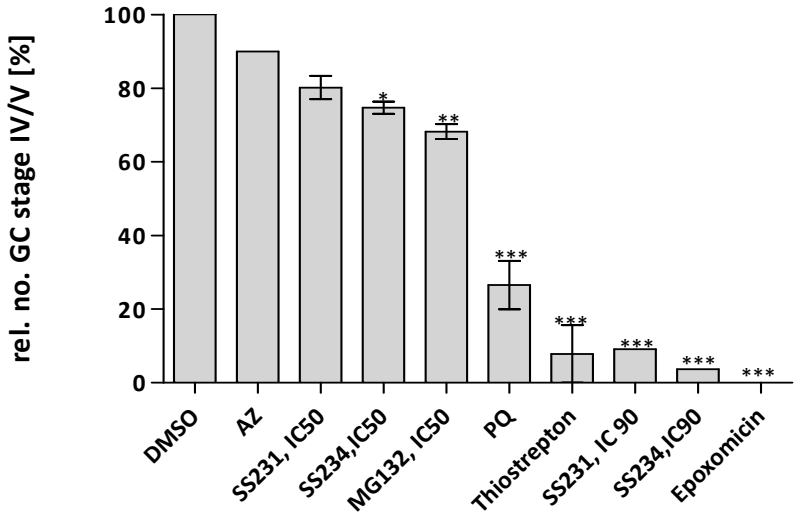

Figure 26. Inhibition of gametocytogenesis. Compounds at IC_{50}s or IC_{90}s or a 0.5% volume of DMSO were added to stage II gametocyte cultures for 2 days. The numbers of stage IV and V gametocytes were counted after 7 days and correlated to the gametocyte numbers of the DMSO control (set to 100%). The graph represents results of at least two independent experiments done in triplicate PQ, SS231 IC50, SS243 IC_{50}, Thiostrepton and MG132 IC_{50} (mean ± SEM) and a single experiment for Epoxomicin, SS231 IC_{90}, SS234 IC_{90} and Azythromicin (AZ) (mean ± SD). Statistical analysis was done using one way ANOVA followed by a *Tukey* test, mean gametocytemia of compounds tested once were compare with mean gametocytemia in DMSO control using t-test (GraphPad Prism 5). Asterisks represent a significant difference between tested compounds and DMSO control, where *** correspond to $P < 0.001$; **correspond to $0.001 < P < 0.01$; * correspond to $0.01 < P < 0.05$ and for $p > 0.05$ the difference in not considered significant and there is no asterisk.

Western blot analysis revealed an accumulation of ubiquitinated proteins in parasites treated with MG132, thiostrepton or derivatives, when compared to 0.5% DMSO-treated control (Figure 27A, upper panel). Labelling for ubiquitinated proteins was particularly strong, when parasites were treated with thiostrepton, SS234 or SS238. No accumulation of ubiquitinated proteins was detected in CQ and SS231 treated parasites (figure 27A, upper panel). As expected, no accumulation was also observed after treatment with ciprofloxacin and derivatives (figure 27B, upper panel) as they are known to target parasite replication. Coomassie-staining of protein gels was used for equal loading control (figure 27A, B, lower panel).

Table 15. Structure of ciprofloxacin and derivatives and their respective IC_{50} and IC80 values

Compounds	structures	IC_{50} (µM) (3D7_48h)	IC_{80} (µM)
Ciprofloxacin	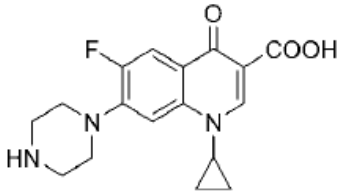	47.0	188
Cipro-Ethyl	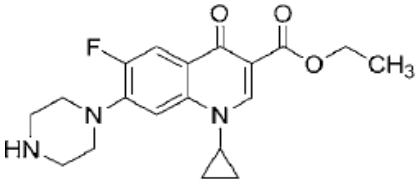	2.33	9.3
Cipro-Ferrocenyl	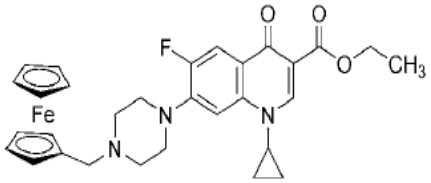	2.63	10.5
Cipro-Benzyl	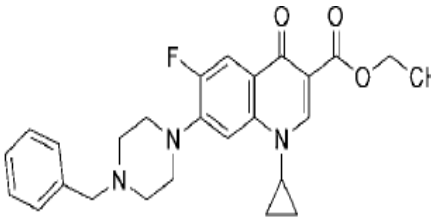	1.08	4.3
Cipro-Adamantyl	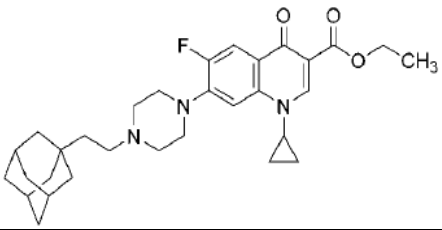	1.00	Not tested

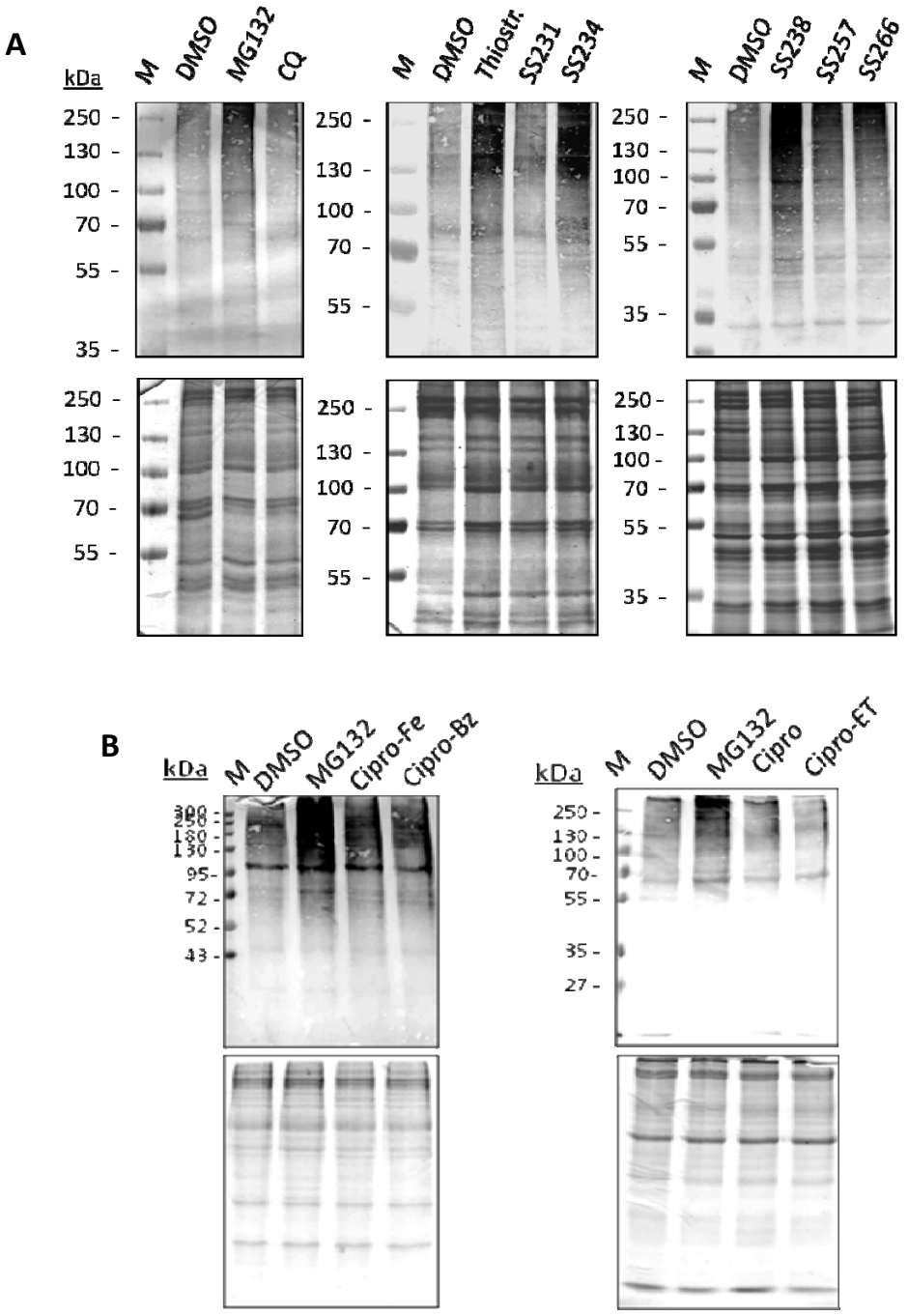

Figure 27. Accumulation of ubiquitinated blood-stage proteins following compound treatment. Synchronized early trophozoites were incubated for 6 h with compounds at IC_{80}s or with a 0.5% volume of DMSO. Parasite extracts were separated by polyacrylamide gel electrophoresis and screened via Western blot analysis. Ubiquitinated parasite proteins were detected with mouse antibody against ubiquitin (A, B, upper). The Coomassie blue staining of protein gels was used to demonstrate the equal loading of parasite protein extract (A, B, lower). For ciprofloxacin (Cipro), 2 x IC_{50} was used.

3.3. The plasmodial proteasome as a potential drug target

3.3.1. Identification of human proteasome subunits homologs in parasite genome

In order to identify parasite homologs of the 26 S proteasomal SUs, we performed a BLAST search using human proteasome SU proteins as queries against the *P. falciparum* 3D7 genome. Predicted homologs of proteasome precursor or SU sequences were ranked as having high score segment pairs and low P-values. The computational analysis revealed plasmodial homologs for all of the human 26S proteasome SUs (table 16).

Table 16. Homologs of 19S and 20S proteasome subunits identified in *P. falciparum* genome

Proteasome subunits	*Homo sapiens* (accession number)	*P. falciparum* (Plasmodb code)	Identities	P-value
CP subunits				
Proteasome subunit α type 1	P25786	PF14_0716	44%	8.7e-52
Proteasome subunit α type 2	P25787	PFF0420c	57%	3.2e-70
Proteasome subunit α type 3	P25788	PFC0745c	34%	3.7e-44
Proteasome subunit α type 4	P25789	PF13_0282	53%	3.4e-66
Proteasome subunit α type 5	P28066	PF07_0112	54%	5.5e-66
Proteasome subunit α type 6	P60900	MAL8P1.128	45%	3.1e-56
Proteasome subunit α type 7	O14818	MAL13P1.270	53%	2.6e-59
Proteasome subunit β type 1	P20618	PFE0915c	43%	4.0e-47
Proteasome subunit β type 2	P49721	PF14_0676	37%	6.3e-33
Proteasome subunit β type 3	P49720	PFA0400c	43%	3.7e-44
Proteasome subunit β type 4	P28070	MAL8P1.142	42%	6.0e-41
Proteasome subunit β type 5	P28074	PF10_0111	53%	1.2e-59
Proteasome subunit β type 6	P28072	PFI1545c	29%	8.3e-27
Proteasome subunit β type 7	Q99436	PF13_0156	53%	1.6e-66
RP base subunits				
26S protease regulatory subunit 7 or RPT1	P35998	PF13_0063	70%	1.2e-159
26S protease regulatory subunit 4 or RPT2	P62191	PF10_0081	77%	1.5e-168
26S protease regulatory subunit 6B or RPT3	P43686	PFD0665c	64%	4.6e-133

26S protease regulatory subunit 10B or RPT4	P62333	PF13_0033	67%	2.8e-142
26S protease regulatory subunit 6A or RPT5	P17980	PF11_0314	71%	7.3e-158
26S protease regulatory subunit 8 or RPT6	P62195	PFL2345c	74%	2.0e-155
26S proteasome non-ATPase regulatory subunit 2 or RPN1	Q13200	PFB0260w	37%	1.5e-143
26S proteasome non-ATPase regulatory subunit 1 or RPN2	Q99460	PF14_0632	43%	1.3e-161
26S proteasome non-ATPase regulatory subunit 4 or RPN10	P55036	PF08_0109	41%	4.6e-37
26S proteasome non-ATPase regulatory subunit RPN13	Q16186	PF14_0138	35%	6.6e-17
RP lid subunits				
26S proteasome non-ATPase regulatory subunit 3 or RPN3	O43242	MAL13P1.190	35%	3.4e-73
26S proteasome non-ATPase regulatory subunit 12 or RPN5	O00232	PF10_0174	39%	1.6e-82
26S proteasome non-ATPase regulatory subunit 4 or RPN6	O00231	PF14_0025	35%	5.3e-51
26S proteasome non-ATPase regulatory subunit 6 or RPN 7	Q15008	PF11_0303	37%	1.1e-76
26S proteasome non-ATPase regulatory subunit 7 or RPN8	P51665	PFI0630w	39%	9.3e-55
26S proteasome non-ATPase regulatory subunit 13 or RPN9	Q9UNM6	PF10_0298	26%	1.2e-38
26S proteasome non-ATPase regulatory subunit 14 or RPN 11	O00487	MAL13P1.343	63%	1.2e-100
26S proteasome non-ATPase regulatory subunit 8 or RPN 12	P48556	PFC0520w	32%	1.6e-25
26S proteasome non-ATPase regulatory subunit RPN 15 or DSS1	P60896	MAL7P1.117	61%	0.53

3.3.2. Expression and sub-cellular localization of the 26S proteasome in blood stages of *P. falciparum*

The identification of genes in the *P. falciparum* genome that are homologous to proteasome subunits of other eukaryotes strongly suggests the presence of a 20S proteasome in the malaria parasite

(Bodzech et al., 2003; Mordmüller et al., 2006). However, before our study no detailed expression and subcellular localization data were available. To study the proteasome expression in blood stage parasites, we performed diagnostic RT-PCR analysis, using primers corresponding to distinct regions in the *α5-SU* and the *β5-SU* gene sequences. Synchronized parasites were harvested in the ring, trophozoite, schizont or gametocyte stages and cDNA was generated from isolated parasite RNA. Quality was verified by monitoring transcripts of stage-specific marker proteins, e.g. *AMA-1* for asexual blood stages or *PfCCp1* for gametocytes (figure 28). For control purposes, RNA samples were treated without reverse transcriptase, and no PCR product was amplified, indicating that genomic DNA-free samples were used. RT-PCR analysis of stage-specific cDNA using α5-SU and β5-SU specific primers revealed corresponding PCR products in all samples, indicating that these putative proteasome-subunits are expressed in these stages. However, transcript for both subunits was less abundant in ring stage parasites than in trophozoites, schizonts and gametocytes (figure 28).

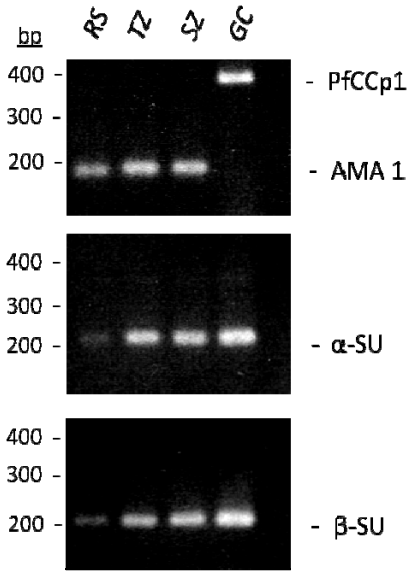

Figure 28. Diagnostic RT-PCR. Analysis of cDNA from ring, trophozoite, schizont, or gametocyte stage indicated transcript expression for proteasome subunits α-SU type 5 (224 bp) and β-SU type *5* (200 bp) in all blood stages with a low transcript abundance in ring stages. The detection of transcript for the asexual marker gene *AMA-1* (189 bp) and the gametocyte marker gene *PfCCp1* (371 bp) were used as quality and equal-loading controls (Leubner, 2010).

For further characterization, the full lenght of *α-SU type 5* and *β-SU type 5* genes were cloned in the pGEX-4T1 plasmid and GST-tagged proteins were expressed in *E.coli* BL21 (DE3) RIL. The purified GST fusion proteins (figure 29) were used to generate antibodies against *P. falciparum* proteasome subunits.

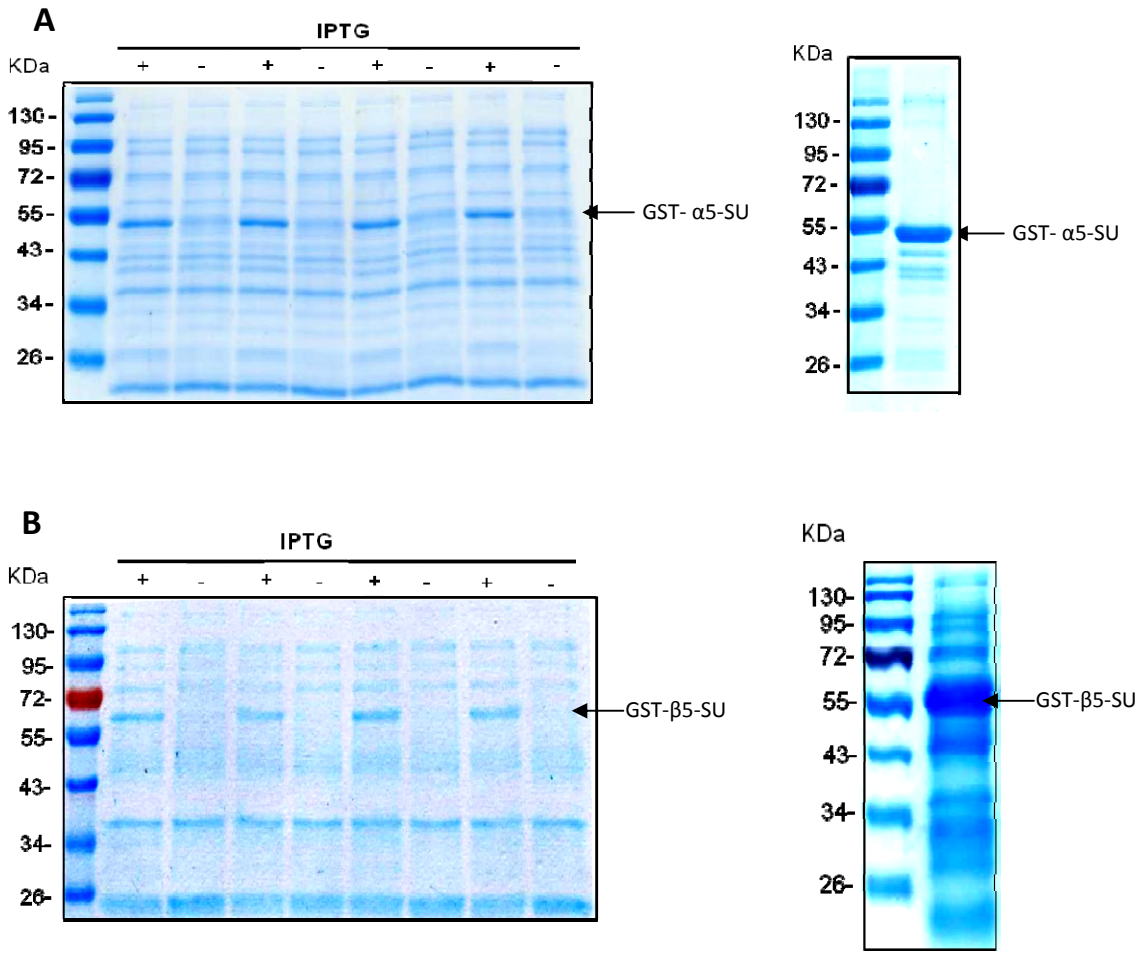

Figure 29. Generation of GST-tagged recombinant proteins. The full length of proteasome α5-SU **(A)** and β5-SU **(B)** homologs were cloned in pGEX-4T1 to generate recombinant proteins. Four colonies (**A** and **B**-left) from the overnight cultures were further cultured in the presence and absence of IPTG to verify expression of GST-tagged recombinant proteins. One of these colonies was selected for purification**.** Purified GST-tagged recombinant proteins were used to immunize six weeks old NMRI mice for polyclonal antibody generation (**A** and **B** -right).

The presence of eukaryotic proteasome in blood stage parasites was subsequently investigated by Western blot analysis. Antisera against recombinant α and β-SU type 5 proteins were generated by the immunization of mice and blotted against SDS PAGE-separated lysates of ring stages, trophozoites, schizonts and mature gametocytes. Western blotting detected one protein band with the expected molecular weight (calculated value: 28.4 kDa) for α-SU type 5, and approximately 25 kDa for β-SU type 5 which is 6 kDa smaller than the calculated value (figure 30-upper panel). The theoretical MW of β-SU type 5 is 30.6 kDa, however, most of the β-type proteasome subunit proteins are known to undergo proteolysis during proteasome maturation (Chen and Hochstrasser, 1995; Seemüller et al., 1995;

Frentzel et al., 1994), thereby releasing the active site residue. Amino acids Gly (-1) and Thr (1) are entirely conserved in all active proteasome beta subunits, with Gly (-1) being important for recognition of the cleavage site and Thr (1) as the catalytic nucleophile (Schmidtke et al., 1996, Seemüller et al., 1996). *P. falciparum* proteasome β-SU type 5 possesses the conserved GTTT active domains described in β-SU type 5 of human and other organisms (figure 31) and the cleavage between Gly (-1) and Thr (1) is predicted to release an active protein with a theoretical size of 23.6 kDa which correlates well with the observed protein band at approximately 25 kDa (figure 30-upper panel, right). The non-processed form of the protein was not detected by our antiserum; this might suggest a rapid processing of the protein. Both proteins were prominent in the trophozoite and schizont stages, but less abundant in ring stages. Blotting against the endoplasmic reticulum-specific protein Pf39 was used for equal loading control (figure 30, lower panel).

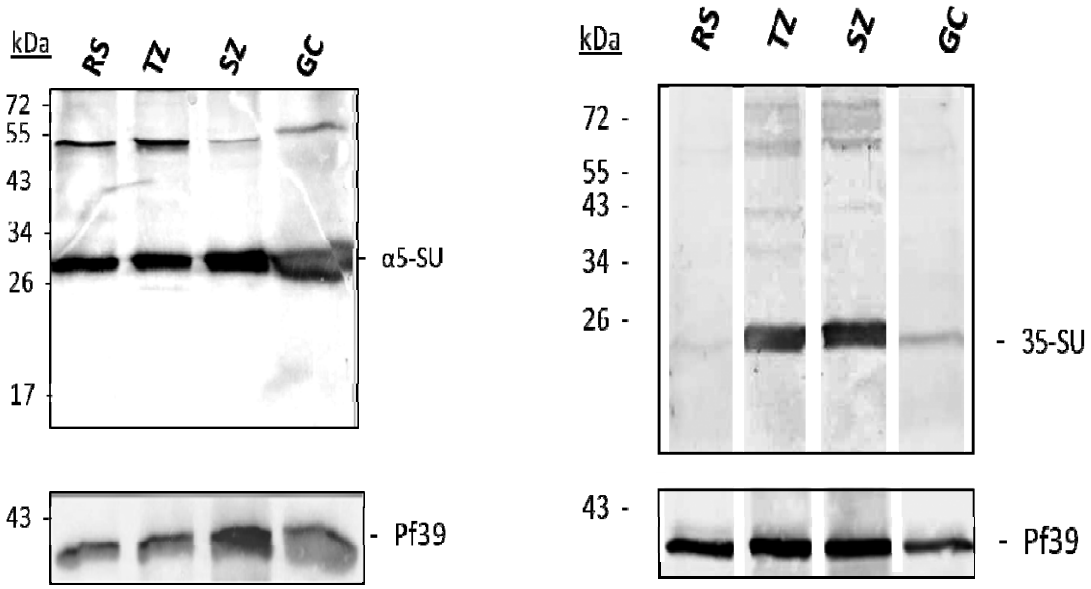

Figure 30. Protein expression of α5-SU and β5-SU in parasite extracts. Proteins presence was demonstrated by Western blot analysis using mouse polyclonal antisera. Screening with antisera against the endoplasmic reticulum protein Pf39 was used to demonstrate the equal loading of parasite extracts (lower). GC, gametocyte; RS, ring stage; SZ, schizont; TZ, trophozoite.

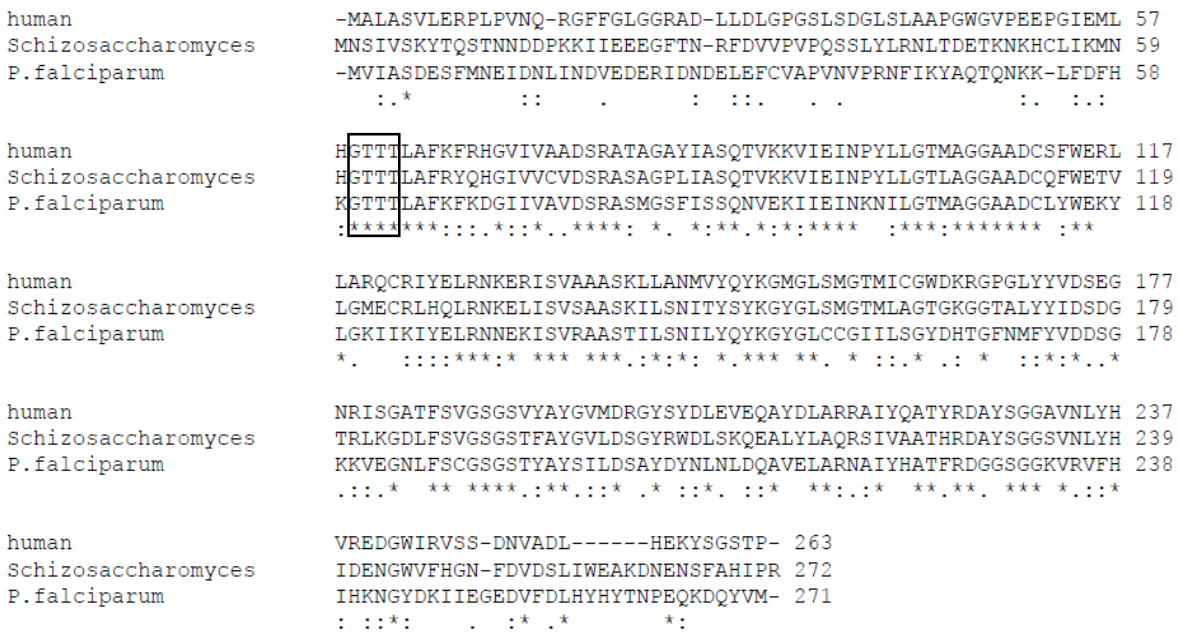

Figure 31. A multiple alignment of three proteasome β5-SU. Protein sequences (Human, *Schizosaccharomyces pombe*, *P. falciparum*) were retrieved from *uniprot* and *plasmo DB*. Multiple sequence alignment of proteasome β5-SU was generated using ClustalW2 (www.ebi.ac.uk/clustalW).The conserved active site in proteasome beta subunit is highlighted in red.

The subcellular localization of α-SU type 5 and β-SU type 5 was also investigated in the parasite blood stages by immunofluorescence assay. While there was only a minor punctuated labelling detected in the ring stages (figure 32A, B; RS), α5-SU and β5-SU were abundantly expressed in trophozoites and schizonts (figure 32A, B; TZ and SZ) where they were present in the cytoplasm and associated with the parasite nucleus. In gametocytes, α5-SU and β5-SU were primarily localized to the cytoplasm and they appeared to be expressed throughout gametocyte maturation (Stage II to V) (figure 32A, B, GC). Uninfected erythrocytes did not label for β5-SU, and sera of non-immunized mice did not result in any labelling of the parasite.

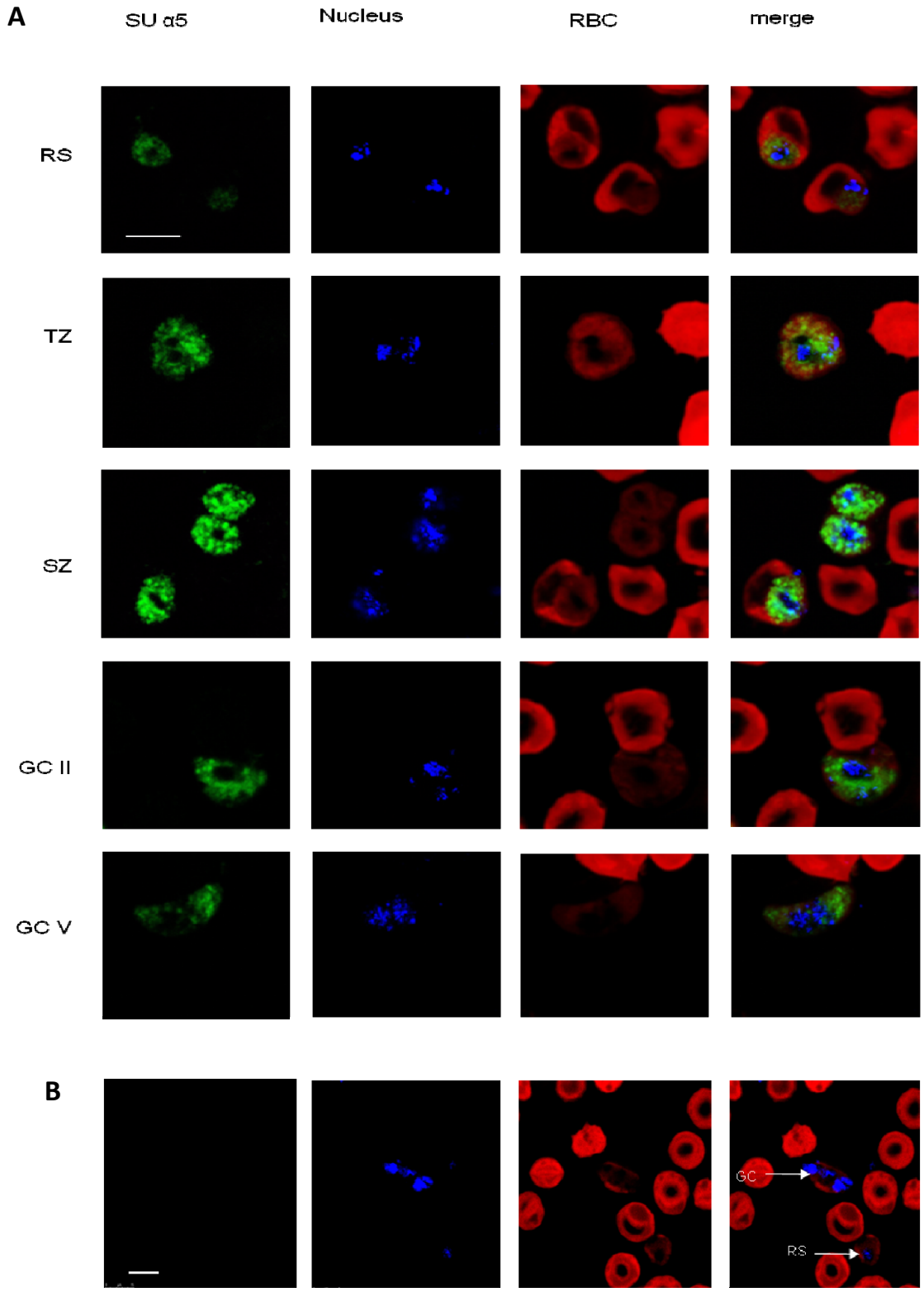

Figure 32. Indirect immunofluorescence assays. *See legend on the next page*

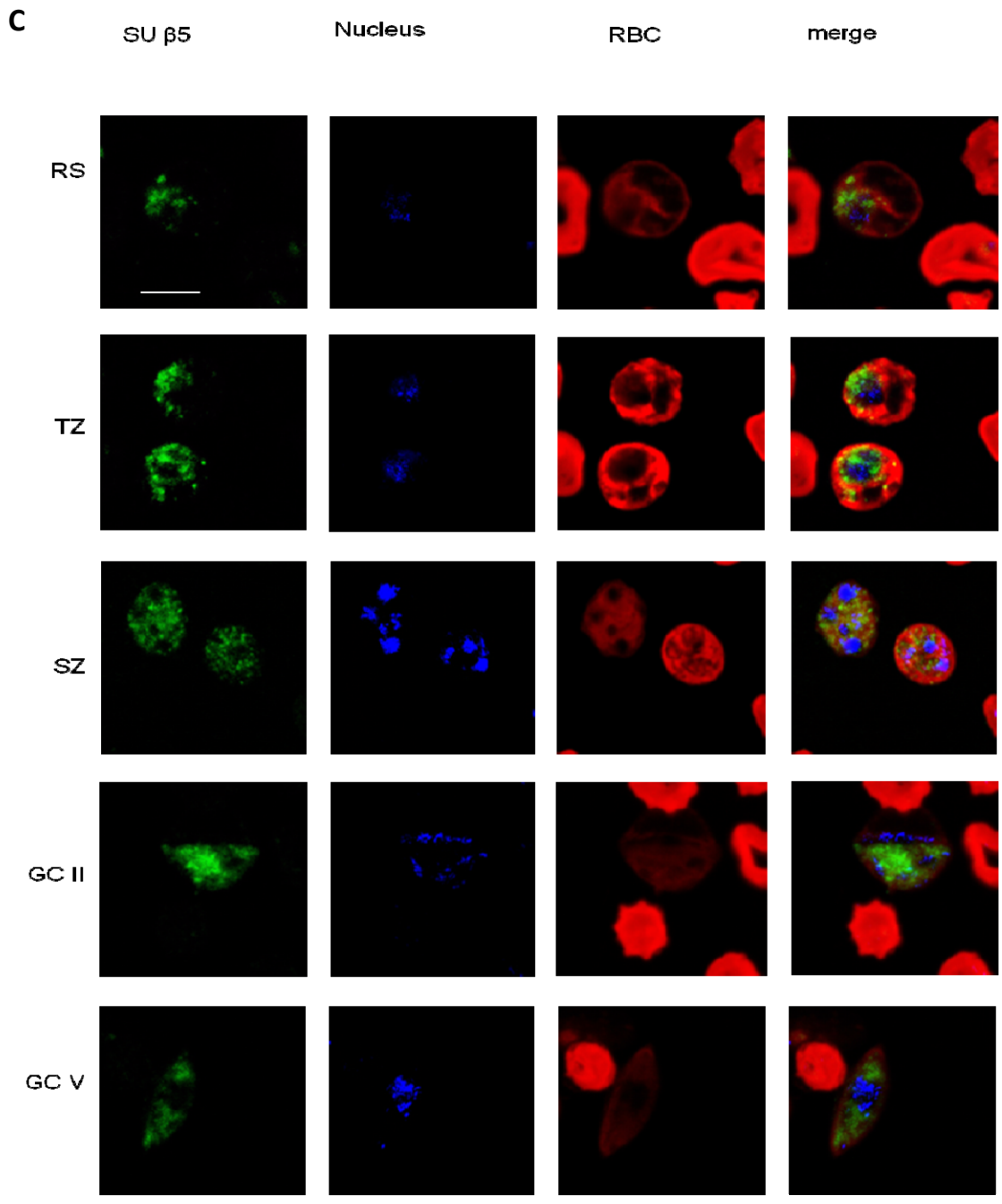

Figure 32. Indirect immunofluorescence assays. Polyclonal antisera against α-SU type 5 **(A)** and β-SU type 5 **(C)** revealed that the two proteins are localized in the asexual blood stages as well as in the gametocyte stages (stages II and V). Nuclei were highlighted by Hoechst nuclear staining (blue); and erythrocytes were counterstained by Evans Blue (red). Neutral mice serum did not stain the parasite (**B**; control) which means the staining was specific. GC, gametocyte; RBC, red blood cell; RS; ring stage, SZ, schizont; TZ, trophozoite. Bar 5 µm. (Images were taken by G. Pradel)

IEM was performed to gain more insight on the sub-localization of the proteasome using anti-β5-SU antibody. IEM revealed that β5-SU is abundantly present in the nuclei of trophozoites and schizonts, but not in the nucleolus (figure 33B). The protein is further present in the cytoplasm of blood stage parasites. No gold labelling was detected in the erythrocyte cytosol, the parasite rhoptries or the food vacuole (figure 33B).

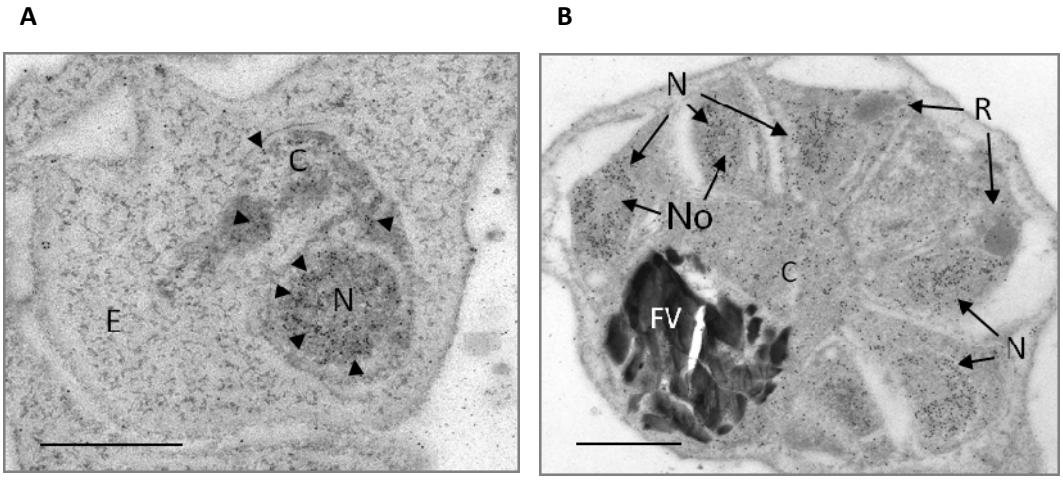

Figure 33. Immunoelectron microscopy. Anti β-SU type 5 antisera in combination with gold (12-nm) coupled secondary antibody indicated the ultrastructural localization of the protein in trophozoites and schizonts. Arrow heads indicate gold particles. Bar 1 µm (Images were taken by G. Pradel)

Lastly we visualized binding of a fluorescent thiostrepton probe (Schoof et al., 2009) to blood stage parasites. Parasites were incubated with the probe for 4 h, fixed with methanol and processed for immunofluorescence assay. The fluorescent probe was mainly localized in schizonts associated with the nuclei in a similar staining pattern described above for the antibodies against proteasome subunits (figure 34). No labelling was detected in the food vacuole of treated parasites (figure 34, arrow), or when the parasites were incubated with a fluorescent control probe, which lacks thiostrepton.

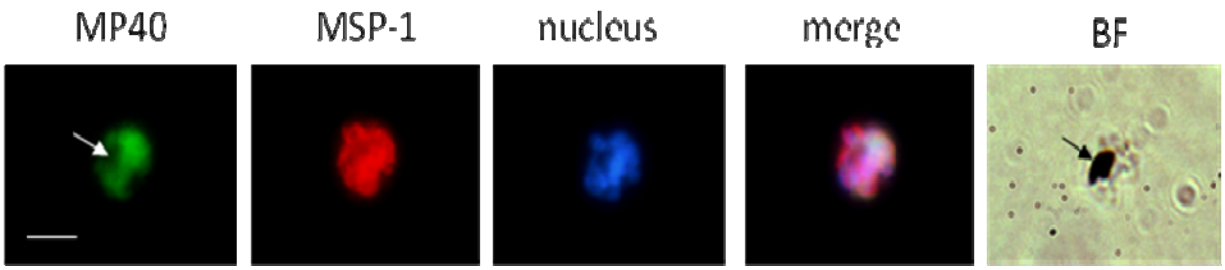

Figure 34. Incubation of asexual blood-stage parasites with a fluorescent thiostrepton probe (MP40). Parasites were visualized by double labeling with anti-MSP-1 antibody (red) and nuclei were highlighted by Hoechst staining (blue). Arrow indicates hemozoin in the parasite food vacuole. Image revealed a subcellular binding of thiostrepton in a schizont. Bar 5 µm. (Images were taken by G. Pradel).

3.3.3. Expression and sub-cellular distribution of the hslV in the gametocytes of *P. falciparum*.

The full characterization and localization of pfhslV was previously reported by Ramasamy et al. (2007), but the study did not include data on gametocytes. To further characterize pfhslV in gametocytes, the full lenght of the *PfhslV* gene encoding protein was cloned in the pGEX-4T1 plasmid and a GST-tagged PfhslV was expressed in *E.coli* BL21 (DE3) RIL. The purified fusion protein (figure 35A) was used to generate antibodies against PfhslV. Sequence alignment of PfHslV with the homologs of HslV in prokaryotes and other protozoan organisms also suggest that the PfhslV mRNA codes for a 37aa long putative pro-sequence followed by the 170 aa of the mature protease. Most importantly, processed plasmodial hslV has the obligatory N-terminal threonine, which is essential for proteolytic activity (Mordmuller et al., 2006). The anti-PfHslV antibodies raised in this study specifically recognized the pro-PfHslV (~22 kDa) and mature-PfHslV (~18 kDa) from the parasite lysate on a Western blot. These results are consistent with previous findings (Ramasamy et al., 2007). We observed that PfhslV was only present in the lysate of asexual stages and not present in the sexual stage lysate (figure 35B, 36) and this observation was confirmed with immunofluorescence assay, which revealed a moderate expression of pfhslV in trophozoites and schizont and no apparent expression in gametocyte stages (figure 35B, 36).

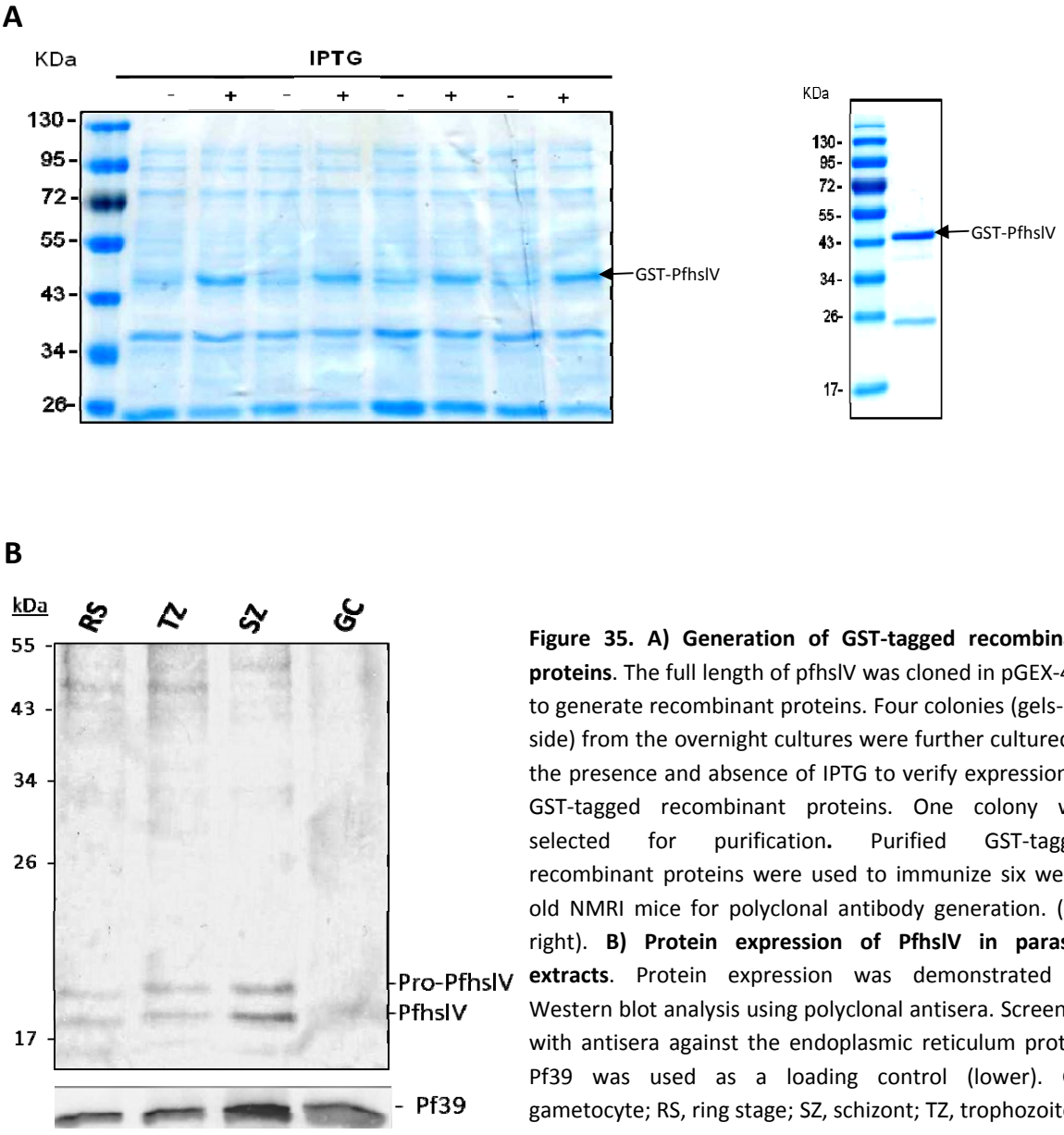

Figure 35. A) Generation of GST-tagged recombinant proteins. The full length of pfhslV was cloned in pGEX-4T1 to generate recombinant proteins. Four colonies (gels-left side) from the overnight cultures were further cultured in the presence and absence of IPTG to verify expression of GST-tagged recombinant proteins. One colony was selected for purification**.** Purified GST-tagged recombinant proteins were used to immunize six weeks old NMRI mice for polyclonal antibody generation. (Gel right). **B) Protein expression of PfhslV in parasite extracts**. Protein expression was demonstrated by Western blot analysis using polyclonal antisera. Screening with antisera against the endoplasmic reticulum protein Pf39 was used as a loading control (lower). GC, gametocyte; RS, ring stage; SZ, schizont; TZ, trophozoite.

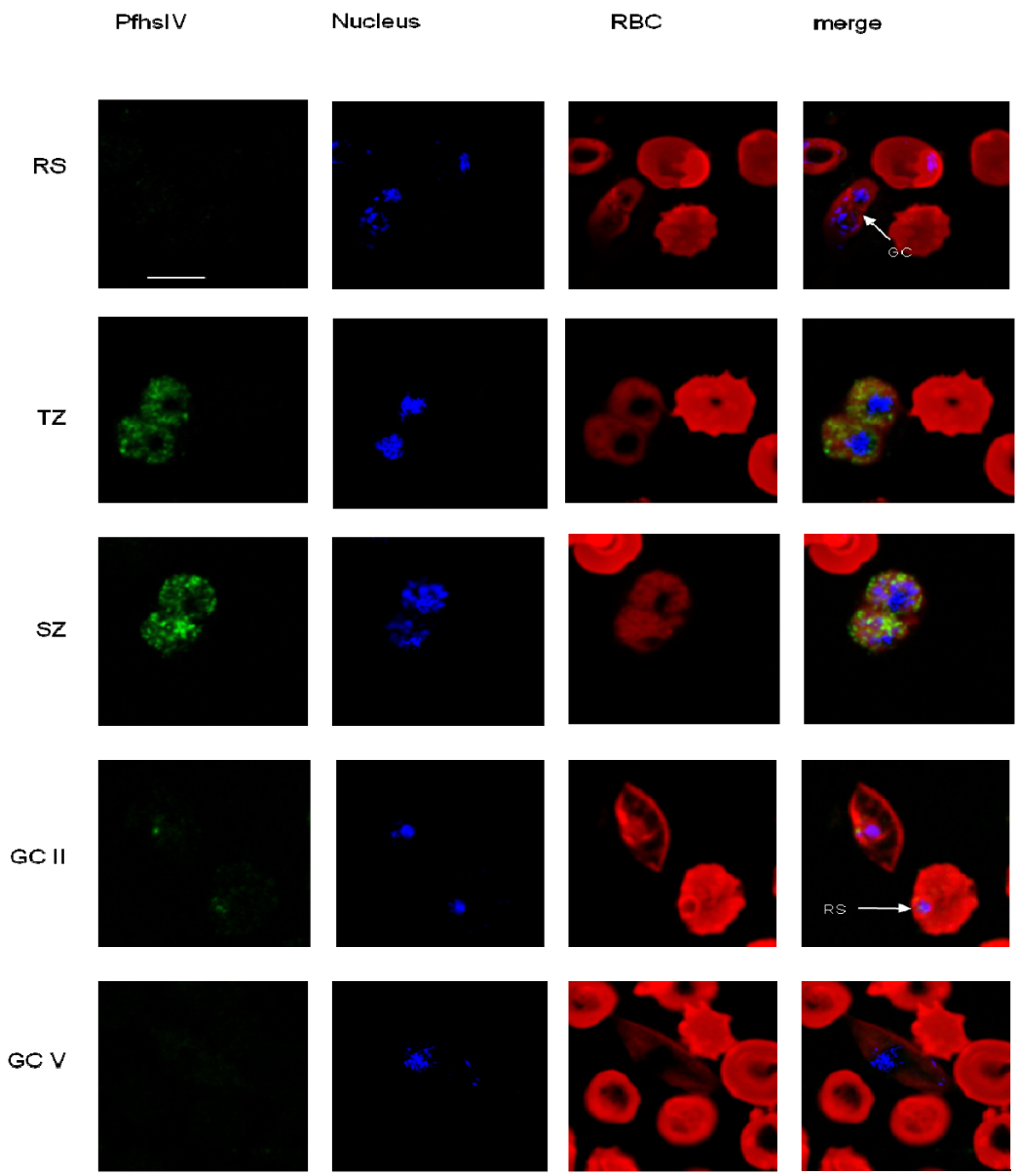

Figure 36. Indirect immunofluorescence assays. Polyclonal antisera against pfhslV revealed localization of the protein in the trophozoite and schizont stages, but not in gametocytes (green). Nuclei were highlighted by Hoechst nuclear staining (blue); and erythrocytes were counterstained by Evans Blue (red). GC, gametocyte; RBC, red blood cell; RS; ring stage, SZ, schizont; TZ, trophozoite. Bar 5 µm (Images were taken by G. Pradel).

3.3.4. Anti-gametocytocidal activity of peptidyl sulfonyl fluorides, a new class of proteasome inhibitors

A new class of compounds namely peptidyl sulfonyl fluorides was further investigated for their gametocytocidal activity. These inhibitors were recently reported for their antiplasmodial properties, and the treatment of parasites with the most active candidate PW28 (500 nM) led to the accumulation of ubiquitinated proteins. PW28 exhibited no cytotoxicity against HeLa cells and HEK 293 cells at 500 µM (Tschan et al., unpublished). The most active PSF were evaluated on gametocyte maturation at their IC_{50} concentrations (table 17; figure 37). Out of the tested compounds, all with the exception of PW40 significantly reduced the number of mature gametocytes ($p < 0.05$) and a strong gametocytocidal activity was observed for AJ34 and AJ38 (figure 37). Noteworthy, the gametocytocidal activities of these two compounds were significantly higher than that of primaquine.

The numbers of gametocyte stages I-V were investigated in the drug-treated samples via immunofluorescence assays in order to assess at which stage the gametocyte is most vulnerable to the compound. The percentages of gametocyte stages that are present in selected drug-treated cultures were determined and compared to the percentages of stages present in DMSO control cultures (figure 38). The evaluation revealed that the potent proteasome inhibitor AJ34 acted immediately on the gametocytes, which were not able to develop further (figure 38). Noteworthy, stage I gametocytes were continuously present in the AJ34-treated cultures even 5 days after removal of the drug, indicating that the growth was inhibited by the inhibitor. Stage I gametocytes that were observed several days after the release of drug pressure represent a new generation of gametocytes formed as a response to drug stress. The moderate proteasome inhibitor PW46 was not able to eliminate all gametocytes at IC_{50} concentrations, and these cells developed into mature gametocytes within the time period of 7 days, though at a slower rate.

To evaluate the potency of proteasome inhibitors for transmission blocking potential, an exflagellation assay with known proteasome inhibitors and thiostrepton at their IC_{80} concentration was carried out. Only epoxomicin significantly reduced the number of exflagellation centers ($P < 0.05$; figure 39), while no reduction was observed with thiostrepton, bortezomib and MG132.

Table 17. Antimalarial activities of peptidyl sulfonyl fluorides Mean IC_{50}s are given in nM and are calculated from at least 2 different experiments (Tschan et al. unpublished).

Peptide backbone	Residues	3D7	D10	Dd2	Name
$(Ile)_2$ThrLeu	R_1=Boc, R_2= H, R_3= Bn	712	378	408	AJ32
	R_1=Ac, R_2= H, R_3= H	966	605	668	AJ49
	R_1=H, R_2= H, R_3= Bn	3687	4150		AJ47
	R_1=Boc, R_2= CH_3, R_3= Bn	4300 3480	20 600 17.900	4540 42 200	PW31*
	R_1=Ac, R_2= CH_3, R_3= H	10 000 23 000	41 400 >150 000	10 000 150 000	PW47*
	R_1=H, R_2= H, R_3= H	> 40 000			AJ48
	R_1=Ac, R_2= H, R_3= Bn	355	247	228	AJ34
	R_1=N_3Ac, R_2= H, R_3= Ac	63.5	37.8	109	PW40
	R_1= N_3Ac, R_2= H, R_3= H	75.0	22.9	85.1	PW46
$(Leu)_3$	R_1= Cbz	308	200	167	AJ38
	R_1= Boc	284	208	215	PW25
	R_1= H	> 40 000			AJ41
	R_1= $PheN_3$	337	101	362	PW35
$(Leu)_4$	R_1= H	9600	11870	11800	PW38
	R_1= Ac	25 176 483	88.7 1670 >5500	198 1900 2600	PW39*
	R_1= Cbz	19.1	16.2	20.2	PW28

*Compounds which loose their activity with time, values of individual experiments are given.

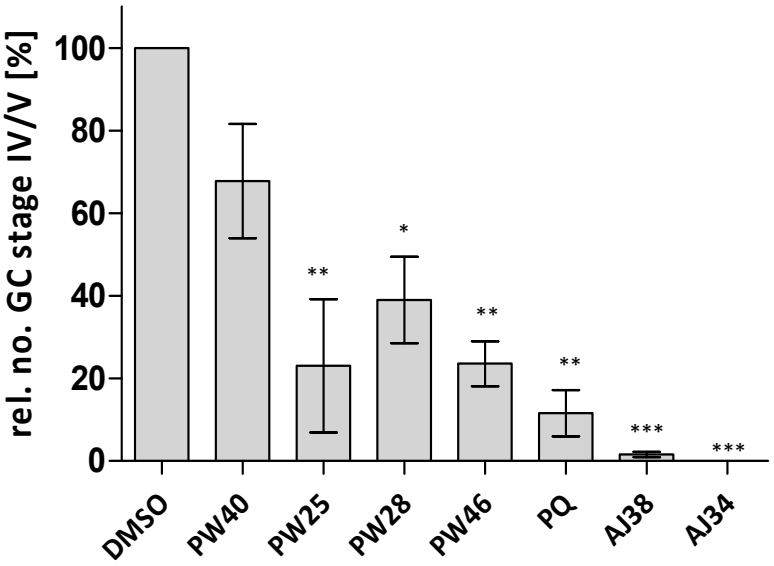

Figure 37. Inhibition of gametocytes maturation. Compounds at IC_{50} or a 0.5% volume of DMSO were added to stage II gametocyte cultures for 2 days. The numbers of stage IV and V gametocytes were counted after 7 days and compared to the gametocyte numbers in the DMSO control (normalized to 100%). The graph represents results of two independent experiments carried out in triplicate (mean ± SEM). Statistical analysis was done using one way ANOVA followed by a *Tukey* test (GraphPad prism 5). Asterisks represent a significant difference between tested compounds and DMSO control, where *** correspond to P < 0.001; **correspond to 0.001 < P <0.01; * correspond to 0.01< P < 0.05 and for p > 0.05 the difference in not considered significant and there is no asterisk. PQ.

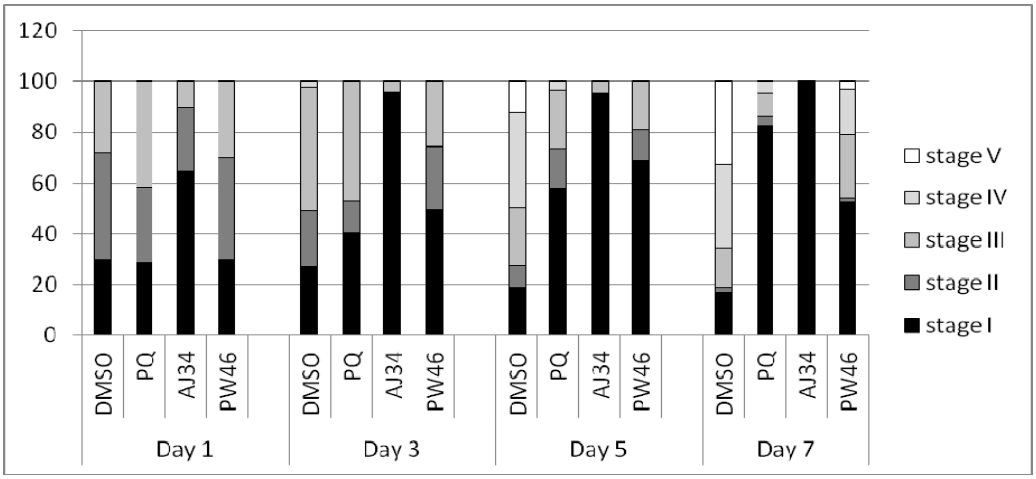

Figure 38. Clearance of gametocyte stages following drug treatment. Compounds at IC_{50} concentrations or 0.5 vol% of DMSO were added to stage II gametocyte cultures for 2 days. The cultures were cultivated for another 5 days after release of drug pressure. Samples were taken at day 1, 3, 5, and 7 of the assay. Gametocytes were detected by IFA, using antibodies against αlpha-tubulin (green). Erythrocytes were counterstained with Evans Blue (red), nuclei were highlighted by Hoechst nuclear stain (blue; see annex). The numbers of gametocytes of stages I to V were counted in a total number of 100 gametocytes in the drug-treated cultures and compared to DMSO control. Primaquine (PQ)-treated cultures were used for positive control.

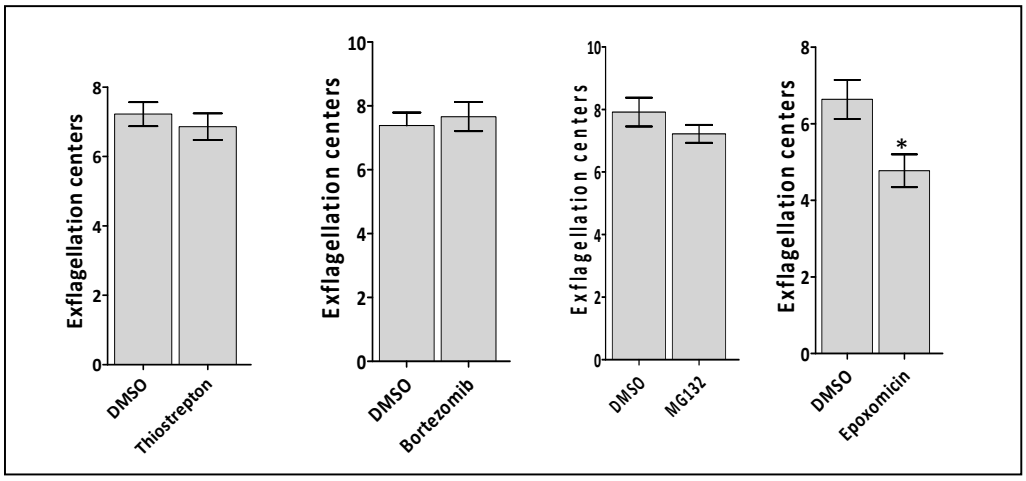

Figure 39. Transmission blocking potential of selected proteasome inhibitors in exflagellation assay. Compounds at IC_{80}s or 1% volume of DMSO were added to mature gametocyte cultures and activated with XA. The number of exflagellation centers were counted 15 min after activation; the number of centers was recorded and compared to the number of centers in the untreated controls. Results of two independent experiments. Mean ± SEM. Statistical analysis was done using t test. *$P < 0.05$, significant.

3.3.5. Expression of the GFP tagged proteins in *P. falciparum*

Parasite transfectants were generated by episomally expressing GFP-tagged proteasomes subunits studied above to have further knowledge on the trafficking of proteasome subunits in the parasite. To confirm the expression of fusion proteins α5-SU-GFP and β5-SU-GFP in our transfectant, antibodies directed against α5- and β5-SU a Western blot analysis were performed. Anti-GFP antibody was used as control. Antibodies against α5-SU and GFP were able to recognize the corresponding fusion protein in Western blot (figure 40B) while the fusion protein β5-SU-GFP was not detected despite the presence of parasites in the selection medium. Untransfected parasites were used as control in Western blot analysis and only a band corresponding to α5-SU was identified (figure 40B). Similarly, the C*andida albicans* protein extract containing GFP (kindly provided by Dr. Sasse) used as control only revealed a single band corresponding to GFP. A single band with a molecular weight of 55 kDa was observed on both gels, corresponding to the sum of molecular weight of α5-SU and GFP, which confirm the expression of the fusion protein in the transfected parasites. We further analyzed localization of the fusion protein in live parasite transfected with pARL- α5-SU-GFP using IFA (figure 40C). The α5-SU GFP tagged protein was abundantly expressed in the parasite cytoplasm and the expression was stable as demonstrated by Western blot (figure 40B).

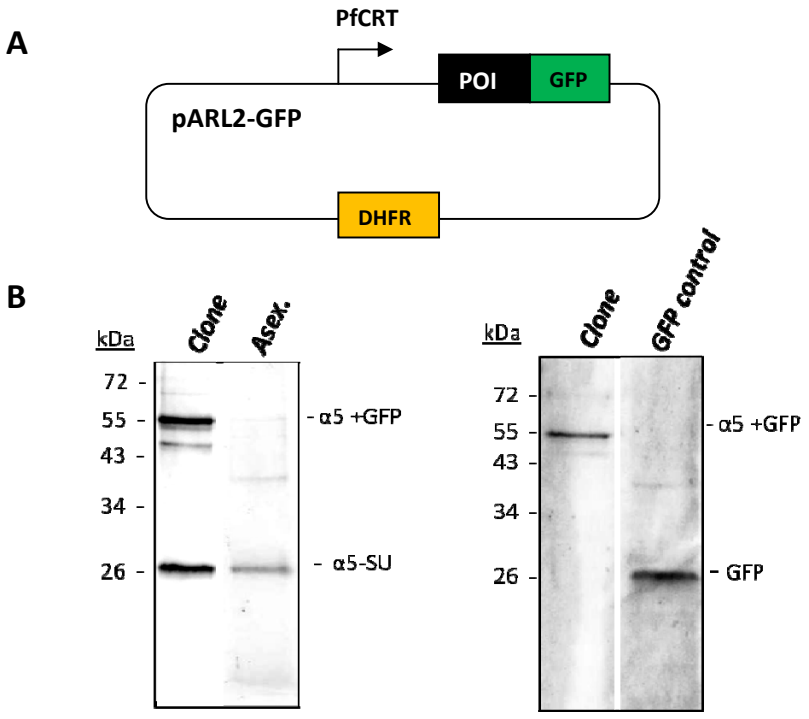

Figure 40. *See legend on the next page*

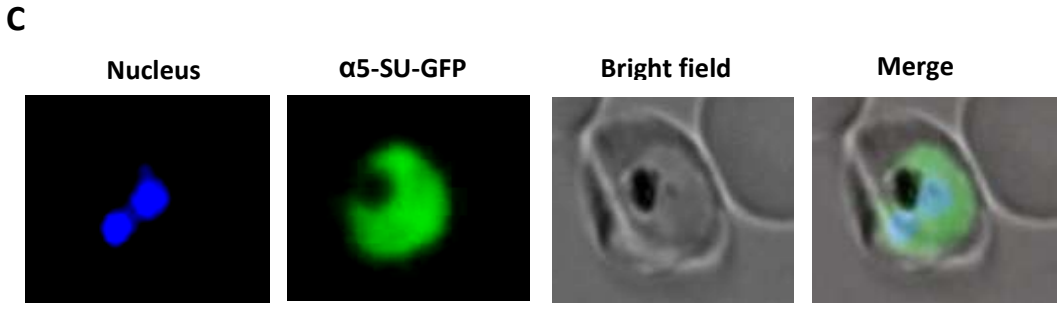

Figure 40. GFP tagged proteasome α5-SU expression in *P. falciparum* blood stages.
A) Construct used to perform transfection of *P. falciparum* NF54. **B)** Protein extracts were prepared from continuous culture of clone pARL-α-GFP and analyzed by Western blot with anti-α5 (left) and anti-GFP (right). Protein extract from 3D7 and protein extract containing GFP were used as negative and positive control respectively. The band migrating at ~55 Kda correspond to fusion protein α-SU5-GFP (28.4 + 27 (GFP) = 55.4 KDa). **C)** The image represents *P. falciparum* α-SU5-GFP chimeric protein expression at the early schizont stage of the parasite, showing parasite cytoplasmic labeling. GFP is not exported into the infected erythrocyte cytoplasm. Parasites were transfected with the pARL-α-GFP vector and the chimera expressed from a stably maintained episome under the control of the crt-promoter. Fluorescence from GFP was captured in live cells using live imaging microscope LEICA AF6000. POI: Protein of interest, Asex.: mixed culture of asexual stages of the parasite.

4. Discussion

4.1. Optimization of HIV-1 screening assay

The development of simple and cost effective platforms for the screening of potential inhibitors is very important in the search for new drugs. Therefore, assays are under constant development and refinement. In our current context, cell-based screening methods offer the potential advantage of investigating different antiviral targets, unlike biochemical (cell free) screening methods which can only be used for the screening against a single target. Single-cycle infectious pseudotyping of HIV-1 using the envelope glycoprotein of the vesicular stomatitis virus (VSV-G), capable of infecting a wide variety of cell types through endocytic pathway (Aiken, 1997), are used for gene delivery *in vitro* (Dull et al., 1998) and were recently exploited for drug screening applications (Cao and Guo, 2008; Garcia et al., 2009). Taking into account that they behave like the wild type virus and they can be manipulated with minimal risk of infection as compared to the wild type HIV-1, we sought to use this reporter virus assay for the screening of hybrid molecules.

With the HIV-1 (VSV-G) used in this study, only inhibitors of reverse transcriptase and integrase could be evaluated since the single-cycle infectious virus has a non functional protease enzyme and the HIV envelop is replaced. The quantification of GFP positive cells using flow cytometry is routinely used to determine the amount of GFP expressing cells, but this method can be cumbersome and time consuming for the screening of several inhibitors, as the flow cytometer used in this study could only measure one sample at a time. To avoid using flow cytometry, several laboratories instead use luciferase or colorimetric assays. A study however reported that the measurement of GFP intensity is a simpler alternative since the reporter is measured directly and doesn't require a substrate or a cofactor for its intrinsic fluorescence (Collins et al., 1998). Therefore, we optimized the reporter virus assay to be compatible with a 96-well format in which 4 or 6 drugs per plate could be screened in triplicate or duplicate, respectively, and in our study, we successfully measured GFP expression by quantifying the intracellular GFP released after cell lysis using a spectrofluorometer.

The method is simple and cost effective, since it doesn't require the use of additional kit. The lysis buffer is simple to prepare and doesn't require a supplement of PIs cocktail. The sensitivity can be considered high because the higher signal varied between 10000-16000 RFU, while the background signal varied between 400-700 RFU. Virus stocks were stable after a long conservation period and a good preparation can be used to screen a large amount of compounds. The method was optimized

using AZT as a reference drug, and the IC_{50} concentrations of AZT varied between 24-80 nM in our assays. This assay is robust to screen HIV inhibitors; however it might be limited since some inhibitors would instead target the fusion mechanism of the VSV-G instead of the post-entry event as expected.This method is particularly suitable for small molecules with known or suspected targets. In this study, we screened AZT derived hybrid molecules, and the assay was suitable as we expected an effect on the virus reverse transcriptase. Nonetheless, hit candidates resulting from such a primary screening must still be investigated on a wild type virus or available biochemical assays.

4.2. Hybrid molecules are potential candidates for HIV/malaria co-infections therapy

The interaction between HIV and malaria infection is bidirectional and synergistic (Skinner-Adams et al., 2007) and currently, there are no specific recommended treatment regimens for malaria and HIV/AIDS co-infection. In this study, we investigated hybrid molecules for their ability to target both *P. falciparum* and HIV. We anticipated that these molecules could be used to treat malaria infected individuals while offering protection against HIV. This strategy could be particularly beneficial for intermittent preventive treatment in HIV infected pregnant women.

Hybrid molecules synthesized in this study showed strong to moderate potency against both, HIV and *P. falciparum*, but most were not investigated further because of their cytotoxicity. Although VAK 87 showed modest cytotoxicity on HeLa cells like VAK 92 and VAK 93, its activity against HIV-1 (VSV-G) was approximately 8 × higher than that of VAK 93, suggesting that the cytotoxicity effect of a compound might not directly affect the outcome of its activity in some cases. Therefore, decisions to interrupt the evaluation of a very potent compound should be taken based on the selectivity index, which estimates the potential of a test compound to kill the parasite without host toxicity. It was nonetheless reasonable to eliminate highly cytotoxic compounds since none of the synthesized hybrid molecules showed a total inhibition at concentrations lower than or equal to 1 µM in our pre-screening phase. Dihyate, the most potent hybrid in our *in vitro* assays has a poor aqueous solubility, thus, likely to have poor bioavailability *in vivo*. However our preliminary data are encouraging as dihyate activity was comparable to that of DHA *in vitro*. DHA is practically insoluble in water just like dihyate and because of its poor aqueous solubility, DHA has only been formulated as oral and rectal tablet preparations (Ansari et al., 2011) and a combination with piperaquine is currently an option for the treatment of uncomplicated malaria. These data suggest that a compound like dihyate could still

be developed if an appropriate formulation is used for its delivery. If successfully developed as drugs, compounds like dihyate could have an advantage over DHA, since they might confer some additional protection against HIV.

Dihyate did not suppress parasite growth *in vivo* when administered orally in pheroid vesicles. This result was not consistent with the data obtained from *in vitro* studies and taking into account that dihyate was administered in pheroid vesicles to improve absorption, at least a moderate antimalarial property was expected. Since unacceptable PK properties is one of the main reasons for clinical failure of drug candidates (Liu et al., 2008), it was therefore necessary to evaluate other factors susceptible to affect dihyate PK, to better understand the failure *in vivo*.

4.3. Pharmacokinetic properties of dihyate

To ensure the success of a drug development, it is essential that a drug candidate has a good bioavailability and a desirable half life. Therefore, an accurate estimate of the PK data and a good understanding of the factors that affect the PK will guide drug design (Lin and Lu, 1997). Our attempt to study PK properties was to use the data as a guide in determining whether or not dihyate was likely to be improved. Therefore we would only discuss dihyate solubility, permeability and stability, the 3 properties that mostly affect bioavailability. The hybridization of AZT and DHA obviously leads to the generation of a higher molecular weight (MW) compound which might explain the predicted poor solubility of dihyate, as the trend towards increased MW is likely to worsen both, aqueous solubility and intestinal permeability (Lipinski, 2000). The reduction in MW is a useful approach in drug development for increasing solubility and might also improve metabolic stability. In our current context we envisaged that the two moieties would remain linked and thus preclude the need to reduce the MW. However the potential benefit of the AZT hybridization strategy, which was primarily the increased solubility and possible enhanced oral bioavailability of these compounds, appeared not to be translated into dihyate, which showed poor solubility and prompted us to dissolve in DMSO for *in vitro* assays and to prepare a formulation for *in vivo* studies, since the later can be used to increase the absorption of the molecule. However, the observed poor solubility is not surprising, considering the point of attachment of AZT to DHA through the primary hydroxyl group of AZT, resulting in dihyate not having a free hydroxyl group. Introduction of hydroxyl groups has been used as a strategy to improve drug solubility, but the solubility of a molecule can also be affected by other factors like lipophilicity and by ionic charge status (Lipinsky, 2000). The absence of a hydroxyl group on dihyate might partly explain the poor aqueous solubility; therefore, derivatives exemplified by Exp 62A, in which the

primary hydroxyl group of AZT is free were expected to have reasonable solubility. However, Exp 62A was predicted by *in silico* tools to have a poorer solubility and permeability than dihyate, suggesting that the poor solubility of dihyate is affected by additional factors.

Although dihyate was further predicted to have an acceptable Caco 2 permeation, the poor solubility of dihyate would led to poor oral bioavailability *in vivo*, hence, administration of dihyate *in vivo* would require an effective formulation strategy. Despite the apparent improved bioavailability observed when formulated in pheroid vesicles, the concentration of dihyate in mice plasma remained low to suppress parasite growth in infected mice and a rapid clearance was observed, thus, suggesting a poor stability of dihyate and a short half life *in vivo*. The O-dealkylation of the oxygen linking AZT and DHA in dihyate predicted by MetaSite appeared to be the main reason for the poor metabolic stability of dihyate. *In vitro* and *in vivo* studies correlated well and showed that dihyate releases AZT, but not DHA. DHA is reported to be metabolized extensively to hydroxylated derivatives by rat liver microsomes (Leskovac and Theoharides, 1991); these data are consistent with MetaSite main metabolism predictions. However a study carried out *in vivo* and *in vitro* using human microsome preparations revealed that DHA is mainly glucuronidated (Ilett, 2002). AZT is also known to be metabolized by glucuronide conjugation to a major inactive metabolite, 3'-azido-3'-deoxy-5'-O-beta-D-glucopyranuronosylthymidine (GZDV; Veal and Back, 1995). Nevertheless, the predicted phase I metabolism could occur in parallel albeit it is obviously not the major metabolism pathway. The hybrid dihyate was synthetized by linking AZT and DHA at their glucuronidation site, (figure 41, Barbier 2000; Ilett et al., 2002), on this basis, dihyate can not be conjugated with glucuronide unless it is first hydroxylated. These data further support the MetaSite predictions which suggested the O-dealkylation as the main biotransformation of dihyate, leading to its instability and cleavage *in vivo*. The DHA moiety released as the result of a cleavage product might have undergone some hydroxylations prior to cleavage, and could not be detected in mouse plasma *in vivo* or in the buffer *in vitro*, as the method was strictly designed to detect DHA and not hydroxylated products.

In this study the phase II metabolism of dihyate was not investigated since the main reason for the lack of *in vivo* activity of dihyate appeared to be its cleavage. These data show that the success of hybrid molecules in clinical settings would mostly depend on their stability.

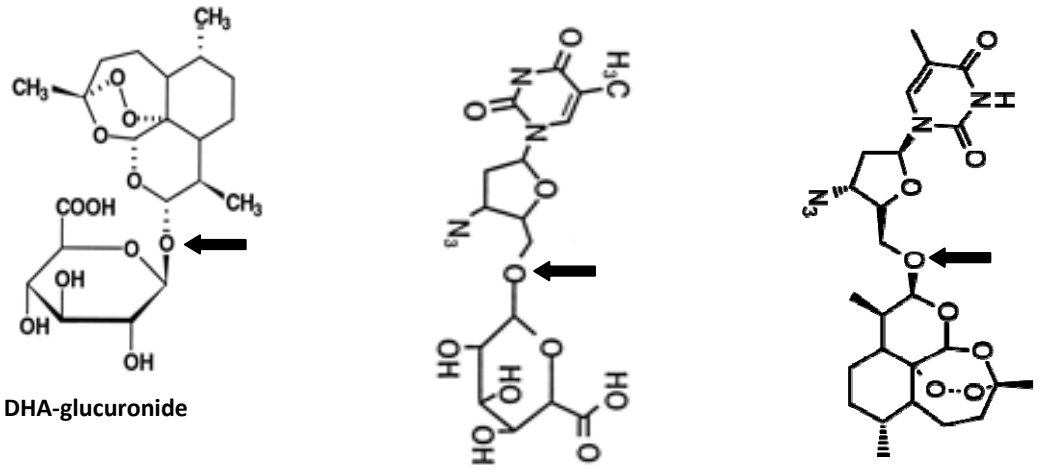

Figure 41. Glucuronide conjugate vs dihyate. A) Structure of DHA-glucuronide, **B)** Structure of AZT-5'-glucuronide, **C)** Dihyate. The arrows depict the AZT and DHA glucuronidation site and AZT-DHA hybrid covalent linkage site.

4.4. Thiostrepton and derivatives are potent inhibitors of P. falciparum asexual and sexual stages development

The spread of resistance to antimalarial drugs is a permanent threat to malaria elimination efforts and there is an urgent need to develop new combination therapy treatment with drugs exhibiting novel modes of action to treat malaria infections. In addition, these new medicines should also be effective against the gametocyte stages of the parasite, which are taken up by the mosquitoes during a blood meal, thereby allowing the parasite to continue the infection cycle in the vector. We evaluated the antimalarial activity of thiostrepton derivatives and we compared them to thiostrepton activity. Among them, five derivatives exhibited higher activity than thiostrepton. We confirmed that thiostrepton and derivatives exhibit a rapid effect since a considerable reduction of the IC_{50} from 48h to 120 h, characteristic of a delayed death was not observed in our assay. Thiostrepton-treated parasites which however escaped killing during the first replication cycle were then arrested in the schizont stage of the second cycle. This can not be considered a typical delayed death event, since the Giemsa stained preparations were obtained from parasites treated with IC_{50} concentration, which might explain the slow killing observed.

Interestingly, the two most active thiostrepton derivatives (SS231, SS234) also exhibited gametocytocidal activity in our gametocyte toxicity assays by blocking the formation or significantly reducing the amount of stage IV-V gametocytes in cultures treated with compounds IC_{90} concentrations. Most of the active thiostrepon-based derivatives do not exhibit toxicity against human cell lines, suggesting a considerable selectivity for the parasite in the cellular environment. Consistent to our data, a dose-response study previously showed that thiostrepton can completely cure *P. bergei*-infected mice with no apparent toxicity up to 500 mg/kg i.p. (Sullivan et al., 2000). In addition the apicoplast-targeting antibiotic thiostrepton inhibited gametocyte maturation but did not inhibit exflagellation at IC_{50} concentration. However, a recent study demonstrated that thiostrepton also inhibits exflagellation (Delves et al., 2012), but in the study, mature gametocytes were incubated for 24 h prior to culture activation with XA, which might explain the difference in our results. Taking all the above mentioned data into account, thiostrepton derivatives described here have a unique feature, by exhibiting potency against all parasite stages; they represent a potential candidate for the malaria elimination project. Thiostrepton has never been advanced to systemic applications due to rather low aqueous solubility and formulation problems (Bagley et al., 2005). Nonetheless, thiostrepton was recently reported to be highly suited as a nanomedicine for treating human cancer when formulated into nanoparticles (Wang and Gartel, 2011). Other thiopeptide antibiotics gave systemically applicable antibiotics after derivatization (Xu et al., 2009). Therefore it can be expected that compounds with improved properties can be obtained following the precedent set. Given the difficulties associated with optimizing bigger molecules like peptides, one could also think of generating peptidomimetics, this would however require the identification of the thiostrepton molecular target.

4.5. Thiostrepton and derivatives target the parasite proteasome

The proteasome has been recently shown to play an important role in protozoan parasites where it is involved in cell differentiation and replication (Paugam et al., 2003). Early studies to decipher the activity of the antibiotic thiostrepton and newly semi-synthetic thiostrepton derivatives revealed that they inhibit the human 20S proteasome *in vitro*, where they preferentially inhibited the caspase-like activity of the proteasome β-subunit type 1 (Schoof et al., 2010). This finding further supported the previous studies carried out by Kwok et al (2008) and Bhat et al (2009a, b) who showed that thiotrepton inhibits cancer cells proliferation by targeting the proteasome.

We here report that the immediate killing effect of thiostrepton and its derivatives is associated to the inhibition of the parasite proteasome, as the treatment of blood stage parasites with MG132 or with

the thiostrepton-based compounds led to accumulation of ubiquitinated proteins while no accumulation was observed in DMSO and CQ treated parasites. This method has been routinely used to show the effect of drugs on the proteasome (Lindenthal et al., 2005; Mordmüller et al., 2006; Prudhomme et al., 2008), but it doesn't reveal the exact target in this multi-protein complex. In addition, treatment of *P. falciparum* blood stages with these compounds results in an immediate killing at the trophozoite stage, similar to the killing mechanism of the proteasome inhibitor MG132. Neither MG132 nor thiostrepton and derivatives are able to eliminate the parasites, when added at the schizont stage, thus after initiation of DNA replication, which is in accordance with previous findings on the antimalarial effect of proteasome inhibitors (Reynolds et al., 2007; Kreidenweiss et al., 2008). Our results show that thiostrepton derivatives do not only inhibit protein synthesis in the apicoplast but also inhibit the proteasome and this might explain why the delayed death effect is not observed. This dual mode of action might be beneficial for the implementation of new combination regimen to reduce resistance development. In a recent study, the authors suggested that thiostrepton inhibit the parasite mitochondrial protein synthesis (Tarr et al. 2011). Taking into account another recent study which demonstrated that the proteasome inhibitor bortezomib inhibit non-proteasomal targets on neuronal cells *in vitro* and on rats and humans *in vivo* (Arastu-Kapur et al., 2011), it is not excluded that thiostrepton might target several pathways in the parasite, since thiostrepton exhibits anti-cancer properties following the same mechanism with proteasome inhibitors. Although *in vitro* studies do not demonstrate the level of inhibition required to be therapeutic relevant, thiostrepton and derivatives could reveal new targetable pathways in the parasite. Second generation of drugs with the ability to inhibit selectively the parasite proteasome could therefore be developed against blood and liver stages.

4.6. The proteasome is expressed in all parasite blood stages and pfhslV is exclusively expressed in asexual blood stages

Despite the increasing evidences on the presence of a proteasome pathway in *P. falciparum*, the precise intracellular localization and characterization of proteasome activity in the different developmental stages of *P. falciparum* have not been studied. We provide evidence on the expression of the malaria proteasome in blood stage parasites by showing that subunits of the 20S proteasome, α5- and β5-SU are predominantly present in trophozoites and schizonts, thus in stages that are metabolically highly active and have to prepare for DNA replication and cell division. Immunoelectron

microscopy confirmed that the proteasome is localized to the cytoplasm and the nucleus of parasites, but not in the nucleolus, and these observations are in accordance with the localization of the 26S proteasome in human cells (Paugam et al., 2003).

We further established one parasite clone which expresses GFP tagged α5-SU, as this approach has been an important application to follow the trafficking pathway of proteins in live *P. falciparum*-infected erythrocytes (Waller et al., 2000; Wickham et al., 2001). The GFP tagged protein appeared to be homogenously distributed in the cytoplasm and does not appear to localize to the nucleus as observed with antibody labelling. It is therefore not clear whether or not the fusion protein localize to the nucleus since the attachment of GFP could affect the transport of the protein of interest. The use of this approach did not bring additional information and a better approach might be to prepare sub-fractions of the parasite using the differential centrifugation method as previously described by Gutiérrez et al (2009).

In addition to the proteasome, the parasite also expresses a homolog of the prokaryotic proteasome subunit, PfhslV. While it is known that PfhslV is abundantly expressed in the asexual blood stages, excluding ring stages (Ramasamy et al., 2007), the expression of this protein in gametocytes was not observed. Since PfhslV is a potential target for chemotherapy, it was important to know if PfhslV is expressed in gametocyte, since targets that are expressed throughout the development cycle are more attractive for the development of multi-stage inhibitors. The attractiveness of PfHslV as a drug target is based on the fact, that it has no homolog in the human host (Ramasamy *et al*., 2007). However future studies have to unveil the function of the bacterial proteasome in *P. falciparum* and the result of this characterization would reveal the suitability of PfhsIV as a valid target for further drug development projects.

4.7. The plasmodial proteasome as a potential novel drug target

Malaria therapy nowadays mostly relies on artemisinin derivatives, and resistances have been reported for all counterpart drugs used in the ACTs, in addition, recent claims of artemisinin resistances where reported in Southeast Asia (Noedl et al., 2008; Dondorp et al., 2009). Consequently, it is necessary to develop new molecules, ideally, molecules targeting distinct pathways from that of drugs in the market, and which exhibit additional transmission blocking properties. Due to the essential roles of the UPS in all eukaryotic cells, one might anticipate that proteasome inhibitors show activities against malaria parasites as well. This study and other studies revealed that proteasome

inhibitors are ideal molecules capable of suppressing the development of liver and erythrocytic (sexual and asexual) stages.

While it was shown in yeast and human that the CP-SUs β1, β2 and β5 display caspase-like, trypsin-like and chymotrypsin-like activities, respectively, such distinct activities have not been confirmed for *Plasmodium*, and interaction of active site-targeting inhibitors with CP-SUs have yet to be demonstrated. However, epoxomicin was reported to bind parasite CP-SUs β2 and β5 (Mordmüller et al., 2006) and bortezomib, which exhibits antiplasmodial activity, has also shown high specificity for β5 (Oerlemans et al., 2008), providing indirect evidence for the proteolytically active sites of the plasmodial proteasome.

In addition, proteasome inhibitors appeared to inhibit the maturation of gametocytes, making the proteasome a suitable target. Gametocyte toxicity was previously described for other antimalarial drugs like primaquine (Pukrittayakamee et al., 2004), and recently was also reported for DHA and partner drugs lumefantrine and pyronaridine (Adjalley et al., 2011). Methylene blue and the proteasome inhibitor epoxomicin were also reported to be potent inhibitors of gametocytes development (Czesny et al., 2009; Adjalley et al., 2011).

In this study we further demonstrate that newly synthesized peptidyl sulfonyl fluorides, a new class of proteasome inhibitors (AJ34, AJ38) and thiostrepton significantly suppressed mature gametocytes formation when administered at their respective IC_{50} concentration, exhibiting a better effect compared to molecules mentioned above, and unlike epoxomicin and thiostrepton, AJ34 and AJ38 were non-toxic to human cells at relatively high concentrations (Tschan et al., unpublished). Molecules that confer protection against sexual and asexual stage will cure the patient and reduce the number of mature gametocytes circulating after treatment, thus reducing or limiting the transmission. However further transmission blocking properties should be evaluated for this compounds, including their ability to inhibit gametocyte activation thereby preventing gamete formation in the mosquito midgut or their ability to reduce oocyst formation thereby preventing the release of infectious sporozoites upon next mosquito bite.

The parasite proteasome has not been isolated; therefore it is not possible to carry out biochemical assays to directly investigate specific inhibitors of *P. falciparum* proteasome. Current proteasome assays are based on purified mammalian proteasome and a number of commercial assays have been developed to investigate all three proteasome enzymatic activities, chymotrypsin-, trypsin-, and caspase-like using the purified proteasome (Schoof et al., 2009). As the parasite proteasome represent a potential target for drugs, the development of a platform to screen inhibitors of *P. falciparum*

proteasome is needed. Recently a number of cell assays based on GFP as a reporter have been described in mammalian cells, the common feature of most of these GFP-fused reporters is that they are based on proteins rapidly degraded by the proteasome under normal conditions, leading to very low fluorescence of the cells, while following inhibition of proteasome activity, the overall fluorescent signal of the cells rapidly increases as a result of accumulation of the reporter proteins (Lavelin et al., 2009). In this same line, interesting data on the ubiquitome of the malaria parasite has presented the first step toward a better understanding of ubiquitylation and its role(s) in the biology of the human malaria parasite (Ponts et al., 2011). These data together with further characterization of ubiquitinated proteins in *P. falciparum* would speed up the discovery of proteins degraded by the ubiquitin-dependent mechanism in *P.falciparum.* These proteins could be ideal candidates for the development of cell-based assays.

5. Future perspectives

HIV and malaria remain the leading cause of mortality in the developing world especially in Africa where most cases occur and where the highest proportion of co-infections are likely to occur. The overlap of these two infections has several implications on their spread. Little is known on the treatment implications when an HIV infected individual is treated for malaria infection. However the WHO has released some warnings regarding some drugs, but so far no specific recommendations are available in endemic regions. It can be seen from data available that adverse drug interactions might occur if ACTs and antiretrovirial combinations are administered together.

The concept of hybrid molecules described here was raised to limit the risk of resistance or improve PK properties while optimizing the activity of the molecule. In this study we reported for the first time the use of hybrid molecules to inhibit two non-related organisms and our data showed that suitable hybrid molecules could lead to suitable applications for HIV/malaria co-infections. It could be advantageous to exploit compounds targeting aspartic proteases as recent studies have shown that clinically approved HIV PIs were able to inhibit malaria parasite growth and to augment the antimalarial action artemisinin *in vitro*. Aspartic proteases could also be evaluated as unique target for hybrid molecules synthesized from two PIs, or a single optimized PI able to effectively inhibit proteases in both, HIV and *P. falciparum*. Hybrid drugs could become an effective strategy to generate chemical entities likely to be more efficacious and less prone to resistance. However, data obtained in this study revealed that some important technical challenges will have to be overcome before hybrid drugs could succeed in the clinical settings.

The use of antibiotics for the treatment of malaria was re-considered following emergence of resistant parasites and antibiotics are currently used as counterparts of fast acting drugs like artemisinin derivatives in the second-line treatment. The introduction of antibiotics with rapid antimalarial activity in the first line treatment might present two avantages; one which is the treatment of malaria infections and a rapid clearance of parasite when administered with a fast acting drug,thus, limiting the amount of circulating gametocytes and reducing transmission. Secondly, it could be exploited in co-infections between malaria and bacterial infections, as the later are sometimes misdiagnosed as malaria. We showed that derivatization of the thiazole antibiotic thiostrepton could lead to the synthesis of more potent molecules with less cytotoxicity. It was further shown that thiostrepton and derivatives exhibit their antimalarial property by targeting the parasite proteasome. Therefore, the parasite proteasome as a target for antimalarial opens door for more studies as it offers the

opportunity to develop drugs that target several parasite stages. A further characterization would be necessary to confirm that the parasite proteasome exhibits the enzymatic activites similar to mammalian proteasome. We would further identify specific target(s) of the proteasome inhibitors within the UPS of *P. falciparum* and develop a cell-based assay to measure the activity of proteasome inhibitors against the proteasome of the malaria parasite.

6. References

Adjalley, S. H., G. L. Johnston, T. Li, R. T. Eastman, E. H. Ekland, A. G. Eappen, A. Richman, B. K. Sim, M. C. Lee, S. L. Hoffman, and D. A. Fidock. 2011. Quantitative assessment of *Plasmodium falciparum* sexual development reveals potent transmission-blocking activity by methylene blue. Proc Natl Acad Sci U S A **108:**E1214-23.

Agarwal, S. 2010. Functional characterization of four CDK-like kinases and one calmodulin-dependent kinase of the malaria parasite *Plasmodium falciparum*, human. **PhD thesis.** University of Würzburg, Germany.

Agnandji, S. T., B. Lell, S. S. Soulanoudjingar, J. F. Fernandes, B. P. Abossolo, C. Conzelmann, B. G. Methogo, Y. Doucka, A. Flamen, B. Mordmuller, S. Issifou, P. G. Kremsner, J. Sacarlal, P. Aide, M. Lanaspa, J. J. Aponte, A. Nhamuave, D. Quelhas, Q. Bassat, S. Mandjate, E. Macete, P. Alonso, S. Abdulla, N. Salim, O. Juma, M. Shomari, K. Shubis, F. Machera, A. S. Hamad, R. Minja, A. Mtoro, A. Sykes, S. Ahmed, A. M. Urassa, A. M. Ali, G. Mwangoka, M. Tanner, H. Tinto, U. D'Alessandro, H. Sorgho, I. Valea, M. C. Tahita, W. Kabore, S. Ouedraogo, Y. Sandrine, R. T. Guiguemde, J. B. Ouedraogo, M. J. Hamel, S. Kariuki, C. Odero, M. Oneko, K. Otieno, N. Awino, J. Omoto, J. Williamson, V. Muturi-Kioi, K. F. Laserson, L. Slutsker, W. Otieno, L. Otieno, O. Nekoye, S. Gondi, A. Otieno, B. Ogutu, R. Wasuna, V. Owira, D. Jones, A. A. Onyango, P. Njuguna, R. Chilengi, P. Akoo, C. Kerubo, J. Gitaka, C. Maingi, T. Lang, A. Olotu, B. Tsofa, P. Bejon, N. Peshu, K. Marsh, S. Owusu-Agyei, K. P. Asante, K. Osei-Kwakye, O. Boahen, S. Ayamba, K. Kayan, R. Owusu-Ofori, D. Dosoo, I. Asante, G. Adjei, D. Chandramohan, B. Greenwood, J. Lusingu, S. Gesase, A. Malabeja, O. Abdul, H. Kilavo, C. Mahende, E. Liheluka, M. Lemnge, et al. 2011. First results of phase 3 trial of RTS,S/AS01 malaria vaccine in African children. N Engl J Med **365:**1863-75.

Aiken, C. 1997. Pseudotyping human immunodeficiency virus type 1 (HIV-1) by the glycoprotein of vesicular stomatitis virus targets HIV-1 entry to an endocytic pathway and suppresses both the requirement for Nef and the sensitivity to cyclosporin A. J Virol **71:**5871-7.

Almond, J. B., and G. M. Cohen. 2002. The proteasome: a novel target for cancer chemotherapy. Leukemia **16:**433-43.

Ansari, M., K. Batty, I. Iqbal, and V. Sunderland. 2011. Improving the solubility and bioavailability of dihydroartemisinin by solid dispersions and inclusion complexes. Archives of Pharmacal Research **34:**757-765.

Arastu-Kapur, S., J. L. Anderl, M. Kraus, F. Parlati, K. D. Shenk, S. J. Lee, T. Muchamuel, M. K. Bennett, C. Driessen, A. J. Ball, and C. J. Kirk. 2011. Nonproteasomal targets of the proteasome inhibitors bortezomib and carfilzomib: a link to clinical adverse events. Clin Cancer Res **17:**2734-43.

Arendt, C.A., and M. Hochstrasser. 1997. Identification of the yeast 20S proteasome catalytic centers and subunit interactions required for active-site formation. Proc. Natl. Acad. Sci. U. S. A. 94, 7156-7161.

Aurrecoechea, C., J. Brestelli, B. P. Brunk, J. Dommer, S. Fischer, B. Gajria, X. Gao, A. Gingle, G. Grant, O. S. Harb, M. Heiges, F. Innamorato, J. Iodice, J. C. Kissinger, E. Kraemer, W. Li, J. A. Miller, V. Nayak, C. Pennington, D. F. Pinney, D. S. Roos, C. Ross, C. J. Stoeckert, Jr., C. Treatman, and H. Wang. 2009. PlasmoDB: a functional genomic database for malaria parasites. Nucleic Acids Res **37:**D539-43.

Bagley, M. C., J. W. Dale, E. A. Merritt, and X. Xiong. 2005. Thiopeptide antibiotics. Chem Rev **105:**685-714.

Balzarini, J., P. Herdewijn, and E. De Clercq. 1989. Differential patterns of intracellular metabolism of 2',3'-didehydro-2',3'-dideoxythymidine and 3'-azido-2',3'-dideoxythymidine, two potent anti-human immunodeficiency virus compounds. J Biol Chem **264:**6127-33.

Barbier, O., D. Turgeon, C. Girard, M. D. Green, T. R. Tephly, D. W. Hum, and A. Belanger. 2000. 3'-azido-3'-deoxythimidine (AZT) is glucuronidated by human UDP-glucuronosyltransferase 2B7 (UGT2B7). Drug Metab Dispos **28:**497-502.

Barnes, K. I., F. Little, P. J. Smith, A. Evans, W. M. Watkins, and N. J. White. 2006. Sulfadoxine-pyrimethamine pharmacokinetics in malaria: pediatric dosing implications. Clin Pharmacol Ther **80:**582-96.

Barthel, D., M. Schlitzer, and G. Pradel. 2008. Telithromycin and quinupristin-dalfopristin induce delayed death in *Plasmodium falciparum*. Antimicrob Agents Chemother **52:**774-7.

Baumann, S., S. Schoof, S. D. Harkal, and H. D. Arndt. 2008. Mapping the binding site of thiopeptide antibiotics by proximity-induced covalent capture. J Am Chem Soc **130:**5664-6.

Bedford, L., S. Paine, P. W. Sheppard, R. J. Mayer, and J. Roelofs. 2010. Assembly, structure, and function of the 26S proteasome. Trends Cell Biol **20:**391-401.

Bellot, F., F. Cosledan, L. Vendier, J. Brocard, B. Meunier, and A. Robert. 2010. Trioxaferroquines as new hybrid antimalarial drugs. J Med Chem **53:**4103-4109.

Bhat, U. G., M. Halasi, and A. L. Gartel. 2009a. FoxM1 is a general target for proteasome inhibitors. PLoS One **4:**e6593.

Bhat, U. G., M. Halasi, and A. L. Gartel. 2009b. Thiazole antibiotics target FoxM1 and induce apoptosis in human cancer cells. PLoS One **4:**e5592.

Boelaert, J. R., K. Sperber, and J. Piette. 2001. The additive *in vitro* anti-HIV-1 effect of chloroquine, when combined with zidovudine and hydroxyurea. Biochem Pharmacol **61:**1531-5.

Bousema, T., and C. Drakeley. 2011. Epidemiology and infectivity of *Plasmodium falciparum* and *Plasmodium vivax* gametocytes in relation to malaria control and elimination. Clin Microbiol Rev **24:**377-410.

Bozdech, Z., M. Llinas, B. L. Pulliam, E. D. Wong, J. Zhu, and J. L. DeRisi. 2003. The transcriptome of the intraerythrocytic developmental cycle of *Plasmodium falciparum*. PLoS Biol **1:**E5.

Burrows, J. N., K. Chibale, and T. N. Wells. 2011. The state of the art in anti-malarial drug discovery and development. Curr Top Med Chem **11:**1226-54.

Cao, Y. L., and Y. Guo. 2008. Screening of HIV-1 replication inhibitors by using pseudotyped virus system. Yao Xue Xue Bao **43:**253-8.

Chadwick, J., R. K. Amewu, F. Marti, F. B. Garah, R. Sharma, N. G. Berry, P. A. Stocks, H. Burrell-Saward, S. Wittlin, M. Rottmann, R. Brun, D. Taramelli, S. Parapini, S. A. Ward, and P. M. O'Neill. 2011. Antimalarial mannoxanes: hybrid antimalarial drugs with outstanding oral activity profiles and a potential dual mechanism of action. ChemMedChem **6:**1357-61.

Chen, P., and M. Hochstrasser. 1995. Biogenesis, structure and function of the yeast 20S proteasome. EMBO J **14:**2620-30.

Chung, D. W., and K. G. Le Roch. 2010. Targeting the *Plasmodium* ubiquitin/proteasome system with anti-malarial compounds: promises for the future. Infect Disord Drug Targets **10:**158-64.

Clough, B., M. Strath, P. Preiser, P. Denny, and I. R. Wilson. 1997. Thiostrepton binds to malarial plastid rRNA. FEBS Lett **406:**123-5.

Collins, L. A., M. N. Torrero, and S. G. Franzblau. 1998. Green fluorescent protein reporter microplate assay for high-throughput screening of compounds against Mycobacterium tuberculosis. Antimicrob Agents Chemother **42:**344-7.

Corson, T. W., N. Aberle, and C. M. Crews. 2008. Design and Applications of Bifunctional Small Molecules: Why Two Heads Are Better Than One. ACS Chem Biol **3:**677-692.

Cosledan, F., L. Fraisse, A. Pellet, F. Guillou, B. Mordmuller, P. G. Kremsner, A. Moreno, D. Mazier, J. P. Maffrand, and B. Meunier. 2008. Selection of a trioxaquine as an antimalarial drug candidate. Proc Natl Acad Sci U S A **105:**17579-84.

Czesny, B., S. Goshu, J. L. Cook, and K. C. Williamson. 2009. The proteasome inhibitor epoxomicin has potent *Plasmodium falciparum* gametocytocidal activity. Antimicrob Agents Chemother **53:**4080-5.

Dahl, E. L, J. L. Shock, B. R. Shenai., J. Gut, J. L. DeRisi, and P. J. Rosenthal. 2006. Tetracyclines specifically target the apicoplast of the malaria parasite *Plasmodium falciparum*. Antimicrob Agents Chemother **50:**3124-3131.

de Bettignies, G., and O. Coux. 2010. Proteasome inhibitors: Dozens of molecules and still counting. Biochimie **92:**1530-45.

Dechy-Cabaret, O., F. Benoit-Vical, A. Robert, and B. Meunier. 2000. Preparation and antimalarial activities of "trioxaquines", new modular molecules with a trioxane skeleton linked to a 4-aminoquinoline. Chembiochem **1:**281-3.

Delves, M., D. Plouffe, C. Scheurer, S. Meister, S. Wittlin, E. A. Winzeler, R. E. Sinden, and D. Leroy. 2012. The activities of current antimalarial drugs on the life cycle stages of *Plasmodium*: a comparative study with human and rodent parasites. PLoS Med **9:**e1001169.

Diallo, D. A., S. N. Cousens, N. Cuzin-Ouattara, I. Nebie, E. Ilboudo-Sanogo, and F. Esposito. 2004. Child mortality in a West African population protected with insecticide-treated curtains for a period of up to 6 years. Bull World Health Organ **82:**85-91.

Dondorp, A. M., F. Nosten, P. Yi, D. Das, A. P. Phyo, J. Tarning, K. M. Lwin, F. Ariey, W. Hanpithakpong, S. J. Lee, P. Ringwald, K. Silamut, M. Imwong, K. Chotivanich, P. Lim, T. Herdman, S. S. An, S. Yeung, P. Singhasivanon, N. P. Day, N. Lindegardh, D. Socheat, and N. J. White. 2009. Artemisinin resistance in *Plasmodium falciparum* malaria. N Engl J Med **361:**455-67.

Dubar, F., G. Anquetin, B. Pradines, D. Dive, J. Khalife, and C. Biot. 2009. Enhancement of the antimalarial activity of ciprofloxacin using a double prodrug/bioorganometallic approach. J Med Chem **52:**7954-7.

Dull, T., R. Zufferey, M. Kelly, R. J. Mandel, M. Nguyen, D. Trono, and L. Naldini. 1998. A third-generation lentivirus vector with a conditional packaging system. J Virol **72:**8463-71.

Eriksen, J., S. Mwankusye, S. Mduma, M. I. Veiga, A. Kitua, G. Tomson, M. G. Petzold, G. Swedberg, L. L. Gustafsson, and M. Warsame. 2008. Antimalarial resistance and DHFR/DHPS genotypes of *Plasmodium falciparum* three years after introduction of sulfadoxine-pyrimethamine and amodiaquine in rural Tanzania. Trans R Soc Trop Med Hyg **102:**137-42.

Etlinger, J. D., and A. L. Goldberg. 1977. A soluble ATP-dependent proteolytic system responsible for the degradation of abnormal proteins in reticulocytes. Proc Natl Acad Sci U S A **74:**54-8.

Fidock, D. A., and T. E. Wellems. 1997. Transformation with human dihydrofolate reductase renders malaria parasites insensitive to WR99210 but does not affect the intrinsic activity of proguanil. Proc Natl Acad Sci U S A **94:**10931-6.

Flateau, C., G. Le Loup, and G. Pialoux. 2011. Consequences of HIV infection on malaria and therapeutic implications: a systematic review. Lancet Infect Dis **11:**541-56.

Flexner, C. 2007. HIV drug development: the next 25 years. Nat Rev Drug Discov **6:**959-66.

Frentzel, S., B. Pesold-Hurt, A. Seelig, and P. M. Kloetzel. 1994. 20 S proteasomes are assembled via distinct precursor complexes. Processing of LMP2 and LMP7 proproteins takes place in 13-16 S preproteasome complexes. J Mol Biol **236:**975-81.

Gallastegui, N., and M. Groll. 2010. The 26S proteasome: assembly and function of a destructive machine. Trends Biochem Sci **35:**634-42.

Gantt, S. M., J. M. Myung, M. R. Briones, W. D. Li, E. J. Corey, S. Omura, V. Nussenzweig, and P. Sinnis. 1998. Proteasome inhibitors block development of *Plasmodium spp*. Antimicrob Agents Chemother **42:**2731-8.

Garcia, J. M., A. Gao, P. L. He, J. Choi, W. Tang, R. Bruzzone, O. Schwartz, H. Naya, F. J. Nan, J. Li, R. Altmeyer, and J. P. Zuo. 2009. High-throughput screening using pseudotyped lentiviral particles: a strategy for the identification of HIV-1 inhibitors in a cell-based assay. Antiviral Res **81:**239-47.

Gediya, L. K., and V. C. O. Njar. 2009. Promise and challenges in drug discovery and development of hybrid anticancer drugs. Expert Opinion on Drug Discovery **4:**1099-1111.

German, P. I., and F. T. Aweeka. 2008. Clinical pharmacology of artemisinin-based combination therapies. Clin Pharmacokinet **47:**91-102.

German, P., B. Greenhouse, C. Coates, G. Dorsey, P. J. Rosenthal, E. Charlebois, N. Lindegardh, D. Havlir, and F. T. Aweeka. 2007. Hepatotoxicity due to a drug interaction between amodiaquine plus artesunate and efavirenz. Clin Infect Dis **44:**889-91.

German, P., S. Parikh, J. Lawrence, G. Dorsey, P. J. Rosenthal, D. Havlir, E. Charlebois, W. Hanpithakpong, N. Lindegardh, and F. T. Aweeka. 2009. Lopinavir/ritonavir affects pharmacokinetic exposure of artemether/lumefantrine in HIV-uninfected healthy volunteers. J Acquir Immune Defic Syndr **51:**424-9.

Glickman, M. H., and A. Ciechanover. 2002. The ubiquitin-proteasome proteolytic pathway: destruction for the sake of construction. Physiol Rev **82:**373-428.

Goodman, C. D., V. Su, and G. I. McFadden. 2007. The effects of anti-bacterials on the malaria parasite *Plasmodium falciparum*. Mol Biochem Parasitol **152:**181-91.

Griffith, D. A., and S. M. Jarvis. 1996. Nucleoside and nucleobase transport systems of mammalian cells. Biochim Biophys Acta **1286:**153-81.

Guantai, E. M., K. Ncokazi, T. J. Egan, J. Gut, P. J. Rosenthal, P. J. Smith, and K. Chibale. 2010. Design, synthesis and *in vitro* antimalarial evaluation of triazole-linked chalcone and dienone hybrid compounds. Bioorg Med Chem **18:**8243-56.

Gutierrez, B., L. Osorio, M. C. Motta, T. Huima-Byron, H. Erdjument-Bromage, C. Munoz, H. Sagua, R. A. Mortara, A. Echeverria, J. E. Araya, and J. Gonzalez. 2009. Molecular characterization and intracellular distribution of the alpha 5 subunit of *Trypanosoma cruzi* 20S proteasome. Parasitol Int **58:**367-74.

Harms, J. M., D. N. Wilson, F. Schluenzen, S. R. Connell, T. Stachelhaus, Z. Zaborowska, C. M. Spahn, and P. Fucini. 2008. Translational regulation via L11: molecular switches on the ribosome turned on and off by thiostrepton and micrococcin. Mol Cell **30:**26-38.

Heinemeyer, W., M. Fischer, T. Krimmer, U. Stachon, and D. H. Wolf. 1997. The active sites of the eukaryotic 20 S proteasome and their involvement in subunit precursor processing. J Biol Chem **272:**25200-9.

Hobbs, C. V., T. Voza, A. Coppi, B. Kirmse, K. Marsh, W. Borkowsky, and P. Sinnis. 2009. HIV protease inhibitors inhibit the development of preerythrocytic-stage *plasmodium* parasites. J Infect Dis **199:**134-41.

Hoffman, I. F., C. S. Jere, T. E. Taylor, P. Munthali, J. R. Dyer, J. J. Wirima, S. J. Rogerson, N. Kumwenda, J. J. Eron, S. A. Fiscus, H. Chakraborty, T. E. Taha, M. S. Cohen, and M. E. Molyneux. 1999. The effect of *Plasmodium falciparum* malaria on HIV-1 RNA blood plasma concentration. AIDS **13:**487-94.

Horrocks, P., and C. I. Newbold. 2000. Intraerythrocytic polyubiquitin expression in *Plasmodium falciparum* is subjected to developmental and heat-shock control. Mol Biochem Parasitol **105:**115-25.

Hyde, J. E. 2005. Drug-resistant malaria. Trends Parasitol **21:**494-8.

Ilett, K. F., B. T. Ethell, J. L. Maggs, T. M. Davis, K. T. Batty, B. Burchell, T. Q. Binh, T. A. Thu le, N. C. Hung, M. Pirmohamed, B. K. Park, and G. Edwards. 2002. Glucuronidation of dihydroartemisinin *in vivo* and by human liver microsomes and expressed UDP-glucuronosyltransferases. Drug Metab Dispos **30:**1005-12.

Jelinek, T., P. Schelbert, T. Loscher, and D. Eichenlaub. 1995. Quinine resistant falciparum malaria acquired in east Africa. Trop Med Parasitol **46:**38-40.

Jongwutiwes, S., P. Buppan, R. Kosuvin, S. Seethamchai, U. Pattanawong, J. Sirichaisinthop, and C. Putaporntip. 2011. *Plasmodium knowlesi* Malaria in humans and macaques, Thailand. Emerg Infect Dis **17:**1799-806.

Kamya, M. R., A. F. Gasasira, A. Yeka, N. Bakyaita, S. L. Nsobya, D. Francis, P. J. Rosenthal, G. Dorsey, and D. Havlir. 2006. Effect of HIV-1 infection on antimalarial treatment outcomes in Uganda: a population-based study. J Infect Dis **193:**9-15.

Kane, R. C., P. F. Bross, A. T. Farrell, and R. Pazdur. 2003. Velcade: U.S. FDA approval for the treatment of multiple myeloma progressing on prior therapy. Oncologist **8:**508-13.

Kariuki, M. M., J. K. Kiaira, F. K. Mulaa, J. K. Mwangi, M. K. Wasunna, and S. K. Martin. 1998. *Plasmodium falciparum*: purification of the various gametocyte developmental stages from *in vitro*-cultivated parasites. Am J Trop Med Hyg **59:**505-8.

Kaumanns, P., I. Hagmann, and M. T. Dittmar. 2006. Human TRIM5alpha mediated restriction of different HIV-1 subtypes and Lv2 sensitive and insensitive HIV-2 variants. Retrovirology **3:**79.

Kerns, E., and L. Di. 2008. Drug-like Properties: Concepts, Structure Design and Methods: from ADME to Toxicity Optimization. 1st ed. pp 138-139.

Khoo, S., D. Back, and P. Winstanley. 2005. The potential for interactions between antimalarial and antiretroviral drugs. AIDS **19:**995-1005.

Kisselev, A. F., and A. L. Goldberg. 2001. Proteasome inhibitors: from research tools to drug candidates. Chem Biol **8:**739-58.

Kiszewski, A. E. 2011. Blocking *Plasmodium falciparum* Malaria Transmission with Drugs: The Gametocytocidal and Sporontocidal Properties of Current and Prospective Antimalarials. Pharmaceuticals **4:**44-68.

Kloetzel, P.-M. 2001. Antigen processing by the proteasome. Nat Rev Mol Cell Biol **2:**179-188.

Kreidenweiss, A., P. G. Kremsner, and B. Mordmuller. 2008. Comprehensive study of proteasome inhibitors against *Plasmodium falciparum* laboratory strains and field isolates from Gabon. Malar J **7:**187.

Kublin, J. G., P. Patnaik, C. S. Jere, W. C. Miller, I. F. Hoffman, N. Chimbiya, R. Pendame, T. E. Taylor, and M. E. Molyneux. 2005. Effect of *Plasmodium falciparum* malaria on concentration of HIV-1-RNA in the blood of adults in rural Malawi: a prospective cohort study. Lancet **365:**233-40.

Kuehn, A., and G. Pradel. 2010. The coming-out of malaria gametocytes. J Biomed Biotechnol **2010:**976827.

Kwok, J. M., S. S. Myatt, C. M. Marson, R. C. Coombes, D. Constantinidou, and E. W. Lam. 2008. Thiostrepton selectively targets breast cancer cells through inhibition of forkhead box M1 expression. Mol Cancer Ther **7:**2022-32.

Lavelin, I., A. Beer, Z. Kam, V. Rotter, M. Oren, A. Navon, and B. Geiger. 2009. Discovery of novel proteasome inhibitors using a high-content cell-based screening system. PLoS One **4:**e8503.

Leskovac, V., and A. D. Theoharides. 1991. Hepatic metabolism of artemisinin drugs--I. Drug metabolism in rat liver microsomes. Comp Biochem Physiol C **99:**383-90.

Leubner, M. 2010. Wirkung von Thiostreptonderivaten auf den Malariaerreger *Plasmodium falciparum* unter besonderer Berücksichtigung des Proteasoms als Angriffsziel. **Bachelor thesis.** University of Würzburg, Germany.

Lindenthal, C., N. Weich, Y. S. Chia, V. Heussler, and M. Q. Klinkert. 2005. The proteasome inhibitor MLN-273 blocks exoerythrocytic and erythrocytic development of *Plasmodium* parasites. Parasitology **131:**37-44.

Lipinski, C. A. 2000. Drug-like properties and the causes of poor solubility and poor permeability. J Pharmacol Toxicol Methods **44:**235-49.

Liu, B., J. Chang, W. P. Gordon, J. Isbell, Y. Zhou, and T. Tuntland. 2008. Snapshot PK: a rapid rodent *in vivo* preclinical screening approach. Drug Discov Today **13:**360-7.

Maier, A. G., B. M. Cooke, A. F. Cowman, and L. Tilley. 2009. Malaria parasite proteins that remodel the host erythrocyte. Nat Rev Micro **7:**341-354.

Makler, M. T., and D. J. Hinrichs. 1993. Measurement of the lactate dehydrogenase activity of *Plasmodium falciparum* as an assessment of parasitemia. Am J Trop Med Hyg **48:**205-10.

Makler, M. T., J. M. Ries, J. A. Williams, J. E. Bancroft, R. C. Piper, B. L. Gibbins, and D. J. Hinrichs. 1993. Parasite lactate dehydrogenase as an assay for *Plasmodium falciparum* drug sensitivity. Am J Trop Med Hyg **48:**739-41.

McConkey, G. A., M. J. Rogers, and T. F. McCutchan. 1997. Inhibition of *Plasmodium falciparum* protein synthesis. Targeting the plastid-like organelle with thiostrepton. J Biol Chem **272:**2046-9.

Mishra, L. C., A. Bhattacharya, M. Sharma, and V. K. Bhasin. 2010. HIV protease inhibitors, indinavir or nelfinavir, augment antimalarial action of artemisinin *in vitro*. Am J Trop Med Hyg **82:**148-50.

Mishra, S., U. Narain, R. Mishra, and K. Misra. 2005. Design, development and synthesis of mixed bioconjugates of piperic acid-glycine, curcumin-glycine/alanine and curcumin-glycine-piperic acid and their antibacterial and antifungal properties. Bioorg Med Chem **13:**1477-86.

Mordmuller, B., R. Fendel, A. Kreidenweiss, C. Gille, R. Hurwitz, W. G. Metzger, J. F. Kun, T. Lamkemeyer, A. Nordheim, and P. G. Kremsner. 2006. Plasmodia express two threonine-peptidase complexes during asexual development. Mol Biochem Parasitol **148:**79-85.

Morphy, R., C. Kay, and Z. Rankovic. 2004. From magic bullets to designed multiple ligands. Drug Discov Today **9:**641-51.

Mosmann, T. 1983. Rapid colorimetric assay for cellular growth and survival: application to proliferation and cytotoxicity assays. J Immunol Methods **65:**55-63.

Muller, O., C. Traore, B. Kouyate, Y. Ye, C. Frey, B. Coulibaly, and H. Becher. 2006. Effects of insecticide-treated bednets during early infancy in an African area of intense malaria transmission: a randomized controlled trial. Bull World Health Organ **84:**120-6.

Muregi, F. W., and A. Ishih. 2010. Next-Generation Antimalarial Drugs: Hybrid Molecules as a New Strategy in Drug Design. Drug Dev Res **71:**20-32.

Noedl, H., Y. Se, K. Schaecher, B. L. Smith, D. Socheat, and M. M. Fukuda. 2008. Evidence of artemisinin-resistant malaria in western Cambodia. N Engl J Med **359:**2619-20.

Nsanzabana, C., and P. J. Rosenthal. 2011. *In vitro* activity of antiretroviral drugs against *Plasmodium falciparum*. Antimicrob Agents Chemother **55:**5073-7.

Nzila, A. 2006. The past, present and future of antifolates in the treatment of *Plasmodium falciparum* infection. J Antimicrob Chemother **57:**1043-54.

Nzila, A., Z. Ma, and K. Chibale. 2011. Drug repositioning in the treatment of malaria and TB. Future Med Chem **3:**1413-26.

Oerlemans, R., N. E. Franke, Y. G. Assaraf, J. Cloos, I. van Zantwijk, C. R. Berkers, G. L. Scheffer, K. Debipersad, K. Vojtekova, C. Lemos, J. W. van der Heijden, B. Ylstra, G. J. Peters, G. L. Kaspers, B. A. Dijkmans, R. J. Scheper, and G. Jansen. 2008. Molecular basis of bortezomib resistance: proteasome subunit beta5 (PSMB5) gene mutation and overexpression of PSMB5 protein. Blood **112:**2489-99.

Oguariri, R. M., J. W. Adelsberger, M. W. Baseler, and T. Imamichi. 2010. Evaluation of the effect of pyrimethamine, an anti-malarial drug, on HIV-1 replication. Virus Res **153:**269-76.

O'Neill, P. M., V. E. Barton, and S. A. Ward. 2010. The molecular mechanism of action of artemisinin--the debate continues. Molecules **15:**1705-21.

Orlowski, R. Z., and D. J. Kuhn. 2008. Proteasome inhibitors in cancer therapy: lessons from the first decade. Clin Cancer Res **14:**1649-57.

Parikh, S., J. Gut, E. Istvan, D. E. Goldberg, D. V. Havlir, and P. J. Rosenthal. 2005. Antimalarial activity of human immunodeficiency virus type 1 protease inhibitors. Antimicrob Agents Chemother **49:**2983-5.

Paugam, A., A. L. Bulteau, J. Dupouy-Camet, C. Creuzet, and B. Friguet. 2003. Characterization and role of protozoan parasite proteasomes. Trends Parasitol **19:**55-9.

Peters, J. M., W. W. Franke, and J. A. Kleinschmidt. 1994. Distinct 19 S and 20 S subcomplexes of the 26 S proteasome and their distribution in the nucleus and the cytoplasm. J Biol Chem **269:**7709-18.

Peters, W. 1975. The chemotherapy of rodent malaria, XXII. The value of drug-resistant strains of *P. berghei* in screening for blood schizontocidal activity. Ann Trop Med Parasitol **69:**155-71.

Pettifor, A., E. Taylor, D. Nku, S. Duvall, M. Tabala, K. Mwandagalirwa, S. Meshnick, and F. Behets. 2009. Free distribution of insecticide treated bed nets to pregnant women in Kinshasa: an effective way to achieve 80% use by women and their newborns. Trop Med Int Health **14:**20-8.

Ponder E. L., and M. Bogyo. 2007. Ubiquitin-like modifiers and their deconjugating enzymes in medically important parasitic protozoa. Eukaryot Cell **6:**1943-52.

Ponts, N., A. Saraf, D. W. Chung, A. Harris, J. Prudhomme, M. P. Washburn, L. Florens, and K. G. Le Roch. 2011. Unraveling the ubiquitome of the human malaria parasite. J Biol Chem **286:**40320-30.

Ponts, N., J. Yang, D. W. Chung, J. Prudhomme, T. Girke, P. Horrocks, and K. G. Le Roch. 2008. Deciphering the ubiquitin-mediated pathway in apicomplexan parasites: a potential strategy to interfere with parasite virulence. PLoS One **3:**e2386.

Pradel, G. 2007. Proteins of the malaria parasite sexual stages: expression, function and potential for transmission blocking strategies. Parasitology **134:**1911-1929.

Pradel, G., and M. Schlitzer. 2010. Antibiotics in malaria therapy and their effect on the parasite apicoplast. Curr Mol Med **10:**335-49.

Prudhomme, J., E. McDaniel, N. Ponts, S. Bertani, W. Fenical, P. Jensen, and K. Le Roch. 2008. Marine actinomycetes: a new source of compounds against the human malaria parasite. PLoS One **3:**e2335.

Pukrittayakamee, S., K. Chotivanich, A. Chantra, R. Clemens, S. Looareesuwan, and N. J. White. 2004. Activities of artesunate and primaquine against asexual- and sexual-stage parasites in *falciparum* malaria. Antimicrob Agents Chemother **48:**1329-34.

Pukrittayakamee, S., W. Supanaranond, S. Looareesuwan, S. Vanijanonta, and N. J. White. 1994. Quinine in severe *falciparum* malaria: evidence of declining efficacy in Thailand. Trans R Soc Trop Med Hyg **88:**324-7.

Radivojac, P., V. Vacic, C. Haynes, R. R. Cocklin, A. Mohan, J. W. Heyen, M. G. Goebl, and L. M. Iakoucheva. 2010. Identification, analysis, and prediction of protein ubiquitination sites. Proteins **78:**365-80.

Ramasamy, G., D. Gupta, A. Mohmmed, and V. S. Chauhan. 2007. Characterization and localization of *Plasmodium falciparum* homolog of prokaryotic ClpQ/HslV protease. Mol Biochem Parasitol **152:**139-48.

Reynolds, J. M., K. El Bissati, J. Brandenburg, A. Gunzl, and C. B. Mamoun. 2007. Antimalarial activity of the anticancer and proteasome inhibitor bortezomib and its analog ZL3B. BMC Clin Pharmacol **7:**13.

Rosenthal, P.J. 2011. Falcipains and other cysteine proteases of malaria parasites. Adv. Exp. Med. Biol. 712, 30-48.

Saadeh, H. A., I. M. Mosleh, and M. S. Mubarak. 2009. Synthesis of novel hybrid molecules from precursors with known antiparasitic activity. Molecules **14:**1483-94.

Savarino, A., L. Gennero, H. C. Chen, D. Serrano, F. Malavasi, J. R. Boelaert, and K. Sperber. 2001b. Anti-HIV effects of chloroquine: mechanisms of inhibition and spectrum of activity. AIDS **15:**2221-9.

Savarino, A., L. Gennero, K. Sperber, and J. R. Boelaert. 2001a. The anti-HIV-1 activity of chloroquine. J Clin Virol **20:**131-5.

Savarino, A., M. B. Lucia, E. Rastrelli, S. Rutella, C. Golotta, E. Morra, E. Tamburrini, C. F. Perno, J. R. Boelaert, K. Sperber, and R. Cauda. 2004. Anti-HIV effects of chloroquine: inhibition of viral particle glycosylation and synergism with protease inhibitors. J Acquir Immune Defic Syndr **35:**223-32.

Schlitzer, M. 2007. Malaria chemotherapeutics part I: History of antimalarial drug development, currently used therapeutics and drugs in clinical development. ChemMedChem **2:**944-86.

Schmidtke, G., R. Kraft, S. Kostka, P. Henklein, C. Frommel, J. Lowe, R. Huber, P. M. Kloetzel, and M. Schmidt. 1996. Analysis of mammalian 20S proteasome biogenesis: the maturation of beta-subunits is an ordered two-step mechanism involving autocatalysis. EMBO J **15:**6887-98.

Schoof, S., G. Pradel, M. N. Aminake, B. Ellinger, S. Baumann, M. Potowski, Y. Najajreh, M. Kirschner, and H. D. Arndt. 2010. Antiplasmodial thiostrepton derivatives: proteasome inhibitors with a dual mode of action. Angew Chem Int Ed Engl **49:**3317-21.

Schoof, S., S. Baumann, B. Ellinger, and H. D. Arndt. 2009. A fluorescent probe for the 70 S-ribosomal GTPase-associated center. Chembiochem **10:**242-5.

Seemuller, E., A. Lupas, and W. Baumeister. 1996. Autocatalytic processing of the 20S proteasome. Nature **382:**468-71.

Seemuller, E., A. Lupas, D. Stock, J. Lowe, R. Huber, and W. Baumeister. 1995. Proteasome from Thermoplasma acidophilum: a threonine protease. Science **268:**579-82.

Sidhu, A. B., Q. Sun, L. J. Nkrumah, M. W. Dunne, J. C. Sacchettini, and D. A. Fidock. 2007. *In vitro* efficacy, resistance selection, and structural modeling studies implicate the malarial parasite apicoplast as the target of azithromycin. J Biol Chem **282:**2494-504.

Singh, B., L. Kim Sung, A. Matusop, A. Radhakrishnan, S. S. Shamsul, J. Cox-Singh, A. Thomas, and D. J. Conway. 2004. A large focus of naturally acquired *Plasmodium knowlesi* infections in human beings. Lancet **363:**1017-24.

Skinner-Adams, T. S., J. S. McCarthy, D. L. Gardiner, P. M. Hilton, and K. T. Andrews. 2004. Antiretrovirals as antimalarial agents. J Infect Dis **190:**1998-2000.

Skinner-Adams, T. S., K. T. Andrews, L. Melville, J. McCarthy, and D. L. Gardiner. 2007. Synergistic interactions of the antiretroviral protease inhibitors saquinavir and ritonavir with chloroquine and mefloquine against *Plasmodium falciparum in vitro*. Antimicrob Agents Chemother **51:**759-62.

Soyinka, J. O., C. O. Onyeji, S. I. Omoruyi, A. R. Owolabi, P. V. Sarma, and J. M. Cook. 2009. Effects of concurrent administration of nevirapine on the disposition of quinine in healthy volunteers. J Pharm Pharmacol **61:**439-43.

Subramaniam, S., A. Mohmmed, and D. Gupta. 2009. Molecular modeling studies of the interaction between *Plasmodium falciparum* HslU and HslV subunits. J Biomol Struct Dyn **26:**473-9.

Sullivan, M., J. Li, S. Kumar, M. J. Rogers, and T. F. McCutchan. 2000. Effects of interruption of apicoplast function on malaria infection, development, and transmission. Mol Biochem Parasitol **109:**17-23.

Talman, A. M., O. Domarle, F. E. McKenzie, F. Ariey, and V. Robert. 2004. Gametocytogenesis: the puberty of *Plasmodium falciparum*. Malar J **3:**24.

Tang, J., K. Maddali, C. D. Dreis, Y. Y. Sham, R. Vince, Y. Pommier, and Z. Wang. 2011a. N-3 Hydroxylation of Pyrimidine-2,4-diones Yields Dual Inhibitors of HIV Reverse Transcriptase and Integrase. ACS Med Chem Lett **2:**63-67.

Tang, J., K. Maddali, C. D. Dreis, Y. Y. Sham, R. Vince, Y. Pommier, and Z. Wang. 2011b. 6-Benzoyl-3-hydroxypyrimidine-2,4-diones as dual inhibitors of HIV reverse transcriptase and integrase. Bioorg Med Chem Lett **21:**2400-2.

Tarr, S. J., R. E. Nisbet, and C. J. Howe. 2011. Transcript-level responses of *Plasmodium falciparum* to thiostrepton. Mol Biochem Parasitol **179:**37-41.

Trape, J. F. 2001. Limits of impregnated bednets for malaria control in tropical Africa. Bull Soc Pathol Exot **94:**174-9.

Tschan, S., A. Kreidenweiss, Y. D. Stierhof, N. Sessler, R. Fendel, and B. Mordmuller. 2010. Mitochondrial localization of the threonine peptidase PfHslV, a ClpQ ortholog in *Plasmodium falciparum*. Int J Parasitol **40:**1517-23.

UNAIDS/WHO. 2009. AIDS epidemics update.
http://data.unaids.org/pub/report/2009/jc1700_epi_update_2009_en.pdf

Veal, G. J., and D. J. Back. 1995. Metabolism of Zidovudine. Gen Pharmacol **26:**1469-75.

Waller, R. F., M. B. Reed, A. F. Cowman, and G. I. McFadden. 2000. Protein trafficking to the plastid of *Plasmodium falciparum* is via the secretory pathway. EMBO J **19:**1794-802.

Walsh, J. J., and A. Bell. 2009. Hybrid drugs for malaria. Curr Pharm Des **15:**2970-85.

Walsh, J. J., D. Coughlan, N. Heneghan, C. Gaynor, and A. Bell. 2007. A novel artemisinin-quinine hybrid with potent antimalarial activity. Bioorg Med Chem Lett **17:**3599-602.

Wang, M., and A. L. Gartel. 2011. Micelle-encapsulated thiostrepton as an effective nanomedicine for inhibiting tumor growth and for suppressing FOXM1 in human xenografts. Mol Cancer Ther **10:**2287-97.

Wang, Z., and R. Vince. 2008a. Design and synthesis of dual inhibitors of HIV reverse transcriptase and integrase: introducing a diketoacid functionality into delavirdine. Bioorg Med Chem **16:**3587-95.

Wang, Z., and R. Vince. 2008b. Synthesis of pyrimidine and quinolone conjugates as a scaffold for dual inhibitors of HIV reverse transcriptase and integrase. Bioorg Med Chem Lett **18:**1293-6.

Wang, Z., E. M. Bennett, D. J. Wilson, C. Salomon, and R. Vince. 2007. Rationally designed dual inhibitors of HIV reverse transcriptase and integrase. J Med Chem **50:**3416-9.

Whitworth, J., D. Morgan, M. Quigley, A. Smith, B. Mayanja, H. Eotu, N. Omoding, M. Okongo, S. Malamba, and A. Ojwiya. 2000. Effect of HIV-1 and increasing immunosuppression on malaria parasitaemia and clinical episodes in adults in rural Uganda: a cohort study. Lancet **356:**1051-1056.

WHO. 2010a**.** Guidelines for the treatment of malaria, 2nd edition.
http://www.who.int/malaria/publications/atoz/9789241547925/en/index.html

WHO. 2010b. Antiretroviral therapy for HIV infection in adults and adolescents.
http://www.who.int/hiv/pub/guidelines/artadultguidelines.pdf

WHO. 2011. World Malaria Report 2011.
http://www.who.int/malaria/world_malaria_report_2011/9789241564403_eng.pdf

Wickham, M. E., M. Rug, S. A. Ralph, N. Klonis, G. I. McFadden, L. Tilley, and A. F. Cowman. 2001. Trafficking and assembly of the cytoadherence complex in *Plasmodium falciparum*-infected human erythrocytes. EMBO J **20:**5636-49.

Xu, L., A. K. Farthing, J. F. Dropinski, P. T. Meinke, C. McCallum, P. S. Leavitt, E. J. Hickey, L. Colwell, J. Barrett, and K. Liu. 2009. Nocathiacin analogs: Synthesis and antibacterial activity of novel water-soluble amides. Bioorg Med Chem Lett **19:**3531-5.

7. Annex

7.1. *P. falciparum* proteasome α-type 5 DNA and protein sequences

Primers for RT-PCR

```
   1  atgttttcaa caaggagtga atatgatagg ggagtaaata ccttttctcc tgaaggacga
        m  f  s  t  r  s  e  y  d  r  g  v  n  t  f  s  p  e  g  r

  61  cttttcaag ttgaatatgc cttaggggcg ataaaacttg gtagtacggc tgtaggtatt
        l  f  q  v  e  y  a  l  g  a  i  k  l  g  s  t  a  v  g  i

 121  tgtgtgaacg atggagtgat attagcatcc gagagaagaa tttcctcaac acttatcgaa
        c  v  n  d  g  v  i  l  a  s  e  r  r  i  s  s  t  l  i  e

 181  aaagattccg ttgagaaatt attatcgata gatgatcata ttggttgtgc gatgagtggt
        k  d  s  v  e  k  l  l  s  i  d  d  h  i  g  c  a  m  s  g

 241  ttgatggctg atgcaagaac attaattgat tatgcaagag tcgagtgtaa tcattataaa
        l  m  a  d  a  r  t  l  i  d  y  a  r  v  e  c  n  h  y  k

 301  tttatttata atgagaatat aaatataaag tcatgtgtag aactaatatc tgaattagct
        f  i  y  n  e  n  i  n  i  k  s  c  v  e  l  i  s  e  l  a

 361  ttagattttt ctaatttgtc tgatagtaaa agaaaaaaga ttatgagcag accattcgga
        l  d  f  s  n  l  s  d  s  k  r  k  k  i  m  s  r  p  f  g

 421  gttgctttat taattggtgg tgtcgataaa aacggaccat gtttatggta tactgaacct
        v  a  l  l  i  g  g  v  d  k  n  g  p  c  l  w  y  t  e  p

 481  tcaggaacca atacaagatt ttcagcagct tctataggtt cagcacaaga aggagcagaa
        s  g  t  n  t  r  f  s  a  a  s  i  g  s  a  q  e  g  a  e

 541  ttattattac aagaaaatta taaaaaagat atgacatttg aacaagctga aattttagct
        l  l  l  q  e  n  y  k  k  d  m  t  f  e  q  a  e  i  l  a

 601  cttacggttt taagacaagt tatggaagat aaactttcaa catcaaatgt tgaaatatgt
        l  t  v  l  r  q  v  m  e  d  k  l  s  t  s  n  v  e  i  c

 661  gctataaaaa aatcagatca aacttttat aaatataata cggatgatat atctagaatt
        a  i  k  k  s  d  q  t  f  y  k  y  n  t  d  d  i  s  r  i

 721  attgacgtat taccatcacc cgtttatccc accatagaca tgacagcata g
        i  d  v  l  p  s  p  v  y  p  t  i  d  m  t  a  -
```

7.2. *P. falciparum* proteasome β-type 5 DNA and protein sequences

Primers for RT-PCR

```
   1  atggtaatag caagtgatga aagctttatg aatgaaattg ataatttaat aaatgatgtg
        m  v  i     a  s  d     e  s  f  m     n  e  i     d  n  l     i  n  d  v

  61  gaagatgaaa gaatagataa tgatgaatta gagttttgtg tagctccagt gaatgtacca
        e  d  e     r  i  d     n  d  e  l     e  f  c     v  a  p     v  n  v  p

 121  agaaatttta taaaatatgc acaaactcaa aataagaaat tatttgattt tcataaaggt
        r  n  f     i  k  y     a  q  t  q     n  k  k     l  f  d     f  h  k  g

 181  actacaactt tagcatttaa atttaaagat gggataatag ttgcagtaga ttcccgagca
        t  t  t     l  a  f     k  f  k  d     g  i  i     v  a  v     d  s  r  a

 241  tctatgggat cttttatatc ttcacagaat gttgaaaaga ttattgaaat aaataaaaat
        s  m  g     s  f  i     s  s  q  n     v  e  k     i  i  e     i  n  k  n

 301  atattaggaa caatggcagg aggagctgct gattgcttat attgggaaaa atatttaggt
        i  l  g     t  m  a     g  g  a  a     d  c  l     y  w  e     k  y  l  g

 361  aaaataataa agatttatga attaagaaat aacgaaaaaa tatcagtacg tgcagctagt
        k  i  i     k  i  y     e  l  r  n     n  e  k     i  s  v     r  a  a  s

 421  actatattaa gtaatatatt atatcaatat aaaggatatg gtttgtgttg tggtattatt
        t  i  l     s  n  i     l  y  q  y     k  g  y     g  l  c     c  g  i  i

 481  ttaagtggtt atgatcatac cggatttaat atgttttatg ttgatgattc aggaaaaaaa
        l  s  g     y  d  h     t  g  f  n     m  f  y     v  d  d     s  g  k  k

 541  gtggaaggaa atttattcag ttgtggtagt ggtagtacat atgcttattc tattttagat
        v  e  g     n  l  f     s  c  g  s     g  s  t     y  a  y     s  i  l  d

 601  tcagcatatg attataattt aaatctagac caagctgttg aattagctag aaatgcaatt
        s  a  y     d  y  n     l  n  l  d     q  a  v     e  l  a     r  n  a  i

 661  tatcatgcta cttttagaga tggtggttca ggaggaaaag taagagtttt tcatattcac
        y  h  a     t  f  r     d  g  g  s     g  g  k     v  r  v     f  h  i  h

 721  aaaaatggat atgacaaaat aattgaagga gaagatgttt tcgatttaca ttaccattat
        k  n  g     y  d  k     i  i  e  g     e  d  v     f  d  l     h  y  h  y

 781  actaatcctg aacaaaagga tcaatatgtt atgtga
        t  n  p     e  q  k     d  q  y  v     m  -
```

7.3. *P. falciparum* hslV DNA and protein sequences

```
  1   atgtttatca gaaactttgt aaatataatt ggatcacaaa aatcaataac caaaacaatt
        m  f  i   r  n  f   v  n  i  i   g  s  q   k  s  i   t  k  t  i

 61   gctagaaatt atttttctga taacagcaag ttgataattc ctcgtcatgg aactaccata
        a  r  n   y  f  s   d  n  s  k   l  i  i   p  r  h   g  t  t  i

121   ttatgtgtta ggaaaaataa tgaagtgtgt ttgatcggtg atggaatggt ttctcaagga
        l  c  v   r  k  n   n  e  v  c   l  i  g   d  g  m   v  s  q  g

181   acgatgatag ttaagggaaa tgcaaaaaag ataagacgtt taaaggacaa tatattaatg
        t  m  i   v  k  g   n  a  k  k   i  r  r   l  k  d   n  i  l  m

241   ggtttcgcag gagctacagc ggattgtttt accttgctag ataaatttga gacaaagatt
        g  f  a   g  a  t   a  d  c  f   t  l  l   d  k  f   e  t  k  i

301   gatgaatatc caaatcaact tttgagaagt tgtgttgagt tagccaaact ttggagaact
        d  e  y   p  n  q   l  l  r  s   c  v  e   l  a  k   l  w  r  t

361   gatagatatt taagacattt agaggccgtt ttaatagtgg ctgataagga tattttgtta
        d  r  y   l  r  h   l  e  a  v   l  i  v   a  d  k   d  i  l  l

421   gaagtaaccg gtaatggtga tgttttagaa ccatcaggaa atgttttagg aacaggatca
        e  v  t   g  n  g   d  v  l  e   p  s  g   n  v  l   g  t  g  s

481   ggaggtccat atgctatggc agctgcaaga gcattgtatg atgtcgaaaa tttaagtgct
        g  g  p   y  a  m   a  a  a  r   a  l  y   d  v  e   n  l  s  a

541   aaagatatag cttataaagc tatgaatatt gctgcagata tgtgttgtca tactaataat
        k  d  i   a  y  k   a  m  n  i   a  a  d   m  c  c   h  t  n  n

601   aattttattt gtgaaacatt gtaa
        n  f  i   c  e  t   l  -
```

7.4. IC_{80} and IC_{90} values of compounds

Compounds	IC_{50} (μM)	$IC_{80(\mu M)}$	$IC_{90(\mu M)}$
Thiostrepton	8.9	35.6	/
SS231	1.0	4.0	9.0
SS234	1.0	4.0	9.0
SS238	2.9	11.6	/
SS257	1.4	5.6	/
SS266	3.5	14	/
Epoxomicin	0.03	0.12	/
MG132	0.05	0.2	/
Bortezomib	0.044	0.18	/
CQ	0.03	0.12	/

IC_{80} and IC_{90} were calculated with GraphPad Prism calculator online: http://graphpad.com/quickcalcs/ECanything2.cfm

7.5. *P. falciparum* gametocyte stages I-V labeled with anti-alpha tubillin

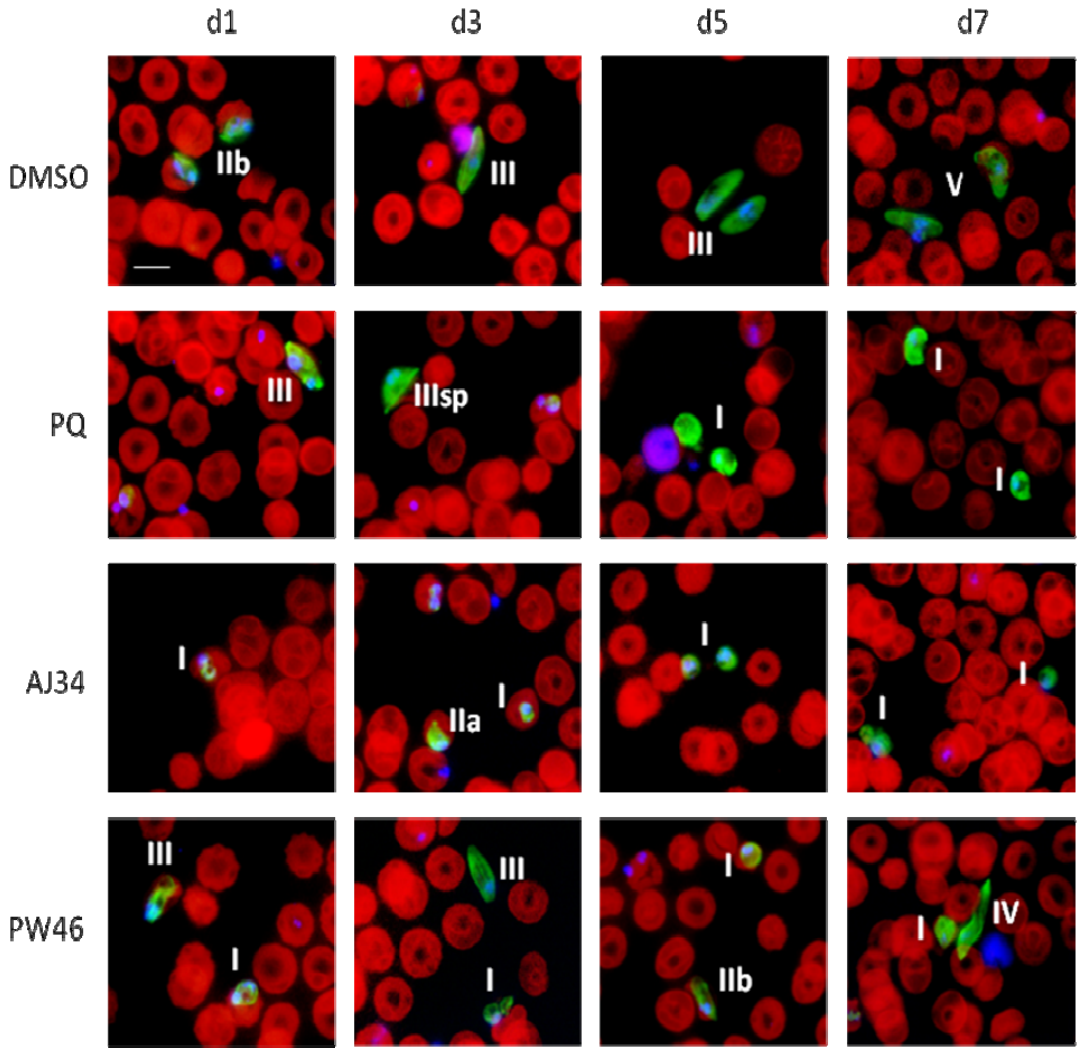

Gametocyte clearance following drug-treatment. Compounds at IC_{50} concentrations or 0.5 vol% of DMSO were added to stage II gametocyte cultures for 2 days. The cultures were cultivated for another 5 days after release of drug pressure. Samples were taken at day 1, 3, 5, and 7 of the assay. Gametocytes were detected by IFA, using antibodies against αlpha-tubulin (green). Erythrocytes were counterstained with Evans Blue (red), nuclei were highlighted by Hoechst nuclear stain (blue). IIIsp, spindle-like structure of a stage III gametocyte; d, day. Bar 5 µm.

7.6. Abbreviations

°C	degree celcius
aa	amino acid
AIDS	acquired immunodeficiency syndrome
AMA	apical membrane antigen
APAD	3-acetylpyridine adenine dinucleotide
APS	ammonium peroxyde sulfate
ATP	adenosine 5'-triphosphate
AZT	azidothymidine or zidovudine
bp	base pair(s)
BSA	bovine serum albumin
cDNA	complementary DNA
CO_2	carbon dioxyde
CQ	chloroquine
d	days
DEPC	diethyl pyrocarbonate
dGTP	2'-deoxyguanosine-5'-triphosphate
dH2O	distilled water
DHA	dihydroartemisinin
DMF	dimethylformamide
DMSO	dimethylsulfoxide
DNA	deoxyribonucleic acid
DNase	deoxyribonuclease
dNTP	deoxynucleotide triphosphate
DTT	dithiothreitol
E. coli	*Escherichia coli*
EDTA	ethylene diamine tetraacetic acid
g	gram
GFP	green fluorscent protein
GST	glutathione-s-transferase
h	hour
HBSS	hank's balanced salt solution
HEPES	*N*-(2-hydroxyethyl)-piperazine-*N*'-2-ethanesulfonic acid
HIV	human immunodeficiency virus
HZ	hemozoin
IC_{50}	Inhibitory concentration 50
IEM	Immunoelectron microscopy
IFA	Immunofluorescence assay
IPTG	Isopropyl-β-D-1-thiogalactopyranoside
kDa	kilodalton
l	liter
M	molar
min	minutes
mRNA	messenger RNA

MW	molecular weight
NAD	nicotinamide adenine dinucleotide
NNRTI	non-nucleoside reverse transcriptase inhibitor
NRTI	nucleoside analogue reverse transcriptase inhibitor
OD	optical density
PAGE	polyacrylamide gel electrophoresis
PBS	phosphate buffered saline
PCR	polymerase chain reaction
PEI	Poly (Ethyleneimine)
PK	pharmacokinetics
RNA	ribonucleic acid
RNase H	Ribonuclease H
rpm	revolutions per minute
RT	room temperature
SDS	sodium dodecyl sulfate
Taq	*thermus aquaticus*
TBDPS	tert-butyldiphenysilyl
TEMED	*N, N, N', N'*-tetramethylethylendiamine
Tris	tris-(hydroxymethyl)-aminomethane
U	unit
UV	ultraviolet
VSV-G	vesicular stomatitis virus G glycoprotein
XA	xanthurenic acid
α5-SU	proteasome alpha 5 subunit
β5-SU	proteasome beta 5 subunit

7.7. Amino Acid Codes

Single letter code	three letter code	Amino acid name
A	Ala	alanine
C	Cys	cysteine
D	Asp	aspartic acid
E	Glu	glutamic acid
F	Phe	phenylalanine
G	Gly	glycine
H	His	histidine
I	Ile	isoleucine
K	lys	Lysine
L	Leu	leucine
M	Met	methionine
N	Asn	asparagine
P	Pro	proline
Q	Gln	glutamine
R	Arg	arginine
S	Ser	serine
T	Thr	threonine
V	Val	valine
W	Trp	tryptophane
Y	Tyr	tyrosine

7.8. Publications

Aminake, M. N., H.-D. Arndt and G. Pradel. **2012.** The proteasome of malaria parasites: A multi-stage drug target for chemotherapeutic intervention? ***International Journal for Parasitology: Drugs and Drug Resistance 2:1-10.***

Aminake, M.N., S. Schoof, L. Sologub, M. Leubner, M. Kirschner, H. D. Arndt, and G. Pradel. **2011.** Thiostrepton and derivatives exhibit antimalarial and gametocytocidal activity by dually targeting parasite proteasome and apicoplast. ***Antimicrob Agents Chemother 55:1338-48.***

Schoof, S., G. Pradel, **M. N. Aminake**, B. Ellinger, S. Baumann, M. Potowski, Y. Najajreh, M. Kirschner, and H. D. Arndt. **2010**. Antiplasmodial thiostrepton derivatives: proteasome inhibitors with a dual mode of action. ***Angew Chem Int Ed Engl 49:3317-21.***